

Climate change is associated with a higher extinction risk of a subshrub in anthropogenic landscapes

A manuscript for consideration as a Research Article for publication in Journal of Ecology

Eva Conquet^{1*}, Arpat Ogzul¹, Susana Gómez-González^{2,3}, Fernando Ojeda², Maria Paniw^{1,4}

1. Department of Evolutionary Biology and Environmental Studies, University of Zurich, Zurich 8057, Switzerland

2. Departamento de Biología-IVAGRO, Universidad de Cádiz, Campus Río San Pedro, 11510 Puerto Real, Spain

3. Center for Climate and Resilience Research, (CR)2, Santiago, Chile

4. Department of Conservation and Global Change, Doñana Biological Station (EBD-CSIC), Seville 41092, Spain

Author's ORCID IDs:

Eva Conquet: 0000-0002-8047-2635

Arpat Ozgul: 0000-0001-7477-2642

Susana Gómez-González: 0000-0002-3779-8701

Fernando Ojeda: 0000-0001-5480-0925

Maria Paniw: 0000-0002-1949-4448

* Corresponding author's email address: eva.conquet@gmail.com

Word count (abstract through references): 12010

Number of citations: 103

Number of tables in main document: 0

Number of figures in main document: 5

Acknowledgments

We are grateful to all the helpers who have contributed to the data collection and to the Spanish military Campo de Adiestramiento de la Armada in Sierra del Retín (Cádiz), who granted access to some study populations. We acknowledge the E-OBS dataset from the EU-FP6 project UERRA (<https://www.uerra.eu>) and the Copernicus Climate Change Service, as well as the data providers in the ECA&D project (<https://www.ecad.eu>). EC was supported by a Swiss National Science Foundation Grant (31003A_182286) to AO. MP was funded by the grant RYC2021-033192-I by MCIN/AEI/10.13039/501100011033 and “European Union NextGenerationEU/PRTR”. SG-G was funded by the Agencia Estatal de Investigación (Spain; PID2019-106908RA-I00/AEI/10.13039/501100011033) and ANID/FONDAP (Chile; 1522A0001).

Author Contributions

Eva Conquet: Conceptualization, Methodology, Software, Validation, Formal analysis, Investigation, Data curation, Writing - Original Draft, Writing - Review and Editing, Visualization. **Arpat Ozgul:** Conceptualization, Methodology, Resources, Writing - Review and Editing, Supervision, Project administration, Funding acquisition. **Susana Gómez-González:** Validation, Investigation, Resources, Writing - Review and Editing. **Fernando Ojeda:** Investigation, Resources, Writing - Review and Editing, Supervision, Project administration, Funding acquisition. **Maria Paniw:** Conceptualization, Methodology, Software, Validation, Formal analysis,

Investigation, Data curation, Writing - Original Draft, Writing - Review and Editing, Supervision, Project administration, Funding acquisition.

Data and Code Availability Statement

The data necessary for reproducing results and graphs presented in this study are available on Zenodo [link] (+ ref). Original data can be requested from Maria Paniw (maria.paniw@ebd.csic.es). Code for formatting data, implementing and running models and analyses, and plotting results is available on GitHub:

<https://github.com/EvaCnqt/DewyPinesLandUseClimateChange>. The version of code used for this study is archived on Zenodo [link] (+ref).

Conflict of Interest Statement

The authors declare no conflict of interest.

Statement on Inclusion

Our work was performed in collaboration with scientists based in the country where the study was initiated and carried out. The perspective of locally based authors who have strong experience with the focal system was paramount to ensure our conclusions took into account the local context. Additionally, we relied on literature previously published by scientists from the region.

1 **Climate change is associated with a higher extinction risk of a**
2 **subshrub in anthropogenic landscapes**

3

4 **Abstract**

- 5 1. In most ecosystems, the increasingly strong effects of climate change on
6 biodiversity co-occur with other anthropogenic pressures, most importantly
7 land-use change. However, many long-term demographic studies focus on
8 populations monitored in protected areas, and our understanding of how
9 climate change will affect population persistence under anthropogenic land
10 use is still limited.
- 11 2. To fill this knowledge gap, we assessed the consequences of co-occurring
12 land-use and climate change on vital rates and population dynamics of a fire-
13 adapted Mediterranean carnivorous subshrub, the dewy pine (*Drosophyllum*
14 *lusitanicum*). We used seven years of individual data on 4,753 plants
15 monitored in three natural heathland sites that experience primarily fire as a
16 disturbance, and five anthropogenic sites, where fires have been replaced by
17 persistent disturbances from browsing or mechanical vegetation removal as a
18 consequence of land-use change. All sites are projected to experience
19 increasingly hotter summers and drier falls and winters. We used generalised
20 additive models to model non-linear responses of survival, growth, and
21 reproduction to rainfall, temperature, size, density, and time since fire in
22 anthropogenic and natural dewy-pine populations. We then projected
23 population dynamics under climate-change scenarios using an individual-
24 based model.

25 3. Our findings reveal that vital rates respond differently to climate change in
26 anthropogenic compared to natural habitats. While extinction risks did not
27 change under climate change in natural habitats, future higher summer
28 temperatures decreased survival and led to population declines and higher
29 extinction probabilities in anthropogenic habitats.

30 4. *Synthesis*: Our results highlight the possible dramatic effects of climate
31 change on populations largely confined to chronically disturbed,
32 anthropogenic habitats and provide a foundation for devising relevant
33 management strategies aiming towards the protection of species in human-
34 disturbed habitats of the Mediterranean habitat. Overall, our findings
35 emphasise the need for more long-term studies in managed landscapes.

36

37 **Keywords**

38 plant population and community dynamics, anthropogenic landscape, climate
39 change, land-use change, disturbance regime, fire adaptation, Mediterranean
40 habitat, population persistence

41

42 **Introduction**

43

44 Land-use change has been identified as the most important driver of
45 biodiversity declines in most ecosystems (Sala et al., 2000; Díaz et al., 2019; IPBES,
46 2019). Across the globe, human expansion has caused habitat loss and
47 fragmentation through the modification of lands for urbanisation or agricultural
48 purposes (Foley et al., 2005), with dire consequences on local and regional species

49 persistence (Selwood et al., 2015) and cascading effects at the community and
50 ecosystem levels (Garnier et al., 2007; Kampichler et al., 2012; Alberti, 2015).
51 Meanwhile, the effects of land-use change on species are increasingly compounded
52 by more severe impacts of climate change on natural systems (Brook et al., 2008;
53 Mantyka-Pringle et al., 2012; Oliver & Morecroft, 2014).

54

55 The complex interplay of land-use and climate change is reshaping ecosystems at
56 an unprecedented rate, with profound implications for the persistence of many
57 species (Pereira et al., 2024). Nonetheless, many studies assess the persistence of
58 populations under climate change in protected areas (Murali et al., 2022)—which are
59 generally sheltered from anthropogenic land use and habitat loss (Geldmann et al.,
60 2013; Watson et al., 2014; but see Clark et al., 2013), and where populations are
61 thus overall doing better than those outside protected regions (Geldmann et al.,
62 2013; Gray et al., 2016). This means that, in many studies, the key role of land-use
63 change in shaping the response of populations to changes in climate is omitted
64 (Titeux et al., 2016). Land-use and climate change can have reciprocal effects on
65 each other, leading to non-additive effects of these pressures on populations and
66 communities (Brook et al., 2008; Mantyka-Pringle et al., 2012; Oliver & Morecroft,
67 2014; Montràs-Janer et al., 2024). Thus, the effects of climate change might differ
68 among land use types, and the consequences of land-use change could depend on
69 the strength of climate change (Mantyka-Pringle et al., 2012). Understanding these
70 dynamics beyond the confines of protected areas is crucial for devising effective
71 conservation strategies.

72

73 Land-use, climate change, and their interaction (Brook et al., 2008) can affect
74 populations via changes in key vital rates through multiple mechanisms such as
75 inbreeding depression (Leimu et al., 2010; Bijlsma & Loeschcke, 2012), physiological
76 stress (Selwood et al., 2015), or phenotypic selection (Alberti, 2015). Negative
77 effects of climate change on survival could be exacerbated by anthropogenic land
78 use, as habitat fragmentation could hamper individual dispersal, thereby preventing
79 populations to shift their habitat range to respond to the new conditions arising under
80 climate change (Lawson et al., 2010; Oliver & Morecroft, 2014). Additionally,
81 negative correlations between adaptations to land use and to climate change could
82 cause the selection for the tolerance of one pressure to reduce the capacity to adapt
83 to the other (Chevin et al., 2010; Oliver & Morecroft, 2014). As population sizes
84 decrease, these detrimental effects could be amplified through demographic
85 stochasticity and inbreeding depression (Fagan & Holmes, 2006), as a decrease in
86 genetic variability and its subsequent fitness reduction would lower the capacity of
87 individuals to cope with challenging environmental conditions (Leimu et al., 2010;
88 Bijlsma & Loeschcke, 2012). Nonetheless, in face of the prevalence of negative
89 effects of both anthropogenic land use and climate change, and given their
90 interacting effects on demographic parameters (Brook et al., 2008; Titeux et al.,
91 2016) and biodiversity (Montràs-Janer et al., 2024), exhaustively assessing
92 population persistence under changing climatic conditions requires studying
93 populations in anthropogenic landscapes.

94

95 Mediterranean biomes are among the most sensitive to interacting pressures derived
96 from land-use and climate change (Newbold et al., 2020). In these ecosystems, fire
97 is a recurrent disturbance that has shaped plant traits over evolutionary time (Keeley

98 et al., 2012) and is essential to the functioning of ecosystems (Pausas & Bond,
99 2020). However, many fire-adapted plant species in the Mediterranean Basin are
100 now largely found in anthropized habitats where fire regimes have been substantially
101 altered or suppressed altogether by changes in land use (Pausas & Keeley, 2014;
102 Ojeda 2020), which can have strong impacts on plant population dynamics (Paniw,
103 Quintana-Ascencio et al., 2017) and wider ecosystem processes, such as nutrient
104 cycling (Pausas & Bond, 2020). Mediterranean plant populations are also
105 increasingly exposed to shorter and drier winters and hotter summers, jeopardising
106 the persistence of shrubland communities (Paniw et al., 2021). While the effects of
107 human activities in fire-disturbed habitats on plant population persistence have
108 previously been studied (e.g. Paniw, Quintana-Ascencio et al., 2017), we still lack a
109 full understanding on population dynamics under the interacting pressures of land-
110 use and climate change.

111

112 Here, we use a Mediterranean, fire-adapted subshrub, the dewy pine (*Drosophyllum*
113 *lusitanicum*), as a case study to investigate the effects of changing climatic
114 conditions on population dynamics in natural and anthropogenic habitats. We used
115 seven years of individual-based data, collected as part of long-term demographic
116 monitoring (since 2011) in natural and anthropogenic (i.e., highly human-dominated
117 permanently disturbed sites) habitats, to parameterize vital-rate responses to
118 interacting climate (temperature and rainfall) and biotic (plant size and intraspecific
119 density) drivers and project resulting population dynamics under climate-change
120 scenarios. We expected higher extinction probabilities in anthropogenic habitats
121 under current climatic conditions, as previous research has shown human
122 disturbances to have a negative effect on population dynamics (Paniw, Quintana-

123 Ascencio et al., 2017; Conquet et al., 2023), and such disturbances are likely to
124 persist in Mediterranean heathlands (Ojeda, 2020). Additionally, given the negative
125 effects of compound anthropogenic pressures on natural systems (Zscheischler et
126 al., 2018), we expected sharper declines in anthropogenic populations than in
127 natural ones under climate change.

128

129 **Methods**

130

131 Study species

132

133 *Life history*

134

135 The dewy pine, *Drosophyllum lusitanicum* (Drosophyllaceae), is a rare
136 carnivorous subshrub endemic to the western end of the Mediterranean basin and
137 tightly associated to fire-prone Mediterranean heathlands of southern Spain,
138 Portugal, and northern Morocco (Correia & Freitas, 2002; Garrido et al., 2003; Paniw
139 et al., 2015). As with many species in fire-prone habitats, dewy pines have adapted
140 their life history to persist under recurring fire regimes that remove all aboveground
141 vegetation. Populations rely on a persistent soil seedbank (Fig. 1), whose dynamics
142 strongly vary with time since fire (TSF_t , where t is the number of years after a fire;
143 Paniw, Quintana-Ascencio et al., 2017; Conquet et al., 2023). When a fire occurs
144 (TSF_0), the combined effect of heat and vegetation and litter removal trigger the
145 germination of the major part of seeds stored in the seedbank (Fig. 1; Appendix S1:
146 Table S1; Cross et al., 2017; Paniw, Quintana-Ascencio et al., 2017; Gómez-
147 González et al., 2018). Germination from the seedbank continues in later post-fire

148 years but greatly decreases from TSF₂. New seedlings mostly grow during the first
149 year after a fire (TSF₁) and become reproductive plants from the second year after
150 the population burned (TSF₂; Fig. 1). The majority of seeds produced by these
151 individuals do not germinate directly but go to the soil seedbank to replenish the
152 population at the next fire (Fig. 1). This occurs because dewy pines are increasingly
153 overgrown by dominant shrub vegetation, which hinders seed germination (Gómez-
154 González et al., 2018) and insect prey capture (Paniw et al., 2018), drastically
155 decreasing the survival of aboveground plants after TSF₄ (Paniw et al., 2015).

156

157 Despite being fire-adapted, active fire suppression and general degradation of
158 heathland habitats under land-use change (for instance through vegetation removal
159 for wide firebreaks or pine afforestations) mean that most populations of dewy pines
160 as well as numerous other heathland species persist in highly and permanently
161 human-disturbed (hereafter anthropogenic) habitats (Paniw et al., 2015) (see
162 Appendix 2: Table S1 for details on study populations). In such habitats, periodic
163 mechanical clearing of vegetation or browsing—of surrounding vegetation but not on
164 dewy pines—and trampling by domestic ungulates act as a constant disturbance
165 resembling the effect of fire by the removal of aboveground vegetation, but lasting
166 much longer. This has led to important changes in the demographic processes of
167 dewy pines (Paniw, Quintana-Ascencio et al., 2017; Conquet et al., 2023).

168 Seedbanks in chronically disturbed, anthropogenic populations are likely depleted
169 because the long-term clearance of vegetation means that relatively more seeds
170 germinate immediately instead of going into the seedbank (Appendix S1: Table S1;
171 Gómez-González et al., 2018). Vital rates of aboveground individuals are affected as
172 well; while juvenile survival rapidly decreases after a fire in natural populations, it

173 remains stable across time under human disturbances. However, smaller mature
174 individuals in anthropogenic populations have a lower survival than in natural
175 populations, and reproduction is decreased as well. Moreover, negative density
176 feedbacks are stronger in anthropogenic populations (Conquet et al., 2023).

177

178 Anthropogenic pressures in dewy pine habitats are also increasingly interacting with
179 climate change. Temperatures have been increasing in the last four decades (on
180 average by 0.033 °C per year) and will continue to do so in the future (Appendix S2:
181 Fig. S1 and S2). Contrastingly, while the recent increase in rainfall variability is
182 predicted to reverse, rainfall is forecasted to be less abundant in the future (-0.16
183 mm per year on average). Such variations in environmental patterns have already
184 shown to lead to population declines in natural shrublands (Paniw et al., 2023).

185 Dewy pines will therefore likely be increasingly affected by interactions of climate
186 change and human disturbance. Therefore, understanding their response to climate
187 effects will help us discern the joint role of different pressures on plants persisting in
188 anthropogenic habitats.

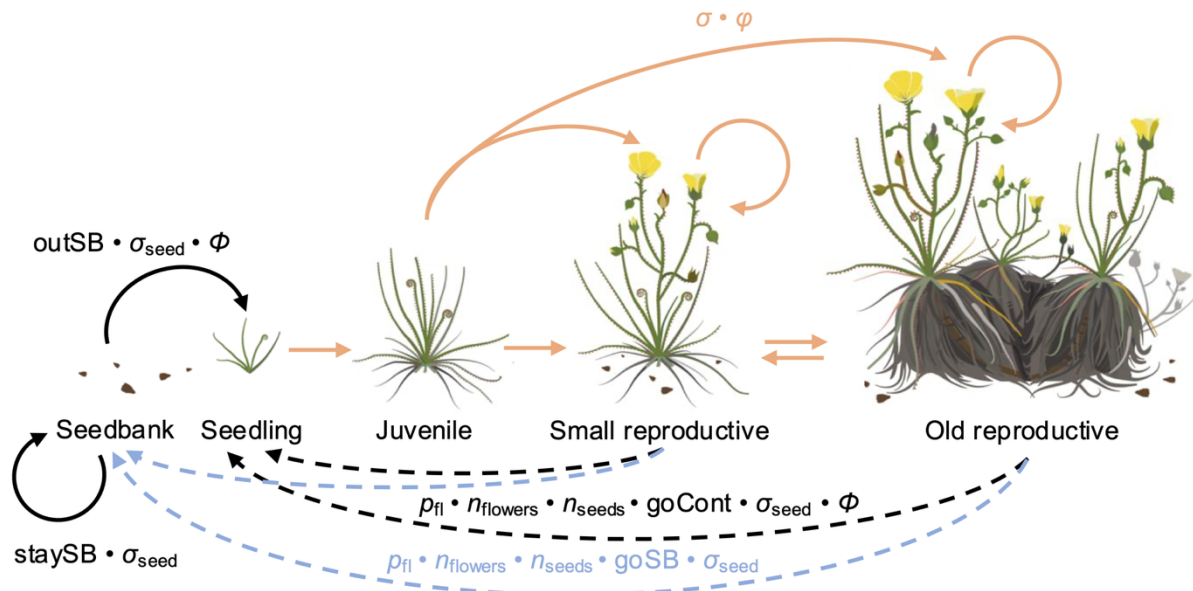
189

190 *Demographic data*

191

192 We used individual demographic data collected on 4753 dewy pines from eight
193 populations of southern Spain, located in two types of habitats: Mediterranean
194 heathlands experiencing recurrent fire regimes and low levels of anthropogenic
195 pressures such as cattle browsing and trampling (natural populations; $n = 3$); and
196 Mediterranean heathlands that have not burned in the past 40 years but where high
197 anthropogenic pressures constantly remove aboveground vegetation (anthropogenic

198 populations; $n = 5$) (Appendix S2: Table S1). In each population, we obtained
 199 information on size, reproduction (probability of flowering and number of flowers), and
 200 survival from individually marked plants located in 40 1×1m plots; all individuals,
 201 including new recruits, in a given plot were marked and censused every spring in the
 202 last week of April or first week of May (see Appendix S1 for details).



203 **Figure 1 – Dewy-pine life cycle.** Conditional on seed survival (σ_{seed}), seeds in
 204 the seedbank germinate, with germination probability $outSB$, to become seedlings of
 205 a given size (Φ), or remain dormant underground ($staySB$). Aboveground individuals
 206 then survive (σ) and grow (φ), depending on their size (size-dependent survival and
 207 growth is highlighted in orange); and become reproductive from two years after a fire
 208 occurred in natural habitats. Reproductive individuals produce seeds conditional on
 209 size-dependent flowering probability (p_{fl}), the number of flowers ($n_{flowers}$), and the
 210 number of seeds per flower (n_{seeds}). These seeds, conditional on their survival (σ_{seed}),
 211 either germinate directly ($goCont$; dashed black arrows) and become seedlings of a
 212 given size (Φ) or contribute to the underground seedbank ($goSB$; dashed blue arrow).
 213

214 Estimation of seedbank parameters

215

216 To parameterize variation among different habitat types in probabilities of seed
217 germination (goCont for seeds germinating without going to the seedbank and outSB
218 for seeds germinating from the seedbank), dormancy (staySB) and transition to the
219 seedbank (goSB) (Fig. 1), we used published data from seed-burial and greenhouse
220 germination experiments (Paniw, Quintana-Ascencio et al., 2017; Gómez-González
221 et al., 2018). Previous research has shown that in natural populations, most
222 produced seeds (97.4%; 95% confidence interval [96.3%–98.4%]) go to the
223 underground seedbank (Appendix S1: Table S1). While 81% [77.4%–85.2%] of the
224 seeds germinate from the seedbank right after a fire (TSF₀), that proportion greatly
225 decreases in later post-fire habitat stages (6.09% [4.44%–7.75%] in TSF₁ and 3.47%
226 [2.31%–4.63%] in later TSFs). In contrast, in chronically disturbed, anthropogenic
227 populations, a much lower proportion of the produced seeds goes to the seedbank
228 (82.2% [65.3%–97.5%]). In these populations, although 59.8% [56.6%–63.0%] of the
229 underground seeds remain underground, seedbanks are depleted due to the
230 decreased proportion of seeds produced by aboveground plants entering dormancy.

231

232 Estimation of aboveground vital rates

233

234 We investigated how rainfall, temperature, and density affect the survival, growth,
235 and reproduction of individuals, for natural and anthropogenic dewy-pine populations
236 separately (Appendix 2: Table S1). We used Generalised Additive Models—fitted
237 with the *gam* function of the *mgcv* package (Wood, 2011; Wood et al., 2016; Wood,
238 2017)—to estimate (1) survival (σ) and flowering probability (p_{fl}) (using a binomial

239 distribution), (2) the number of flowers per individual (n_{flowers} ; using a negative
240 binomial distribution instead of a simple Poisson model as the data were
241 overdispersed), and (3) growth (φ) and seedling size (Φ), with size = log(number of
242 leaves \times length of the longest leaf (cm)) (Fig. 1; Paniw, Quintana-Ascencio et al.,
243 2017). We modelled the latter two vital rates using a scaled t distribution (“scat” in
244 the family parameter of the *gam* function) instead of a Gaussian distribution to
245 accommodate the heavy-tailed nature of the response variables (see Appendix 1:
246 Table S4). We tested for the nonlinear responses of all vital rates to lag cumulative
247 rainfall and average daily maximum temperature, and aboveground density of large
248 (i.e., size > 4.5) intraspecific neighbours. In addition, to account for effects of post-
249 fire habitat stages, we tested for nonlinear effects of time since fire (TSF) on vital
250 rates of natural populations. We used a cubic spline basis with three dimensions ($k =$
251 3) for all these covariates (except for the size effect on the number of flowers, where
252 we used $k = 4$ to model a decline in the number of flowers of large individuals as has
253 been observed in all populations), and a gamma value of 1.4, as is commonly used
254 to reduce the risk of overfitting (Wood, 2017). We also included random year and
255 population effects on the model intercept in all models using a random-effect spline.
256 We performed all analyses in R 4.2.2 via RStudio (R Core Team, 2022; Posit team,
257 2023).

258

259 *Vital-rate responses to climatic variables (cumulative rainfall and*
260 *average maximum daily temperature)*

261

262 We chose rainfall and maximum temperatures as climatic predictors based on recent
263 publications showing the importance of these two drivers on vital rates of

264 Mediterranean plants (García-Callejas et al., 2017; Paniw et al., 2023) and based on
265 our a priori expectations given the biology of the study species (Appendix 1: Table
266 S2). We extracted daily rainfall and maximum temperature data with a resolution of
267 0.1 degree for all dewy-pine population locations from the E-OBS dataset from the
268 EU-FP6 project UERRA and the Copernicus Climate Change Service (Cornes et al.,
269 2018; see Appendix S2 for details). We obtained the monthly cumulative rainfall and
270 average maximum temperature in each population by averaging the values recorded
271 within a buffer of 0.1×1.5 degrees (i.e. 1.5 times the grid resolution) around the
272 population coordinates. We assessed the presence of rainfall and temperature lag
273 effects on dewy-pine vital rates using GAMs including cumulative rainfall and
274 average maximum daily temperature across several biologically relevant periods. We
275 defined these periods based on prior knowledge of seasonal climatic effects in
276 Mediterranean shrublands (Paniw et al. 2023; Appendix 1, Table S2); and did not
277 use a sliding-window approach to assess lagged effects to avoid spurious
278 correlations (Evers et al., 2021). For survival and growth, we assessed the effect of
279 climate following the annual population census (set to the 1st of May), while for
280 reproductive parameters (i.e., flowering probability, number of flowers, and seedling
281 size), we assessed the effect of climate in periods prior to the census. More
282 specifically, we considered the effect of post-census average maximum temperature
283 in summer (May–September) and of cumulative rainfall in fall (September–
284 November), winter (January–April), or both (September–April), on survival and
285 growth. We tested for the effect of pre-census average maximum daily temperature
286 in winter (January–April), and of cumulative rainfall in fall (September–November)
287 and winter (January–April) on reproductive rates. We considered that the effects of
288 longer lag periods are effectively absorbed by changes in plant size.

289

290 *Vital-rate responses to large aboveground individual density*

291

292 To understand how intraspecific interactions affect dewy-pine vital rates, we included
293 in our models the density of aboveground individuals, specific to a 1-m² quadrat in a
294 given population. This spatial resolution matches the study design—where plants are
295 censused in four transects of ten 1-m² quadrats (Paniw, Quintana-Ascencio et al.,
296 2017)—and corresponds to the observed scale at which the plant-plant interactions
297 affecting the demography of dewy pines occur. We only considered individuals of
298 size > 4.5, which corresponds to the minimum observed size of reproductive plants.
299 Smaller plants are largely seedlings which have relatively weak effects on plant vital
300 rates, as large individuals are unlikely to be affected by small plants and small plants
301 are primarily affected by large shrubs (Brewer et al., 2021). We did not use a
302 spatially explicit formulation of density dependence (e.g. using the crowding
303 approach described in Adler et al., 2010), as such an approach requires knowledge
304 of the spatial distribution of individuals and seeds, which we lacked for some sites
305 and years.

306

307 *Vital-rate model selection*

308

309 We selected the best vital-rate models using the Akaike Information Criterion (AIC,
310 using a threshold of $\Delta AIC > 2$ to identify a model as performing better than another;
311 Burnham et al., 2011; Wood, 2017) and the number of degrees of freedom. Prior to
312 model selection, we standardised and checked for correlations between all
313 covariates (see Appendix S1 for more details). We first selected the best lag period

314 for the effect of rainfall and temperature and then added—in a forward selection
315 framework—density and size to the model selection and, for natural populations,
316 time since last fire (Appendix S1: Table S3 for more details). We considered two-way
317 interactions among the climatic variables, density, size, and TSF as well as site-
318 specific random slopes (e.g., site-specific effects of density or size) in our model
319 selection, using random-effect splines.

320

321 Population projections under climate change scenarios

322

323 *Individual-Based Model definition*

324

325 We used the estimated vital rates to parameterize an Individual-Based Model (IBM)
326 and project each natural and anthropogenic dewy-pine population under current and
327 predicted climate conditions. The following is a summary of the IBM specificities; a
328 more detailed description of the different modules of the projection model following
329 the ODD (Overview, Design concepts, Details) protocol (Grimm et al., 2006; 2020)
330 can be found in Appendix S3. We performed 500 30-year projections of each dewy-
331 pine population under two scenarios: (1) a control scenario corresponding to current
332 climatic conditions where 30 years—and the corresponding rainfall and temperature
333 values—were sampled at random among the past observed ones (2016–2021); and
334 (2) two climate-change scenario where the rainfall and temperature values
335 corresponded to projected climatic conditions from 2021 to 2050 according to the
336 RCP4.5 and RCP8.5 climate-change scenarios (Riahi et al., 2011). The climate-
337 change scenario comprised 11 sets of 500 population projections, each set
338 corresponding to future rainfall and temperature conditions extracted from 11 global

339 circulation models (GCM; Appendix S2: Table S2) from the Coupled Model
340 Intercomparison Project 6 (CMIP6; Eyring et al., 2016; Pascoe et al., 2020; Waliser
341 et al., 2020) available from the Earth System Grid Federation's (ESFG; Petrie et al.,
342 2021) web application accessible at <https://aims2.llnl.gov/search>. These models
343 have been used in several studies on ecological systems (Tredennick et al., 2016;
344 Paniw et al., 2022) and differ in their parameterisation, enabling us to project the
345 dewy-pine populations under a wide range of possible future climatic conditions and
346 thereby reduce bias in our population projections (Sanderson et al., 2015).

347

348 Because most GCMs comprised projected rainfall and temperature values beyond
349 the values observed in our populations, we capped these values to the maximum
350 and minimum observed. This approach allowed us to investigate the response of
351 dewy-pine populations to substantial increases in the frequency of extreme climatic
352 conditions, rather than changes in absolute rainfall and temperature values.

353

354 Each population projection started with a population vector of z-sized individuals
355 from 2021—the last year used to estimate vital rates—, and the initial population
356 thus comprised individuals observed in the population in that year. This also applies
357 to the initial rainfall and temperature values, and the aboveground density of large
358 individuals. While we assumed no fire occurred in anthropogenic populations, we
359 simulated a sequence of 30 post-fire habitat stages for each projection of natural
360 populations. The first post-fire state corresponded to the one observed in 2021, and
361 the subsequent ones were determined based on a Markov matrix containing the
362 among-TSF transition probabilities based on a fire frequency of 1/30 representing

363 the stochastic fire regime occurring in natural dewy-pine populations (see Appendix
364 S3 for details; see also Conquet et al., 2023).

365

366 We projected each initial population in discrete yearly steps determining which
367 aboveground individuals reproduced, survived, and grew, and how many seeds
368 germinated—from the seedbank or directly after reproduction—or entered or
369 remained in the seedbank. Each of these processes was represented by a sub-
370 model within the general IBM. As annual censuses took place during the flowering
371 period (pre-reproductive census), each projected year started with the reproduction
372 sub-model. This sub-model sampled reproductive individuals (0 or 1) based on a
373 binomial distribution parameterised with the estimated mean flowering probability
374 (p_{fi}). If any individual reproduced, its number of flowers was sampled from a negative
375 binomial distribution based on the estimated mean number of flowers per plant
376 ($n_{flowers}$); and the number of seeds per flower (n_{seeds}) was sampled from a Poisson
377 distribution with a mean of 9.8—the average number of seeds per flower used in
378 Paniw et al. (2017). To avoid excessive reproductive values in natural populations,
379 we capped the number of flowers per individual to the maximum observed number of
380 flowers in each population. In natural populations, where fires could occur, the
381 reproduction sub-model was skipped in the first year after fire, as dewy pine adults
382 are killed by fire and postfire recruits do not reproduce until two years after
383 germination.

384

385 The reproduction sub-model was followed by the survival and growth sub-model,
386 which sampled the surviving individuals from a binomial distribution based on the
387 mean estimated survival rate, and assigned them a size to which they would grow at

388 the next time step by sampling from a scaled t distribution (to accommodate for
389 heavy-tailed size values when fitting the growth model) based on the mean, standard
390 deviation, and degrees of freedom of the fitted growth model. Sporadically sampled
391 positive infinite sizes were set to the maximum observed size in the population in the
392 currently projected year, while negative infinite sizes were set to zero.

393

394 Finally, at the end of each projected year, the seedbank sub-model sampled seeds
395 from the seedbank that remained dormant or germinated from binomial distributions
396 based on the respective probabilities (staySB and outSB). The seeds that did not
397 survive—i.e., neither germinated or stayed dormant—were removed from the
398 seedbank. The seeds germinating without going through the seedbank were
399 sampled from a binomial distribution based on the probability of continuous
400 germination (goCont). Some seedbank processes are hidden processes that cannot
401 be easily determined in the field without perturbing the populations. To reduce the
402 resulting bias, we applied a correction factor representing seed survival (σ_{seed}) to the
403 seedbank parameters in anthropogenic populations (see Appendix S1 and Paniw,
404 Quintana-Ascencio et al., 2017 for more details), and further corrected outSB and
405 goCont in Sierra Carbonera Disturbed by reducing them to 40 % of their values. We
406 also capped the number of recruits to the maximum number of seedlings observed in
407 all natural populations as well as in two anthropogenic populations: Bujeo and Sierra
408 Carbonera Disturbed. Ultimately, all recruits were assigned a size by sampling from
409 a scaled t distribution based on the estimated mean seedling size as well as its
410 standard deviation and degrees of freedom.

411

412 At the end of a projected year, we updated the size of individuals that grew during
413 the previous year as well as the aboveground density for each 1-m² quadrat in the
414 population. We also calculated and recorded the annual population growth rate
415 (annual $\log \lambda$), which we used to calculate the stochastic growth rate $\log \lambda_S$ for each
416 projection (see Appendix S3 for more details; see also Conquet et al., 2023). In each
417 projection, the population was considered extinct if it went below the quasi-extinction
418 threshold set at 5 aboveground individuals and 50 seeds in the seedbank.

419

420 *Model validation*

421

422 We calibrated our vital-rate and individual-based models by projecting each dewy-
423 pine population from the year it was first censused to 2022. We then compared
424 observed and projected aboveground population sizes and population growth rates,
425 as well as individual size distributions across time. For natural populations, we used
426 the observed post-fire habitat stages and did not simulate fire frequencies. This
427 process enabled us to validate our IBM by assessing its ability to well represent the
428 dynamics of the dewy-pine populations in years that were not used in the model-
429 fitting part of our analysis (i.e., years before 2016 when available, and 2022).

430

431 *Sensitivity analyses*

432

433 We assessed which demographic rates contribute most to changes in population
434 dynamics under climate change in anthropogenic and natural populations. To do so,
435 we repeated climate-change projections, as described in the previous section, for
436 each population, but we changed climatic drivers under the RCP 8.5 climate-change

437 scenario in specific vital rate models only (survival, growth, flowering probability,
438 number of flowers or seedling size), while assuming current climatic conditions in the
439 remaining vital rates. We performed 100 30-year projections, and calculated
440 sensitivities as:

441

$$442 \quad \text{Sensitivity} = \frac{\sum_{i=1}^{n=100} (\log \lambda_{S_perturbed_i} - \log \lambda_{S_control_i}) / \log \lambda_{S_control_i}}{n},$$

443

444 where i = one of 100 $\log \lambda_S$, and $\log \lambda_{S_control}$ represent population dynamics
445 assuming current climatic conditions in all vital rates. We calculated 500 sensitivity
446 values for each population by randomly sampling 100 $\log \lambda_{S_control}$ from the 500
447 available and comparing them to the 100 available $\log \lambda_{S_perturbed}$.

448

449 **Results**

450

451 Vital-rate responses to habitat disturbance

452

453 Dewy-pine vital rates varied between natural and anthropogenic habitats (Fig.
454 2). Survival was on average higher in anthropogenic (mean = 0.42 and 95%
455 confidence interval = [0.18, 0.70]) than in natural habitats (0.27 [0.17, 0.40]; Fig. 2).
456 In contrast, we found the opposite pattern for growth (i.e., plant size at $t+1$), which
457 was higher in natural (size 5.0 [4.7, 5.2] at the next time step, calculated as
458 $\log(\text{number of leaves} \times \text{length of the longest leaf (cm)})$) than in anthropogenic sites
459 (4.7 [4.4, 4.9]), as well as flowering probability (0.039 [0.013, 0.11] in natural and
460 0.025 [0.013, 0.045] in anthropogenic populations), and seedling size (3.4 [3.2, 3.5]
461 and 3.0 [2.8, 3.3], respectively; Fig. 2). However, there was no difference between

462 habitat types in the number of flowers per individual (6.9 [6.2, 7.7] on average in
463 natural populations and 6.7 [5.8, 7.8] in anthropogenic populations; Fig. 2). Notably,
464 we found more among-site variation in anthropogenic than in natural conditions,
465 possibly because the level of anthropogenic disturbance differed between sites
466 (Appendix S1: Fig. S3).

467
468
469
470
471
472
473
474
475
476
477
478
479
480
481
482
483
484
485
486
487

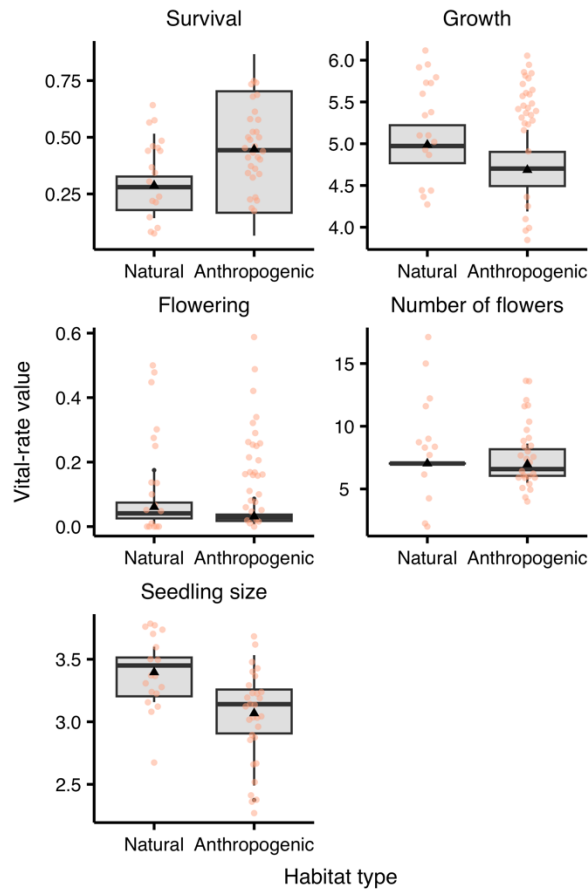
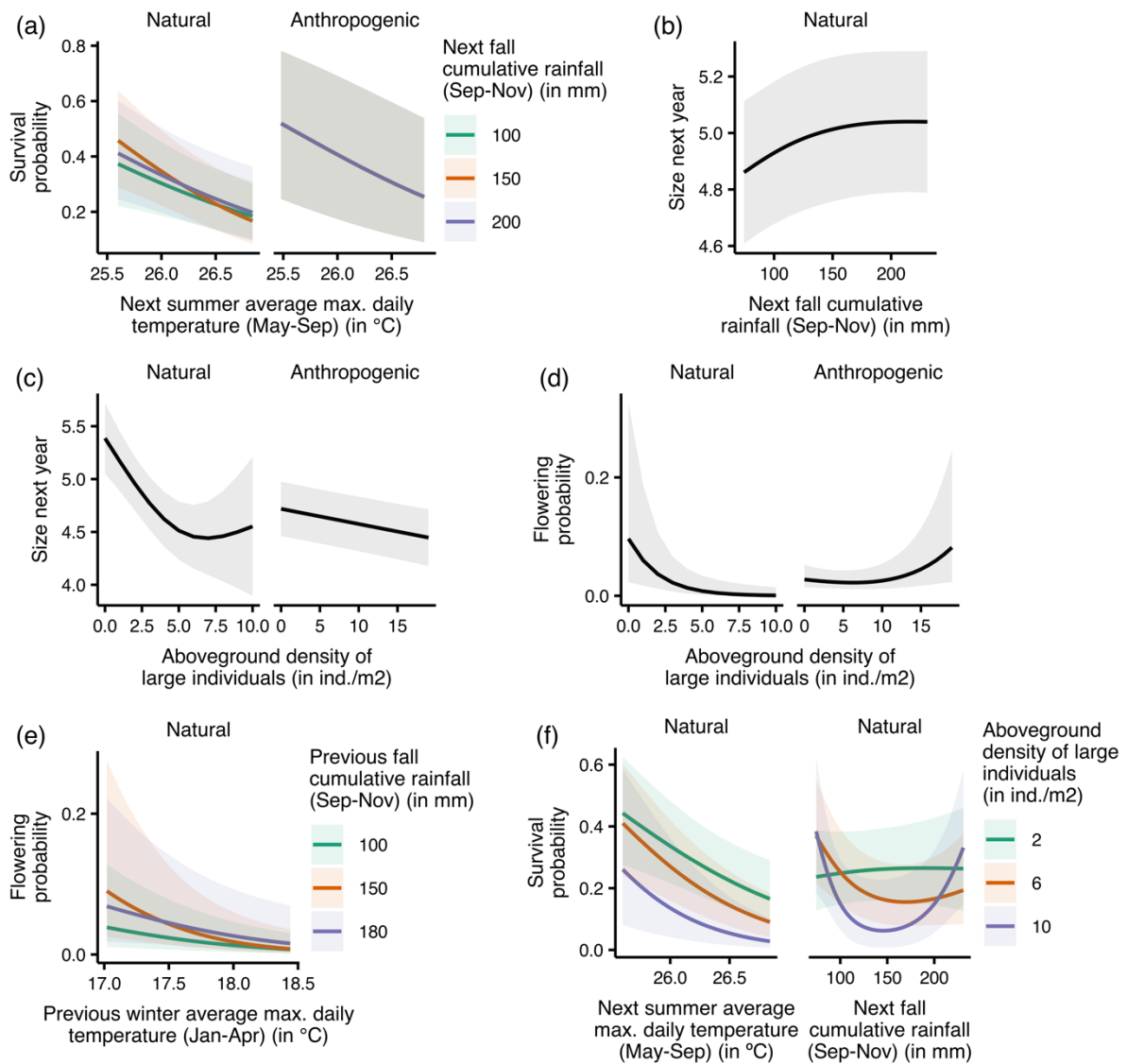


Figure 2 – Predicted and observed average vital-rate values in natural and anthropogenic populations. The boxplots represent the distribution of the predicted average values of habitat-specific survival, growth, i.e., $\log(\text{number of leaves} \times \text{length of the longest leaf (cm)})$, and flowering rates, as well as the number of flowers and seedling size estimated for each population and year from GAMs. The whiskers represent the 2.5th and 97.5th percentiles and the black triangle the mean estimate. We kept covariates at their mean values (scaled value = 0) except for the number of flowers, where we used the mean size of reproducing individuals. The coloured dots represent the observed average vital rates in each population and year.

488 Vital-rate responses to climatic variables

489

490 In both anthropogenic and natural habitats, the variation of most vital rates was
491 associated with changes in at least one of the two climatic variables considered in
492 our analysis: monthly cumulative rainfall (hereafter rainfall) or monthly average daily
493 maximum temperature (hereafter temperature) (Fig. 3; Appendix S1: Table S4). Most
494 vital rates were more strongly associated with the same climatic variable in the same
495 period of the year in both habitats (e.g. variation in survival was associated with
496 changes in summer temperatures and fall rainfall in both natural and anthropogenic
497 populations). Overall, larger variations in vital rates were associated with changes in
498 temperature than with rainfall (Fig. 3; Appendix S1: Table S4).



499 **Figure 3 – Relationships between dewy-pine vital rates and climatic**
500 **variables and aboveground density of large individuals.** Predictions from the
501 GAM models show variation in (a) survival and (b) flowering probability with changes
502 in temperature (next summer and previous winter, respectively) and rainfall (next and
503 previous fall), (c) flowering probability with changes in previous fall rainfall and
504 density, and growth, i.e., $\log(\text{number of leaves} \times \text{length of the longest leaf (cm)})$, with
505 (d) changes in next fall rainfall, and (e) aboveground density of large individuals (size
506 > 4.5). Lines show the mean vital-rate values and shaded areas the associated 95%
507 confidence interval.

508

509 In both natural and anthropogenic populations, survival was the only vital rate for
510 which variation was associated with changes in both rainfall and temperature (i.e.,
511 the fixed effects of both climatic variables were retained in the model selection). With
512 all other covariates held constant at their average value in the respective habitat
513 types, survival was negatively associated with an increase in summer temperatures
514 (i.e., average maximum daily temperature from May to September) (Fig. 3a). For
515 example, when temperature increased from 25.5 to 26.5 °C, the average survival
516 rate decreased from 0.47 [0.29, 0.66] to 0.23 [0.14, 0.35] in natural populations, and
517 from 0.51 [0.24, 0.78] to 0.31 [0.12, 0.60] under anthropogenic conditions. In both
518 habitats, variation in survival was also associated with changes in the amount of
519 rainfall in fall (i.e., September–November; Fig. 3a, Appendix S1: Table S4 and Fig.
520 6e). In natural populations, this association was on average positive (from 0.25 [0.14,
521 0.39] under 80 mm of rain to 0.28 [0.16, 0.45] under 200 mm). In contrast, in
522 anthropogenic populations, average survival across sites did not change with rainfall,
523 but investigating this relationship at the site level revealed important among-
524 population variability, with positive associations in some sites (e.g. from 0.39 [0.16,
525 0.67] under 80 mm of rain to 0.46 [0.21, 0.74] under 200 mm in Sierra del Retín
526 Disturbed) and negative associations in others (e.g. from 0.46 [0.21, 0.74] to 0.36
527 [0.15, 0.65] in Prisioneros; Appendix S1: Fig. S3). Such among-site differences were
528 almost ubiquitous across vital rates in anthropogenic populations (Appendix S1: Fig.
529 S4), but not in natural habitats. For example, on average across all natural sites,
530 individuals grew more with higher amounts of rainfall. More specifically, the longest
531 leaf of an average-sized individual grew from 4.3 to 4.9 [4.6, 5.1] in a year under 80
532 mm of rain but to 5.0 [4.8, 5.3] under 200 mm (Fig. 3b).

533

534 Vital-rate responses to aboveground density of large plants

535

536 In both anthropogenic and natural habitats, plants grew less when densities of
537 large individuals increased (Fig. 3c). Under human disturbance, an average-sized
538 individual grew from 4.1 to 4.7 [4.4, 4.9] in a year with 2 large individuals/m² but to
539 4.6 [4.3, 4.8] with 10 ind./m² (Fig. 3c). In natural conditions, an individual grew from
540 4.3 to 5.0 [4.7, 5.2] with a density of 2 ind./m² but only to 4.6 [3.9, 5.2] with 10 ind./m²
541 (Fig. 3c). Seedling size also decreased with higher numbers of large individuals
542 aboveground (Appendix S1: Fig. S5a). Interestingly, the direction of the association
543 between density and flowering probability differed between habitat types, as the
544 flowering rate was positively associated with density in anthropogenic populations
545 (from 0.50 [0.28, 0.72] with 2 ind./m² to 0.65 [0.35, 0.86] with 15 ind./m²), but strongly
546 negatively in natural ones (from 0.68 [0.41, 0.87] with 2 ind./m² to 0.10 [0.013, 0.50]
547 with 7 ind./m²) (Fig. 3d).

548

549 Vital-rate responses to interactions between climate, density, size,
550 and post-fire habitat conditions

551

552 In natural—but not in anthropogenic—populations, high amounts of rainfall
553 mitigated the strength of the negative association between temperature and survival,
554 which decreased from 0.48 [0.30, 0.67] at 25.5 °C to 0.23 [0.14, 0.36] at 26.5 °C
555 under 150 mm of rainfall but only from 0.43 [0.26, 0.63] at 25.5 °C to 0.25 [0.13,
556 0.41] at 26.5 °C under 200 mm (Fig. 3a). We found a similar pattern for the
557 association between previous winter temperatures and flowering probability, which

558 decreased from 0.72 [0.45, 0.89] at 17.5 °C to 0.29 [0.076, 0.66] at 18.5 °C with 150
559 mm of rain but only from 0.73 [0.43, 0.90] to 0.46 [0.15, 0.80] with 180 mm (Fig. 3e).
560
561 Additionally, in natural populations, survival increased with rainfall at low densities
562 (Fig. 3f; from 0.26 [0.16, 0.40] to 0.28 [0.16, 0.44] for 100 and 200 mm of rain at 2
563 ind./m²); but these variables had a u-shaped relationship at high densities, with
564 lowest survival rates reached for about 145 mm of rain (e.g. 0.076 [0.021, 0.24] at 10
565 ind./m²). The decline in survival with increasing summer temperatures was also
566 weaker at low (e.g. from 0.47 [0.29, 0.66] at 25.5 °C to 0.22 [0.14, 0.35] at 26.5 °C
567 with 2 ind./m²) than at high densities (from 0.45 [0.26, 0.65] to 0.14 [0.077, 0.25] with
568 6 ind./m²) (Fig. 3f). We also found density-dependent variation in flowering
569 probability and growth with rainfall and seedling size with temperature (Appendix S1:
570 Fig. S5). Additionally, the strength and direction of the association between survival
571 rates and both rainfall and temperature in natural populations were also size
572 dependent (Appendix S1: Fig. S6g,h).

573

574 Individual Based Model

575

576 *Population projections*

577

578 The projections of our individual-based model over the observed period
579 showed that our parameterization enabled us to correctly represent the population-
580 specific pattern of changes in mean annual change in aboveground population size
581 and of population abundance (Fig. 4; Appendix S1: Fig. S1). Additionally, observed

582 and projected time-varying size distributions were largely overlapping, with a slight
583 bias towards small individuals in some populations (Appendix S1: Fig. S2).

584 Discrepancies between projection and observed population dynamics
585 occurred both at observed abundance peaks and troughs, and this may in part be
586 explained by the fact that the GAMs parameterized to predict vital rates were
587 smoothed to avoid overfitting to extreme data values. This then constrained
588 estimates of population dynamics (Paniw et al. 2021), but, at the same time, did not
589 extrapolate the latter beyond biologically realistic values. In addition, discrepancies
590 between projection and observed population dynamics may also occur because our
591 models did not consider (due to a lack of data) other processes that may affect vital
592 rates and thus population dynamics, such as density dependent germination of
593 seeds from the seedbank or interspecific interactions (Brewer et al. 2021).

594

595

596

597

598

599

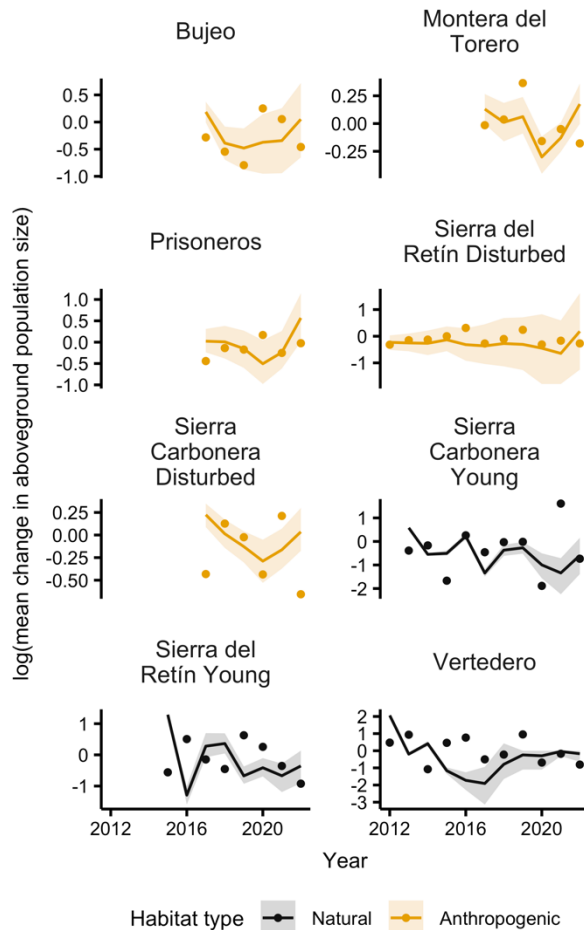
600

601

602

603

604



619 **Figure 4 – Observed and projected average change in aboveground**
620 **population abundance.** We projected each natural and anthropogenic population
621 for 500 times across the range of observed years available for each population
622 (maximum range from 2011 to 2022) to perform an out-of-sample validation of our
623 individual-based model parameterization. For each projection, we calculated the log
624 of the average change in aboveground population abundance between years (i.e.,
625 $\log(N_t/N_{t-1})$ with N_t the aboveground population size in year t) and obtained the
626 average (line) and 25th and 95th percentile of the population-specific distribution
627 (shaded ribbon). We compared these projected values to the observed ones (dots).
628

629 Projecting natural and anthropogenic populations under a control scenario (i.e.,
630 assuming similar environmental conditions in the future as currently observed)
631 showed that the average population growth rates ($\log \lambda_s$) did not vary much between
632 habitat types (mean = -0.15, 2.5 and 97.5% quantiles = [-0.62, 0.33] in natural and -
633 0.19 [-0.89, 0.63] in anthropogenic populations; Fig. 5). On the other hand, the
634 probability of quasi-extinction (p_{q-ext}) was on average higher in anthropogenic (0.56
635 [0.026, 1.0]) than in natural populations (0.17 [0.062, 0.26]). Extinction probabilities
636 also varied much more among anthropogenic than among natural populations in the
637 control scenario (Fig. 5). In natural populations, the stochastic fire regime in our
638 projections increased the population growth rate substantially after fires, avoiding the
639 quasi-extinction threshold (i.e., 5 aboveground individuals and 50 seeds in the
640 seedbank) in simulations where fires occurred regardless of the population (Conquet
641 et al., 2023). Anthropogenic populations, on the other hand, varied substantially in
642 size, and the high variation in p_{q-ext} reflects the consistently higher variation in
643 dynamics among populations (Appendix S1: Fig. S7).

644
645
646
647
648
649
650
651
652
653
654
655
656
657
658
659
660
661
662
663
664
665
666
667

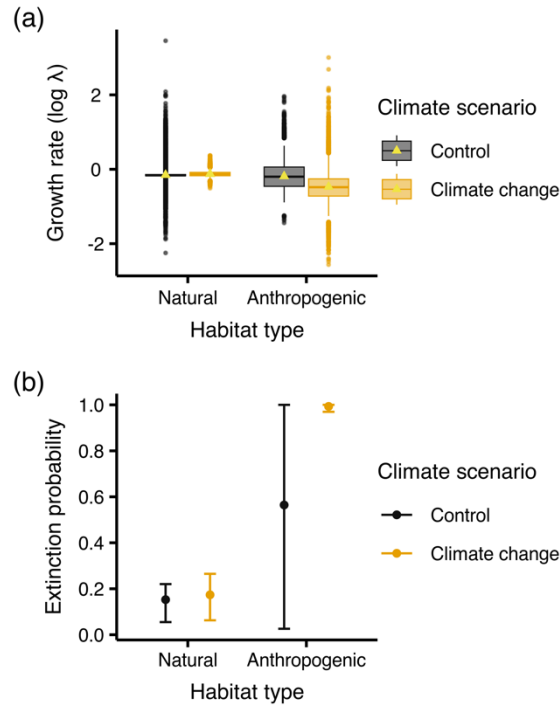


Figure 5 – Demographic consequences of climate change in natural and anthropogenic populations of dewy pines. We projected each natural and anthropogenic population 500 times for 30 years under a control (keeping temperature and rainfall conditions as currently observed) and two climate-change scenarios (RCP4.5 and RCP8.5). Here, results from scenario RCP8.5 are shown. To assess the demographic consequences of climate change in populations experiencing different levels of human disturbance, we computed for each population: (a) the stochastic population growth rate across 30 years for each population projection ($\log \lambda_s$; including both the seedbank and aboveground individuals) and (b) the probability of quasi-extinction (p_{q-ext}). Here we summarise these metrics per habitat type, and the variability in the values therefore correspond to among-population and among-projection differences.

668 In contrast with the control scenario, population growth rates differed between
669 habitats under climate change (Fig. 5). While the population growth rate (-0.12 [-
670 0.28, 0.072]) and extinction probability (0.17 [0.070, 0.26]) of natural populations did
671 not vary under climate change, under climate change scenario RCP8.5, our
672 projections show a decrease in $\log \lambda_S$ in anthropogenic sites (-0.47 [-1.3, 0.45]),
673 accompanied by an increase in the extinction probability (0.99 [0.97, 1.0]) (Fig. 5).
674 Results were very similar for scenario RCP4.5 (Appendix S2: Fig. S3), highlighting
675 that anthropogenic populations are at a high risk of local extinction even under
676 moderate climate change. In anthropogenic habitats, changes in population
677 dynamics under climate change were largely driven by the adverse effects of climate
678 change on plant survival (Appendix S4: Figs. S1-S2). In natural habitats, climate
679 change effects on survival and growth increased $\log \lambda_S$ in some populations, likely
680 through compensatory density feedbacks, and only climate change effects on
681 reproduction resulted in consistent decreases in $\log \lambda_S$ compared to the control
682 scenario (Appendix S4: Figs. S1-S2).

683

684 **Discussion**

685

686 Our individual-based models projecting natural and anthropogenic populations
687 of dewy pines using habitat-specific survival, growth, and reproductive rates revealed
688 that the current decline of anthropogenic populations will worsen under climate
689 change, leading to increased extinction risk. While the increasing frequency of
690 extreme high summer temperatures affected both natural and anthropogenic
691 populations negatively, occasionally high rainfall and compensatory density
692 dependence greatly reduced this effect in natural populations. Under chronic,

693 anthropogenic disturbance, however, the decline in survival was not compensated by
694 either of these factors. Consequently, with the frequency of extreme climatic
695 conditions increasing under climate change, populations in anthropogenic habitats—
696 which are currently already decreasing—were negatively affected by future climatic
697 conditions. Habitat dynamics shaped by fires also dominated the effects of
698 environmental perturbations in natural habitats, highlighting the importance of fire
699 regimes in Mediterranean heathlands (Ojeda, Pausas, and Verdú, 2010; Keeley et
700 al., 2011). Adaptations to anthropogenic disturbances meanwhile can lead to
701 changes in vital-rate responses to climate and density, with detrimental
702 consequences on population persistence. The implications of our findings extend
703 beyond ecological theory, offering tangible guidance for conservation policies. Under
704 contrasting responses of natural and anthropogenic populations to climate change,
705 management would need to be adapted to allow periodic vegetation clearance (most
706 importantly through burning) in heathlands which would provoke mass germination
707 from the seed bank of dewy pines and other seeder species, increasing local
708 biodiversity (Fernandes et al., 2013; Ojeda, 2020). In anthropogenic habitats, on the
709 other hand, further disturbances should be prevented (Lawson et al. 2010). As our
710 results highlight climate changes drives population dynamics through adverse effects
711 on survival in anthropogenic habitats, management should focus on improving the
712 survival of large plants, for instance by allowing for moderate shrub cover that
713 shields dewy pines from climatic extremes (Brewer et al. 2021).

714

715 Land-use change (e.g. grazing) often has stronger effects on populations than
716 climate change (Sirami et al., 2017). However, few studies assess how interactions
717 between these two environmental pressures affect different vital rates and how such

718 effects then scale to population dynamics, despite evidence of land-use change
719 mediating the effect of climate change on species abundance and diversity
720 (Mantyka-Pringle, Martin, and Rhodes, 2012; Oliver and Morecroft, 2014). Such
721 interactions are likely to be strong drivers of vital-rate responses in habitats such as
722 Mediterranean heathlands, which are among the ecosystems most affected by
723 climate and land-use change (Newbold et al., 2020), the latter leading to changes in
724 disturbance regimes in the habitats. Consequently, interactions between these two
725 pressures might have strong effects on systems such as the dewy pine, where we
726 observe differences among disturbance levels in vital-rate responses to climate,
727 density, and their interactions among natural and highly disturbed habitats.

728

729 Our projections of natural and anthropogenic dewy-pine populations under climate
730 change indicate that future changes in climate will spare populations in natural
731 habitats but will have adverse effects on populations experiencing anthropogenic
732 disturbances, which is the majority of dewy pine populations (Garrido et al., 2003),
733 as well as many other Mediterranean shrublands (Newbold et al., 2020). We also
734 note that we capped the effects of projected climate extremes to the maximum past
735 observed values in order to not project population dynamics outside the observed
736 range of responses to climate (Fronzek et al., 2010). However, climate-change
737 projections show increases in extreme temperature values that are clearly outside
738 the range of past observed values (Fig. S1), indicating that our projections are likely
739 conservative and local extinction risks for this endangered species may be further
740 exacerbated.

741

742 As previously observed in our study populations, anthropogenic disturbances not
743 only lead to increased continuous seed germination and decreased seed dormancy
744 (Appendix S1), but also allowed aboveground individuals to survive longer in the
745 absence of shrub encroachment (Paniw, Quintana-Ascencio et al., 2017).
746 Consequently, dewy pines in chronically disturbed, anthropogenic habitats reached
747 higher sizes than those in natural habitats. This is contrary to many studies
748 assessing trait-level consequences of land-use change—and more specifically
749 grazing—on plants. In these studies, plants in grazed sites adapted to this
750 disturbance by shrinking over time to avoid being consumed by herbivores (Fischer
751 et al., 2011; Kerns et al., 2011; Völler et al., 2017). However, with their mucilage-
752 covered leaves, dewy pines are not palatable to herbivores (Ojeda et al., 2021), and
753 therefore do not require such an adaptation. On the contrary, the small amount or
754 absence of damage dealt to plants by herbivores along with the removal of other
755 plants and the subsequent release of both intra- and interspecific competition, might
756 allow dewy pines in anthropogenic populations to grow without surrounding
757 vegetation hampering their nutrient acquisition (Paniw et al., 2018) and growth
758 (Grime, 1973; Hjalten et al., 1993; Kambatuku et al., 2011; Fig. 3c).

759

760 While anthropogenic disturbances allow dewy pine plants to survive and grow better
761 than in natural conditions, this comes at the cost of reproduction, with flowering
762 probability decreasing in the largest individuals. Although the consequences of land-
763 use change on plant reproduction are clearly species- and site-dependent (Kerns et
764 al., 2011; Völler et al., 2017), tradeoffs similar to those observed in our populations
765 are common across taxa (Stearns, 1989). Such negative correlations between vital
766 rates might be more striking under stressful conditions such as low resource

767 availability (Villemas & García, 2018). This might be the case in anthropogenic
768 populations of dewy pines particularly. Plants rely almost exclusively on capturing
769 prey invertebrates for nutrient uptake (Paniw, Gil-Cabeza et al., 2017; Skates et al.,
770 2019). In natural populations, invertebrates, especially insect pollinators, are
771 abundant after fires, when many post-fire ephemeral species flower, and dewy pine
772 plants are more conspicuous to insects, thus facilitating prey capture and nutrient
773 uptake (Paniw et al., 2018). In anthropogenic habitats, intense browsing or
774 mechanical vegetation removal are likely to decrease invertebrate abundances with
775 respect to natural sites (Mayer, 2004; Carpio et al., 2014). When shrub cover is
776 chronically low or sparse, dewy pine plants are more conspicuous to prey insects but
777 they may also be more exposed to wind and solar radiation, thus resulting in
778 relatively more stressful environmental conditions (Paniw et al., 2018). In turn, while
779 populations in these chronically disturbed, anthropogenic habitats appear to persist,
780 a low reproductive output may generate an extinction debt, where the population
781 structure is skewed towards old individuals that cannot be replaced in the long term
782 (Matías et al., 2019).

783

784 Adverse disturbance effects on vital rates can be exacerbated under unfavourable
785 climatic conditions (e.g. Hindle et al., 2023; see also; Nolan et al., 2021 and
786 references therein). Plants commonly suffer from extreme temperatures and drought,
787 which affect individuals through processes such as heat stress, photosynthesis
788 inhibition, or reduced soil moisture and water resources (e.g. Larcher, 2000;
789 McDowell et al., 2008; Nolan et al., 2021). While dewy pines are somewhat adapted
790 to dry and hot summer conditions (Darwin 1875; Adlassnig et al., 2006; Adamec,
791 2009), survival greatly decreased with increasing summer temperatures. In addition

792 to the aforementioned processes reducing the survival of plants experiencing high
793 temperatures, such extreme conditions could lead to a great reduction in prey
794 availability. These carnivorous subshrubs indeed rely on droplets of mucilage on
795 their leaves to capture insects, from which they obtain nutrients (Paniw, Gil-Cabeza
796 et al., 2017). However, increasing temperatures and the subsequent decrease in
797 humidity could prevent plants from forming these droplets, and thereby from
798 accessing these resources.

799

800 Rainfall also played an important role in shaping dewy-pine demography. In addition
801 to limiting water resources (McDowell et al., 2008), extremely low amounts of rain do
802 not provide enough moisture for dewy pines to produce mucilage on their leaf-traps
803 (Darwin 1875; Adlassnig et al., 2006; Adamec, 2009). As a result, plants might not
804 get enough nutrients to allocate to the different demographic processes. However, in
805 natural populations, high amounts of rainfall seemed to slightly buffer negative
806 temperature effects, likely by compensating the low humidity and water resources
807 under high temperatures. This process did not seem to occur in anthropogenic
808 populations, where the increased exposure to extreme temperatures due to sparse
809 vegetation cover might be too intense to counterbalance.

810

811 In addition to interactions between climatic variables, density-dependent effects of
812 climate are common across taxa and can play a key role in shaping population
813 dynamics, for example by enhancing or mitigating adverse environmental effects
814 (Gamelon et al., 2017; Paniw et al., 2019). In plant populations, vital-rate density
815 dependence can be attributed to two main biological processes: competition (e.g. for
816 light or pollinators; Craine & Dybzinski, 2013) and facilitation (i.e., the positive effect

817 of neighbours on a focal individual, e.g., through shading or protection from
818 herbivory; Callaway & Pugnaire, 2007; Graff et al., 2007; Le Bagousse-Pinguet et al.,
819 2012). According to the stress-gradient hypothesis, variations in environmental
820 conditions can lead to shifts between these two processes in a given population
821 (Bertness & Callaway, 1994; Maestre et al., 2005), for example under increased
822 levels of disturbance (Graff et al., 2007; Villarreal-Barajas & Martorell, 2009; Le
823 Bagousse-Pinguet et al., 2012) or extreme climatic conditions (Callaway & Pugnaire,
824 2007; Grant et al., 2014; Olsen et al., 2016). This was the case in dewy pines, where
825 intraspecific density had opposite effects on some vital rates between natural—
826 where competition prevailed—and anthropogenic populations—where facilitation
827 was at play.

828

829 As commonly observed in plant communities (Villalobos et al., 2016; Adler et al.,
830 2018), increasing intraspecific densities in natural conditions led to declining
831 survival—with the exception of early post-fire conditions, where facilitation generally
832 predominates in fire-adapted plant communities (Vilà & Sardans, 1999; Paniw et al.,
833 2018). For dewy pines, in addition to the more common resources for which plants
834 compete (e.g. light or pollinators), such negative effects of conspecifics on survival
835 could arise from competition for prey (Craine & Dybzinski, 2013). Contrastingly,
836 individuals in anthropogenic populations benefited from higher intraspecific densities.
837 In addition to the competition release stemming from the removal of surrounding
838 vegetation (Catling et al., 2024), increasing levels of disturbance such as browsing
839 might lead to a shift from competition to facilitation, as neighbours might act as a
840 barrier against browsers (Le Bagousse-Pinguet et al., 2012).

841

842 In addition to the consequences on vital rates, future increases in temperatures and
843 decreases in rainfall under climate change are expected to lead to higher frequency
844 and intensity of wildfires (Turco et al., 2019; Nolan et al., 2021). In populations where
845 land-use change led to seedbank depletions through increase in continuous
846 germination and dormancy loss, returning fire regimes will likely have strong
847 negative consequences on population persistence, as reduced soil seedbanks will
848 not be enough to replenish populations following the removal of aboveground
849 individuals by fire. Decrease in the ability of fire-adapted plants to germinate or
850 resprout after more frequent and intense fire could have dramatic consequences for
851 the persistence of plant communities in fire-prone habitats (Enright et al., 2015;
852 Nolan et al., 2021).

853

854 Overall, our findings highlight the existence of demographic responses to climate
855 and land-use change and call for conservation policies taking into account the
856 detrimental effects of climate change on populations persisting under human
857 alterations to their habitats, more specifically in fire-adapted systems. Moreover,
858 species-specific effects of interactions between climate and land-use change
859 highlight the need for studies assessing these effects at the community level—
860 accounting for the effects of both climate and intra- and inter-specific density—to
861 understand how interactions between these pressures might affect fire-prone and
862 more generally anthropogenic landscapes.

863 **References**

864

865 Adamec, L. (2009). Ecophysiological Investigation on *Drosophyllum Lusitanicum*:

866 Why Doesn't the Plant Dry Out? *Carnivorous Plant Newsletter*, **38**(3), 71–74.

867 <https://doi.org/10.55360/cpn383.la180>

868 Adlassnig, W., Peroutka, M., Eder, G., Pois, W., & Lichtscheidl, I. K. (2006).

869 Ecophysiological Observations on *Drosophyllum Lusitanicum*. *Ecological*

870 *Research*, **21**(2), 255–62. <https://doi.org/10.1007/s11284-005-0116-z>

871 Adler, P. B., Ellner, S. P., & Levine, J. M. (2010). Coexistence of Perennial Plants:

872 An Embarrassment of Niches. *Ecology Letters*, **13**(8), 1019–29.

873 <https://doi.org/10.1111/j.1461-0248.2010.01496.x>

874 Adler, P. B., Smull, D., Beard, K. H., Choi, R. T., Furniss, T., Kulmatiski, A., Meiners,

875 J. M., Tredennick, A. T., & Veblen, K. E. (2018). Competition and Coexistence

876 in Plant Communities: Intraspecific Competition Is Stronger than Interspecific

877 Competition. *Ecology Letters*, **21**(9), 1319–29.

878 <https://doi.org/10.1111/ele.13098>

879 Alberti, M. (2015). Eco-Evolutionary Dynamics in an Urbanizing Planet. *Trends in*

880 *Ecology & Evolution*, **30**(2), 114–26. <https://doi.org/10.1016/j.tree.2014.11.007>

881 Bertness, M. D., & Callaway, R. (1994). Positive Interactions in Communities. *Trends*

882 *in Ecology & Evolution*, **9**(5), 191–93. <https://doi.org/10.1016/0169->

883 [5347\(94\)90088-4](https://doi.org/10.1016/0169-5347(94)90088-4)

884 Bijlsma, R., & Loeschcke, V. (2012). Genetic Erosion Impedes Adaptive Responses

885 to Stressful Environments. *Evolutionary Applications*, **5**(2), 117–29.

886 <https://doi.org/10.1111/j.1752-4571.2011.00214.x>

887 Brewer, J. S., Paniw, M., & Ojeda, F. (2021). Plant Behavior and Coexistence: Stem

888 Elongation of the Carnivorous Subshrub *Drosophyllum Lusitanicum* within
889 Xerophytic Shrub Canopies. *Plant Ecology*, **222**(11), 1197–1208.
890 <https://doi.org/10.1007/s11258-021-01170-0>

891 Brook, B. W., Sodhi, N. S., & Bradshaw, C. J. A. (2008). Synergies among Extinction
892 Drivers under Global Change. *Trends in Ecology & Evolution*, **23**(8), 453–60.
893 <https://doi.org/10.1016/j.tree.2008.03.011>

894 Burnham, K. P., Anderson, D. R., & Huyvaert, K. P. (2011). AIC Model Selection and
895 Multimodel Inference in Behavioral Ecology: Some Background,
896 Observations, and Comparisons. *Behavioral Ecology and Sociobiology*, **65**(1),
897 23–35. <https://doi.org/10.1007/s00265-010-1029-6>

898 Callaway, R. M., & Pugnaire, F. I. (2007). Facilitation in Plant Communities. In F. I.
899 Pugnaire, & F. Valladares (Eds.), *Functional Plant Ecology* (2nd ed., pp. 435–
900 55). CRC Press.

901 Carpio, A. J., Castro–López, J., Guerrero–Casado, J., Ruiz–Aizpurua, L., Vicente, J.,
902 & Tortosa, F. S. (2014). Effect of Wild Ungulate Density on Invertebrates in a
903 Mediterranean Ecosystem. *Animal Biodiversity and Conservation*, **37**(2), 115–
904 25. <https://doi.org/10.32800/abc.2014.37.0115>

905 Catling, A. A., Mayfield, M. M., & Dwyer, J. M. (2024). Individual Vital Rates Respond
906 Differently to Local-Scale Environmental Variation and Neighbour Removal.
907 *Journal of Ecology*, **112**(6), 1369–82. [https://doi.org/10.1111/1365-
908 2745.14308](https://doi.org/10.1111/1365-2745.14308)

909 Chevin, L.-M., Lande, R., & Mace, G. M. (2010). Adaptation, Plasticity, and
910 Extinction in a Changing Environment: Towards a Predictive Theory. *PLOS*
911 *Biology*, **8**(4), e1000357. <https://doi.org/10.1371/journal.pbio.1000357>

912 Clark, N. E., Boakes, E. H., McGowan, P. J. K., Mace, G. M., & Fuller, R. A. (2013).

913 Protected Areas in South Asia Have Not Prevented Habitat Loss: A Study
914 Using Historical Models of Land-Use Change. *PLOS ONE*, **8**(5), e65298.
915 <https://doi.org/10.1371/journal.pone.0065298>

916 Conquet, E., Ozgul, A., Blumstein, D. T., Armitage, K. B., Oli, M. K., Martin, J. G. A.,
917 Clutton-Brock, T. H., & Paniw, M. (2023). Demographic Consequences of
918 Changes in Environmental Periodicity. *Ecology*, **104**(3), e3894.
919 <https://doi.org/10.1002/ecy.3894>

920 Cornes, R. C., van der Schrier, G., van den Besselaar, E. J. M., & Jones, P. D.
921 (2018). An Ensemble Version of the E-OBS Temperature and Precipitation
922 Data Sets. *Journal of Geophysical Research: Atmospheres*, **123**(17), 9391–
923 409. <https://doi.org/10.1029/2017JD028200>

924 Correia, E., & Freitas, H. (2002). *Drosophyllum Lusitanicum*, an Endangered West
925 Mediterranean Endemic Carnivorous Plant: Threats and Its Ability to Control
926 Available Resources. *Botanical Journal of the Linnean Society*, **140**(4), 383–
927 90. <https://doi.org/10.1046/j.1095-8339.2002.00108.x>

928 Craine, J. M., & Dybzinski, R. (2013). Mechanisms of Plant Competition for
929 Nutrients, Water and Light. *Functional Ecology*, **27**(4), 833–40.
930 <https://doi.org/10.1111/1365-2435.12081>

931 Cross, A. T., Paniw, M., Ojeda, F., Turner, S. R., Dixon, K. W., & Merritt, D. J.
932 (2017). Defining the Role of Fire in Alleviating Seed Dormancy in a Rare
933 Mediterranean Endemic Subshrub. *AoB PLANTS*, **9**(5), plx036.
934 <https://doi.org/10.1093/aobpla/plx036>

935 Darwin, C. (1875). *Insectivorous Plants*. John Murray, London.
936 <https://doi.org/10.1017/CBO9780511694127>

937 Díaz, S., Settele, J., Brondízio, E. S., Ngo, H. T., Agard, J., Arneeth, A., Balvanera, P.,

938 Brauman, K. A., Butchart, S. H. M., Chan, K. M. A., Garibaldi, L. A., Ichii, K.,
939 Liu, J., Subramanian, S. M., Midgley, G. F., Miloslavich, P., Molnár, Z., Obura,
940 D., Pfaff, A., ... Polasky, S. (2019). Pervasive Human-Driven Decline of Life
941 on Earth Points to the Need for Transformative Change. *Science*, **366**(6471),
942 eaax3100. <https://doi.org/10.1126/science.aax3100>

943 Enright, N. J., Fontaine, J. B., Bowman, D. M. J. S., Bradstock, R. A., & Williams, R. J.
944 (2015). Interval Squeeze: Altered Fire Regimes and Demographic Responses
945 Interact to Threaten Woody Species Persistence as Climate Changes.
946 *Frontiers in Ecology and the Environment*, **13**(5), 265–72.
947 <https://doi.org/10.1890/140231>

948 Evers, S. M., Knight, T. M., Inouye, D. W., Miller, T. E. X., Salguero-Gómez, R., Iler,
949 A. M., & Compagnoni, A. (2021). Lagged and Dormant Season Climate Better
950 Predict Plant Vital Rates Than Climate During the Growing Season. *Global*
951 *Change Biology*, **27**(9), 1927–1941. <https://doi.org/10.1111/gcb.15519>

952 Eyring, V., Bony, S., Meehl, G. A., Senior, C. A., Stevens, B., Stouffer, R. J., &
953 Taylor, K. E. (2016). Overview of the Coupled Model Intercomparison Project
954 Phase 6 (CMIP6) Experimental Design and Organization. *Geoscientific Model*
955 *Development*, **9**(5), 1937–58. <https://doi.org/10.5194/gmd-9-1937-2016>

956 Fagan, W. F., & Holmes, E. E. (2006). Quantifying the Extinction Vortex. *Ecology*
957 *Letters*, **9**(1), 51–60. <https://doi.org/10.1111/j.1461-0248.2005.00845.x>

958 Fernandes, P. M., Davies, G. M., Ascoli, D., Fernandez, C., Moreira, F., Rigolot, E.,
959 Stoof, C. R., Vega, J.A., & Molina, D. (2013). Prescribed Burning in Southern
960 Europe: Developing Fire Management in a Dynamic Landscape. *Frontiers in*
961 *Ecology and the Environment*, **11**(s1), e4–e14. <https://doi.org/10.1890/120298>

962 Fischer, M., Weyand, A., Rudmann-Maurer, K., & Stöcklin, J. (2011). Adaptation of

963 Poa Alpina to Altitude and Land Use in the Swiss Alps. *Alpine Botany*, **121**(2),
964 91–105. <https://doi.org/10.1007/s00035-011-0096-2>

965 Foley, J. A., DeFries, R., Asner, G. P., Barford, C., Bonan, G., Carpenter, S. R.,
966 Chapin, F. S., Coe, M. T., Daily, G. C., Gibbs, H. K., Helkowski, J. H.,
967 Holloway, T., Howard, E. A., Kucharik, C. J., Monfreda, C., Patz, J. A.,
968 Prentice, I. C., Ramankutty, N., & Snyder, P. K. (2005). Global Consequences
969 of Land Use. *Science*, **309**(5734), 570–74.
970 <https://doi.org/10.1126/science.1111772>

971 Fronzek, S., Carter, T. R., Räisänen, J., Ruokolainen, L., & Luoto, M. (2010).
972 Applying Probabilistic Projections of Climate Change With Impact Models: A
973 Case Study for sub-Arctic Palsa Mires in Fennoscandia. *Climate Change*, **99**,
974 515–534. <https://doi.org/10.1007/s10584-009-9679-y>

975 Gamelon, M., Grøtan, V., Nilsson, A. L. K., Engen, S., Hurrell, J. W., Jerstad, K.,
976 Phillips, A. S., Røstad, O. W., Slagsvold, T., Walseng, B., Stenseth, N. C.,
977 Sæther, B.-E. (2017). Interactions between Demography and Environmental
978 Effects Are Important Determinants of Population Dynamics. *Science*
979 *Advances*, **3**(2), e1602298. <https://doi.org/10.1126/sciadv.1602298>

980 Garnier, E., Lavorel, S., Ansquer, P., Castro, H., Cruz, P., Dolezal, J., Eriksson, O.,
981 Fortunel, C., Freitas, H., Golodets, C., Grigulis, K., Jouany, C., Kazakou, E.,
982 Kigel, J., Kleyer, M., Lehsten, V., Lepš, J., Meier, T., Pakeman, R., ... Zarovali,
983 M. P. (2007). Assessing the Effects of Land-Use Change on Plant Traits,
984 Communities and Ecosystem Functioning in Grasslands: A Standardized
985 Methodology and Lessons from an Application to 11 European Sites. *Annals*
986 *of Botany*, **99**(5), 967–85. <https://doi.org/10.1093/aob/mcl215>

987 García-Callejas, D., Molowny-Horas, R., & Retana, J. (2017). Projecting the

988 Distribution and Abundance of Mediterranean Tree Species Under Climate
989 Change: A Demographic Approach. *Journal of Plant Ecology*, **10**(5), 731–743.
990 <https://doi.org/10.1093/jpe/rtw081>

991 Garrido, B., Hampe, A., Marañón, T., & Arroyo, J. (2003). Regional Differences in
992 Land Use Affect Population Performance of the Threatened Insectivorous
993 Plant *Drosophyllum Lusitanicum* (Droseraceae). *Diversity and Distributions*,
994 **9**(5), 335–50. <https://doi.org/10.1046/j.1472-4642.2003.00029.x>

995 Geldmann, J., Barnes, M., Coad, L., Craigie, I. D., Hockings, M., & Burgess, N. D.
996 (2013). Effectiveness of Terrestrial Protected Areas in Reducing Habitat Loss
997 and Population Declines. *Biological Conservation*, **161**(May), 230–38.
998 <https://doi.org/10.1016/j.biocon.2013.02.018>

999 Gómez-González, S., Paniw, M., Antunes, K., & Ojeda, F. (2018). Heat Shock and
1000 Plant Leachates Regulate Seed Germination of the Endangered Carnivorous
1001 Plant *Drosophyllum Lusitanicum*. *Web Ecology*, **18**(1), 7–13.
1002 <https://doi.org/10.5194/we-18-7-2018>

1003 Graff, P., Aguiar, M. R., & Chaneton, E. J. (2007). Shifts in Positive and Negative
1004 Plant Interactions Along a Grazing Intensity Gradient. *Ecology*, **88**(1), 188–99.
1005 [https://doi.org/10.1890/0012-9658\(2007\)88\[188:SIPANP\]2.0.CO;2](https://doi.org/10.1890/0012-9658(2007)88[188:SIPANP]2.0.CO;2)

1006 Grant, K., Kreyling, J., Heilmeyer, H., Beierkuhnlein, C., & Jentsch, A. (2014).
1007 Extreme Weather Events and Plant–Plant Interactions: Shifts between
1008 Competition and Facilitation among Grassland Species in the Face of Drought
1009 and Heavy Rainfall. *Ecological Research*, **29**(5), 991–1001.
1010 <https://doi.org/10.1007/s11284-014-1187-5>

1011 Gray, C. L., Hill, S. L. L., Newbold, T., Hudson, L. N., Börger, L., Contu, S., Hoskins,
1012 A. J., Ferrier, S., Purvis, A., & Scharlemann, J. P. W. (2016). Local

1013 Biodiversity Is Higher inside than Outside Terrestrial Protected Areas
1014 Worldwide. *Nature Communications*, **7**(1), 12306.
1015 <https://doi.org/10.1038/ncomms12306>

1016 Grime, J. P. (1973). Competitive Exclusion in Herbaceous Vegetation. *Nature*,
1017 **242**(5396), 344–47. <https://doi.org/10.1038/242344a0>

1018 Grimm, V., Berger, U., Bastiansen, F., Eliassen, S., Ginot, V., Giske, J., Goss-
1019 Custard, J., Grand, T., Heinz, S. K., Huse, G., Huth, A., Jepsen, J. U.,
1020 Jørgensen, C., Mooij, W. M., Müller, B., Pe'er, G., Piou, C., Railsback, S. F.,
1021 Robbins, A. M., ... DeAngelis, D. L. (2006). A Standard Protocol for
1022 Describing Individual-Based and Agent-Based Models. *Ecological Modelling*,
1023 **198**(1), 115–26. <https://doi.org/10.1016/j.ecolmodel.2006.04.023>

1024 Grimm, V., Railsback, S. F., Vincenot, C. E., Berger, U., Gallagher, C., DeAngelis, D.
1025 L., Edmonds, B., Ge, J., Giske, J., Groeneveld, J., Johnston, A. S. A., Milles,
1026 A., Nabe-Nielsen, J., Polhill, J. G., Radchuk, V., Rohwäder, M.-S., Stillman, R.
1027 A., Thiele, J. C., & Ayllón, D. (2020). The ODD Protocol for Describing Agent-
1028 Based and Other Simulation Models: A Second Update to Improve Clarity,
1029 Replication, and Structural Realism. *Journal of Artificial Societies and Social*
1030 *Simulation*, **23**(2), 7. <https://doi.org/10.18564/jasss.4259>

1031 Hindle, B. J., Quintana-Ascencio, P. F., Menges, E. S., & Childs, D. Z. (2023). The
1032 Implications of Seasonal Climatic Effects for Managing Disturbance
1033 Dependent Populations under a Changing Climate. *Journal of Ecology*,
1034 **111**(8), 1749–61. <https://doi.org/10.1111/1365-2745.14143>

1035 Hjalten, J., Danell, K., & Ericson, L. (1993). Effects of Simulated Herbivory and
1036 Intraspecific Competition on the Compensatory Ability of Birches. *Ecology*,
1037 **74**(4), 1136–42. <https://doi.org/10.2307/1940483>

1038 IPBES. (2019). Global Assessment Report on Biodiversity and Ecosystem Services
1039 of the Intergovernmental Science-Policy Platform on Biodiversity and
1040 Ecosystem Services. E. S. Brondizio, J. Settele, S. Díaz, & H. T. Ngo (Eds.).
1041 IPBES secretariat, Bonn, Germany. <https://doi.org/10.5281/zenodo.6417333>

1042 Kambatuku, J. R., Cramer, M. D., & Ward, D. (2011). Intraspecific Competition
1043 between Shrubs in a Semi-Arid Savanna. *Plant Ecology*, **212**(4), 701–13.
1044 <https://doi.org/10.1007/s11258-010-9856-0>

1045 Kampichler, C., van Turnhout, C. A. M., Devictor, V., & van der Jeugd, H. P. (2012).
1046 Large-Scale Changes in Community Composition: Determining Land Use and
1047 Climate Change Signals. *PLOS ONE*, **7**(4), e35272.
1048 <https://doi.org/10.1371/journal.pone.0035272>

1049 Keeley, J. E., Bond, W. J., Bradstock, R. A., Pausas, J. G., & Rundel, P. W. (2012).
1050 *Fire in Mediterranean Ecosystems: Ecology, Evolution and Management*.
1051 Cambridge University Press.

1052 Kerns, B. K., Buonopane, M., Thies, W. G., & Niwa, C. (2011). Reintroducing Fire
1053 into a Ponderosa Pine Forest with and without Cattle Grazing: Understory
1054 Vegetation Response. *Ecosphere*, **2**(5), art59. [https://doi.org/10.1890/ES10-](https://doi.org/10.1890/ES10-00183.1)
1055 [00183.1](https://doi.org/10.1890/ES10-00183.1)

1056 Larcher, W. (2000). Temperature Stress and Survival Ability of Mediterranean
1057 Sclerophyllous Plants. *Plant Biosystems - An International Journal Dealing*
1058 *with All Aspects of Plant Biology*, **134**(3), 279–95.
1059 <https://doi.org/10.1080/11263500012331350455>

1060 Lawson, D. M., Regan, H. M., Zedler, P. H., & Franklin, J. (2010). Cumulative Effects
1061 of Land Use, Altered Fire Regime and Climate Change on Persistence of
1062 *Ceanothus Verrucosus*, a Rare, Fire-Dependent Plant Species. *Global*

1063 *Change Biology*, **16**(9), 2518–29. <https://doi.org/10.1111/j.1365->
1064 [2486.2009.02143.x](https://doi.org/10.1111/j.1365-2486.2009.02143.x)

1065 Le Bagousse-Pinguet, Y., Gross, E. M., & Straile, D. (2012). Release from
1066 Competition and Protection Determine the Outcome of Plant Interactions
1067 along a Grazing Gradient. *Oikos*, **121**(1), 95–101.
1068 <https://doi.org/10.1111/j.1600-0706.2011.19778.x>

1069 Leimu, R., Vergeer, P., Angeloni, F., & Ouborg, N. J. (2010). Habitat Fragmentation,
1070 Climate Change, and Inbreeding in Plants. *Annals of the New York Academy*
1071 *of Sciences*, **1195**(1), 84–98. <https://doi.org/10.1111/j.1749->
1072 [6632.2010.05450.x](https://doi.org/10.1111/j.1749-6632.2010.05450.x)

1073 Maestre, F. T., Valladares, F., & Reynolds, J. F. (2005). Is the Change of Plant–Plant
1074 Interactions with Abiotic Stress Predictable? A Meta-Analysis of Field Results
1075 in Arid Environments. *Journal of Ecology*, **93**(4), 748–57.
1076 <https://doi.org/10.1111/j.1365-2745.2005.01017.x>

1077 Mantyka-Pringle, C. S., Martin, T. G., & Rhodes, J. R. (2012). Interactions between
1078 Climate and Habitat Loss Effects on Biodiversity: A Systematic Review and
1079 Meta-Analysis. *Global Change Biology*, **18**(4), 1239–52.
1080 <https://doi.org/10.1111/j.1365-2486.2011.02593.x>

1081 Matías, L., Abdelaziz, M., Godoy, O., & Gómez-Aparicio, L. (2019). Disentangling the
1082 Climatic and Biotic Factors Driving Changes in the Dynamics of *Quercus*
1083 Suber Populations across the Species' Latitudinal Range. *Diversity and*
1084 *Distributions*, **25**(4), 524–35. <https://doi.org/10.1111/ddi.12873>

1085 Mayer, C. (2004). Pollination Services under Different Grazing Intensities.
1086 *International Journal of Tropical Insect Science*, **24**(1), 95–103.
1087 <https://doi.org/10.1079/IJT20047>

1088 McDowell, N., Pockman, W. T., Allen, C. D., Breshears, D. D., Cobb, N., Kolb, T.,
1089 Plaut, J., Sperry, J., West, A., Williams, D. G., & Yepez, E. A. (2008).
1090 Mechanisms of Plant Survival and Mortality during Drought: Why Do Some
1091 Plants Survive While Others Succumb to Drought? *New Phytologist*, **178**(4),
1092 719–39. <https://doi.org/10.1111/j.1469-8137.2008.02436.x>

1093 Montràs-Janer, T., Suggitt, A. J., Fox, R., Jönsson, M., Martay, B., Roy, D. B.,
1094 Walker, K. J., & Auffret, A. G. (2024). Anthropogenic Climate and Land-Use
1095 Change Drive Short- and Long-Term Biodiversity Shifts across Taxa. *Nature*
1096 *Ecology & Evolution*, **8**(4), 739–51. [https://doi.org/10.1038/s41559-024-](https://doi.org/10.1038/s41559-024-02326-7)
1097 [02326-7](https://doi.org/10.1038/s41559-024-02326-7)

1098 Murali, G., de Oliveira Caetano, G. H., Barki, G., Meiri, S., & Roll, U. (2022).
1099 Emphasizing Declining Populations in the Living Planet Report. *Nature*,
1100 **601**(7894), E20–24. <https://doi.org/10.1038/s41586-021-04165-z>

1101 Newbold, T., Oppenheimer, P., Etard, A., & Williams, J. J. (2020). Tropical and
1102 Mediterranean Biodiversity Is Disproportionately Sensitive to Land-Use and
1103 Climate Change. *Nature Ecology & Evolution*, **4**(12), 1630–38.
1104 <https://doi.org/10.1038/s41559-020-01303-0>

1105 Nolan, R. H., Collins, L., Leigh, A., Ooi, M. K. J., Curran, T. J. Fairman, T. A., Resco
1106 de Dios, V., & Bradstock, R. (2021). Limits to Post-Fire Vegetation Recovery
1107 under Climate Change. *Plant, Cell & Environment*, **44**(11), 3471–89.
1108 <https://doi.org/10.1111/pce.14176>

1109 Ojeda, F., Carrera, C., Paniw, M., García-Moreno, L., Barbero, G. F., & Palma, M.
1110 (2021). Volatile and Semi-Volatile Organic Compounds May Help Reduce
1111 Pollinator-Prey Overlap in the Carnivorous Plant *Drosophyllum lusitanicum*
1112 (*Drosophyllaceae*). *Journal of Chemical Ecology*, **47**(1), 73–86.

1113 <https://doi.org/10.1007/s10886-020-01235-w>

1114 Ojeda, F., Pausas, J. G., & Verdú, M. (2010). Soil Shapes Community Structure
1115 through Fire. *Oecologia*, **163**(3), 729–35. [https://doi.org/10.1007/s00442-009-](https://doi.org/10.1007/s00442-009-1550-3)
1116 [1550-3](https://doi.org/10.1007/s00442-009-1550-3)

1117 Ojeda, F. (2020). Pine Afforestation, Herriza and Wildfire: A Tale of Soil Erosion and
1118 Biodiversity Loss in the Mediterranean Region. *International Journal of*
1119 *Wildland Fire*, **29**, 1142–1146. <https://doi.org/10.1071/WF20097>

1120 Oliver, T. H., & Morecroft, M. D. (2014). Interactions between Climate Change and
1121 Land Use Change on Biodiversity: Attribution Problems, Risks, and
1122 Opportunities. *WIREs Climate Change*, **5**(3), 317–35.
1123 <https://doi.org/10.1002/wcc.271>

1124 Olsen, S. L., Töpper, J. P., Skarpaas, O., Vandvik, V., & Klanderud, K. (2016). From
1125 Facilitation to Competition: Temperature-Driven Shift in Dominant Plant
1126 Interactions Affects Population Dynamics in Seminatural Grasslands. *Global*
1127 *Change Biology*, **22**(5), 1915–26. <https://doi.org/10.1111/gcb.13241>

1128 Paniw, M., Duncan, C., Groenewoud, F., Drewe, J. A., Manser, M., Ozgul, A., &
1129 Clutton-Brock, T. (2022). Higher Temperature Extremes Exacerbate Negative
1130 Disease Effects in a Social Mammal. *Nature Climate Change*, **12**(3), 284–90.
1131 <https://doi.org/10.1038/s41558-022-01284-x>

1132 Paniw, M., García-Callejas, D., Lloret, F., Bassar, R. D., Travis, J., & Godoy, O.
1133 (2023). Pathways to Global-Change Effects on Biodiversity: New
1134 Opportunities for Dynamically Forecasting Demography and Species
1135 Interactions. *Proceedings of the Royal Society B: Biological Sciences*,
1136 **290**(1993), 20221494. <https://doi.org/10.1098/rspb.2022.1494>

1137 Paniw, M., Gil-Cabeza, E., & Ojeda, F. (2017). Plant Carnivory beyond Bogs:

1138 Reliance on Prey Feeding in *Drosophyllum Lusitanicum* (Drosophyllaceae) in
1139 Dry Mediterranean Heathland Habitats. *Annals of Botany*, **119**(6), 1035–41.
1140 <https://doi.org/10.1093/aob/mcw247>

1141 Paniw, M., Maag, N., Cozzi, G., Clutton-Brock, T. H., & Ozgul, A. (2019). Life History
1142 Responses of Meerkats to Seasonal Changes in Extreme Environments.
1143 *Science*, **363**(6427), 631–35. <https://doi.org/10.1126/science.aau5905>

1144 Paniw, M., Quintana-Ascencio, P. F., Ojeda, F., & Salguero-Gómez, R. (2017).
1145 Interacting Livestock and Fire May Both Threaten and Increase Viability of a
1146 Fire-Adapted Mediterranean Carnivorous Plant. *Journal of Applied Ecology*,
1147 **54**(6), 1884–94. <https://doi.org/10.1111/1365-2664.12872>

1148 Paniw, M., de la Riva, E. G., & Lloret, F. (2021). Demographic Traits Improve
1149 Predictions of Spatiotemporal Changes in Community Resilience to Drought.
1150 *Journal of Ecology*, **109**(9), 3233–45. [https://doi.org/10.1111/1365-](https://doi.org/10.1111/1365-2745.13597)
1151 [2745.13597](https://doi.org/10.1111/1365-2745.13597)

1152 Paniw, M., Salguero-Gómez, R., & Ojeda, F. (2015). Local-Scale Disturbances Can
1153 Benefit an Endangered, Fire-Adapted Plant Species in Western
1154 Mediterranean Heathlands in the Absence of Fire. *Biological Conservation*,
1155 **187**(July), 74–81. <https://doi.org/10.1016/j.biocon.2015.04.010>

1156 Paniw, M., Salguero-Gómez, R., & Ojeda, F. (2018). Transient Facilitation of
1157 Resprouting Shrubs in Fire-Prone Habitats. *Journal of Plant Ecology*, **11**(3),
1158 475–83. <https://doi.org/10.1093/jpe/rtx019>

1159 Pascoe, C., Lawrence, B. N., Guilyardi, E., Jukes, M., & Taylor, K. E. (2020).
1160 Documenting Numerical Experiments in Support of the Coupled Model
1161 Intercomparison Project Phase 6 (CMIP6). *Geoscientific Model Development*,
1162 **13**(5), 2149–67. <https://doi.org/10.5194/gmd-13-2149-2020>

1163 Pausas, J. G., & Bond, W. J. (2020). On the Three Major Recycling Pathways in
1164 Terrestrial Ecosystems. *Trends in Ecology and Evolution*, **35**(9), 767–775.
1165 <https://doi.org/10.1016/j.tree.2020.04.004>

1166 Pausas, J. G., & Keeley, J. E. (2014). Abrupt Climate-Independent Fire Regime
1167 Changes. *Ecosystems*, **17**(6), 1109–20. [https://doi.org/10.1007/s10021-014-](https://doi.org/10.1007/s10021-014-9773-5)
1168 [9773-5](https://doi.org/10.1007/s10021-014-9773-5)

1169 Pereira, H. M., Martins, I. S., Rosa, I. M. D., Kim, H., Leadley, P., Popp, A., Van
1170 Vuuren, D. P., Hurtt, G., Quoss, L., Arneth, A., Baisero, D., Bakkenes, M.,
1171 Chaplin-Kramer, R., Chini, L., Di Marco, M., Ferrier, S., Fujimori, S., Guerra,
1172 C. A., Harfoot, M., ... Alkemade, R. (2024). Global trends and scenarios for
1173 terrestrial biodiversity and ecosystem services from 1900 to 2050. *Science*,
1174 **384**(6694), 458–465. <https://doi.org/10.1126/science.adn3441>

1175 Petrie, R., Denvil, S., Ames, S., Levavasseur, G., Fiore, S., Allen, C., Antonio, F.,
1176 Berger, K., Bretonnière P.-A., Cinquini, L., Dart, E., Dwarakanath, P., Drukem,
1177 K., Evans, B., Franchistéguy, L., Gardoll, S., Gerbier, E., Greenslade, M.,
1178 Hassell, D., ... Wagner, R. (2021). Coordinating an Operational Data
1179 Distribution Network for CMIP6 Data. *Geoscientific Model Development*,
1180 **14**(1), 629–44. <https://doi.org/10.5194/gmd-14-629-2021>

1181 Posit team. (2023). RStudio: Integrated Development Environment for R. Posit
1182 Software, PBC, Boston, MA. <http://www.posit.co/>

1183 R Core Team. (2022). R: A Language and Environment for Statistical Computing.
1184 Vienna, Austria: R Foundation for Statistical Computing. [https://www.R-](https://www.R-project.org/)
1185 [project.org/](https://www.R-project.org/)

1186 Riahi, K., Rao, S., Krey, V., Cho, C., Chirkov, V., Fischer, G., Kindermann, G.,
1187 Nakicenovic, N., & Rafaj, P. (2011). RCP 8.5—A Scenario of Comparatively

1188 High Greenhouse Gas Emissions. *Climatic Change*, **109**(1), 33.
1189 <https://doi.org/10.1007/s10584-011-0149-y>

1190 Sala, O. E., Chapin III, F. S., Armesto, J. J., Berlow, E., Bloomfield, J., Dirzo, R.,
1191 Huber-Sanwald, E., Huenneke, L. F., Jackson, R. B., Kinzig, A., Leemans, R.,
1192 Lodge, D. M., Mooney, H. A., Oesterheld, M., Poff, N. L., Sykes, M. T.,
1193 Walker, B. H., Walker, M., & Wall, D. H. (2000). Global Biodiversity Scenarios
1194 for the Year 2100. *Science*, **287**(5459), 1770–74.
1195 <https://doi.org/10.1126/science.287.5459.1770>

1196 Sanderson, B. M., Knutti, R., & Caldwell, P. (2015). A Representative Democracy to
1197 Reduce Interdependency in a Multimodel Ensemble. *Journal of Climate*,
1198 **28**(13), 5171–94. <https://doi.org/10.1175/JCLI-D-14-00362.1>

1199 Selwood, K. E., McGeoch, M. A., & Mac Nally, R. (2015). The Effects of Climate
1200 Change and Land-Use Change on Demographic Rates and Population
1201 Viability. *Biological Reviews*, **90**(3), 837–53. <https://doi.org/10.1111/brv.12136>

1202 Sirami, C., Caplat, P., Popy, S., Clamens, A., Arlettaz, R., Jiguet, F., Brotons, L., &
1203 Martin, J.-L. (2017). Impacts of Global Change on Species Distributions:
1204 Obstacles and Solutions to Integrate Climate and Land Use. *Global Ecology*
1205 *and Biogeography*, **26**(4), 385–94. <https://doi.org/10.1111/geb.12555>

1206 Skates, L. M., Paniw, M., Cross, A. T., Ojeda, F., Dixon, K. W., Stevens, J. C., &
1207 Gebauer, G. (2019). An Ecological Perspective on ‘Plant Carnivory beyond
1208 Bogs’: Nutritional Benefits of Prey Capture for the Mediterranean Carnivorous
1209 Plant *Drosophyllum Lusitanicum*. *Annals of Botany*, **124**(1), 65–76.
1210 <https://doi.org/10.1093/aob/mcz045>

1211 Stearns, S. C. (1989). Trade-Offs in Life-History Evolution. *Functional Ecology*, **3**(3),
1212 259–68. <https://doi.org/10.2307/2389364>

- 1213 Titeux, N., Henle, K., Mihoub, J.-B., Regos, A., Geijzendorffer, I. R., Cramer, W.,
1214 Verburg, P. H., & Brotons, L. (2016). Biodiversity Scenarios Neglect Future
1215 Land-Use Changes. *Global Change Biology*, **22**(7), 2505–15.
1216 <https://doi.org/10.1111/gcb.13272>
- 1217 Tredennick, A. T., Hooten, M. B., Aldridge, C. L., Homer, C. G., Kleinhesselink, A.
1218 R., & Adler, P. B. (2016). Forecasting Climate Change Impacts on Plant
1219 Populations over Large Spatial Extents. *Ecosphere*, **7**(10), e01525.
1220 <https://doi.org/10.1002/ecs2.1525>
- 1221 Turco, M., Jerez, S., Augusto, S., Tarín-Carrasco, P., Ratola, N., Jiménez-Guerrero,
1222 P., & Trigo, R. M. (2019). Climate Drivers of the 2017 Devastating Fires in
1223 Portugal. *Scientific Reports*, **9**(1), 13886. [https://doi.org/10.1038/s41598-019-](https://doi.org/10.1038/s41598-019-50281-2)
1224 [50281-2](https://doi.org/10.1038/s41598-019-50281-2)
- 1225 Vilà, M., & Sardans, J. (1999). Plant Competition in Mediterranean-Type Vegetation.
1226 *Journal of Vegetation Science*, **10**(2), 281–94.
1227 <https://doi.org/10.2307/3237150>
- 1228 Villalobos, F. J., Sadras, V. O., & Fereres, E. (2016). Plant Density and Competition.
1229 In F. J. Villalobos & E. Fereres (Eds.), *Principles of Agronomy for Sustainable*
1230 *Agriculture* (pp. 159–168). Springer International Publishing.
1231 https://doi.org/10.1007/978-3-319-46116-8_12
- 1232 Villarreal-Barajas, T., & Martorell, C. (2009). Species-Specific Disturbance
1233 Tolerance, Competition and Positive Interactions along an Anthropogenic
1234 Disturbance Gradient. *Journal of Vegetation Science*, **20**(6), 1027–40.
1235 <https://doi.org/10.1111/j.1654-1103.2009.01101.x>
- 1236 Villellas, J., & García, M. B. (2018). Life-History Trade-Offs Vary with Resource
1237 Availability across the Geographic Range of a Widespread Plant. *Plant*

1238 *Biology*, **20**(3), 483–89. <https://doi.org/10.1111/plb.12682>

1239 Völler, E., Bossdorf, O., Prati, D., & Auge, H. (2017). Evolutionary Responses to
1240 Land Use in Eight Common Grassland Plants. *Journal of Ecology*, **105**(5),
1241 1290–97. <https://doi.org/10.1111/1365-2745.12746>

1242 Waliser, D., Gleckler, P. J., Ferraro, R., Taylor, K. E., Ames, S., Biard, J., Bosilovich,
1243 M. G., Brown, O., Chepfer, H., Cinquini, L., Durack, P.J., Eyring, V., Mathieu,
1244 P.-P., Lee, T., Pinnock, S., Potter, G. L., Rixen, M., Saunders, R., Schulz, J.,
1245 Thépaut, J.-N., Tuma, M. (2020). Observations for Model Intercomparison
1246 Project (Obs4MIPs): Status for CMIP6. *Geoscientific Model Development*,
1247 **13**(7), 2945–58. <https://doi.org/10.5194/gmd-13-2945-2020>

1248 Watson, J. E. M., Dudley, N., Segan, D. B., & Hockings, Marc. (2014). The
1249 Performance and Potential of Protected Areas. *Nature*, **515**(7525), 67–73.
1250 <https://doi.org/10.1038/nature13947>

1251 Wood, S. N. (2011). Fast Stable Restricted Maximum Likelihood and Marginal
1252 Likelihood Estimation of Semiparametric Generalized Linear Models. *Journal*
1253 *of the Royal Statistical Society Series B: Statistical Methodology*, **73**(1), 3–36.
1254 <https://doi.org/10.1111/j.1467-9868.2010.00749.x>

1255 Wood, S. N. (2017). *Generalized Additive Models: An Introduction with R, Second*
1256 *Edition*. CRC Press.

1257 Wood, S. N., Pya, N., & Säfken, B. (2016). Smoothing Parameter and Model
1258 Selection for General Smooth Models. *Journal of the American Statistical*
1259 *Association*, **111**(516), 1548–63.
1260 <https://doi.org/10.1080/01621459.2016.1180986>

1261 Zscheischler, J., Westra, S., van den Hurk, B. J. J. M., Seneviratne, S. I., Ward, P.
1262 J., Pitman, A., AghaKouchak, A., Bresh, D. N., Leonard, M., Wahl, T., &

- 1263 Zhang, X. (2018). Future Climate Risk from Compound Events. *Nature*
- 1264 *Climate Change*, **8**(6), 469–77. <https://doi.org/10.1038/s41558-018-0156-3>

1 Appendix S1 – Methodological details and additional results

2 3 1. Seedbank parameters

4
5 We used previously published data obtained from seed-burial and
6 greenhouse-germination experiments to parameterise the transitions of dewy-pine
7 seeds from and to the soil seedbank and to continuous germination (Table S1). More
8 specifically, following Paniw et al. (2017b), we used data on seeds buried in habitat
9 conditions characteristic of early (i.e., recently burned) or late post-fire stages (i.e.,
10 long unburned) to estimate seed survival in the soil (i.e., seedbank stasis; staySB)
11 and the probability of germinating from the seedbank at least two years after burial
12 (outSB). We used estimates from recently burned habitats for anthropogenic
13 populations, which experience constant anthropogenic disturbances mimicking the
14 effects of fire (Paniw et al., 2017b). For natural populations, we used estimates from
15 burned habitats in early post-fire stages (i.e., TSF₂ for staySB and TSF₁ for outSB),
16 and from unburned habitats in later post-fire stages (i.e., from TSF₃ for staySB and
17 from TSF₂ to TSF₄ for outSB). To more accurately describe the observed seedbank
18 dynamics in the first TSFs (i.e., TSF₀ and TSF₁ for staySB and TSF₀ for outSB), we
19 used previously published parameters representing the characteristically high
20 germination rates from the seedbank (outSB) in a fire year (TSF₀), and low
21 germination rates in late TSFs (TSF₅), as well as the very low seedbank stasis
22 (staySB) following a fire (TSF₀ and TSF₁) (Paniw et al., 2017b; Conquet et al., 2023).
23
24 To estimate the probability of seeds germinating continuously without contributing to
25 the seedbank (goCont) and its opposite parameter determining the probability of

26 seeds contributing to the seedbank (goSB), we used data from a growth-chamber
27 germination experiment (see details in Gómez-González et al., 2018). Seeds from 15
28 individual dewy pines growing in natural or anthropogenic habitats were monitored to
29 obtain the proportion of surviving seeds germinating (goCont) and remaining
30 dormant (goSB = 1 - goCont). We used estimates from the corresponding habitat to
31 parameterise seedbank transitions of our natural and anthropogenic populations. In
32 natural populations, however, continuous germination and contribution to the
33 seedbank only starts in TSF₂ and is extremely low from TSF₅. We therefore fixed the
34 values for goCont and goSB using previously published data (Paniw et al., 2017b;
35 Conquet et al., 2023) for these TSFs to represent these observed processes (Table
36 S1). Because natural populations still experience fires, we defined time-since-fire-
37 specific parameter values for these populations. Additionally, to take advantage of
38 the population-specific data available from the germination experiment for several
39 anthropogenic sites, we defined population-specific goCont and goSB values for
40 anthropogenic populations.

41

42 **Table S1 – Seedbank parameters obtained from seed-burial and germination**

43 **experiments.** We used previously published data from a seed-burial experiment in
44 recently burned and long unburned dewy-pine habitats to estimate the proportion of
45 seeds remaining in (staySB) or germinating from the seedbank (outSB). Additionally,
46 we used data from a germination experiment on seeds from natural and
47 anthropogenic habitats to estimate the proportion of seeds contributing to the
48 seedbank (goSB) or germinating continuously (goCont). The table contains
49 parameter means and, wherever available, 95% confidence intervals (with binomial

50 standard deviations calculated as $\sqrt{\frac{\mu \times (1-\mu)}{N}}$ where μ is the parameter mean and N the

51 sample size). Asterisks indicate parameter values adapted from previously published
 52 values (Paniw et al., 2017b; Conquet et al., 2023), and for which the confidence
 53 interval could not be calculated.

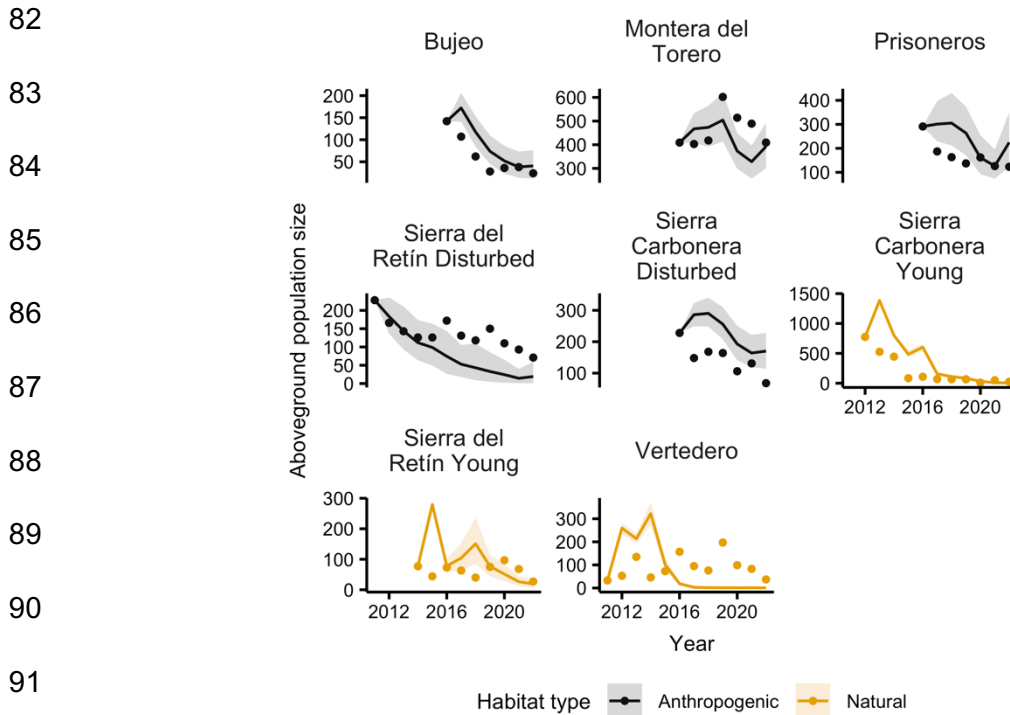
Natural populations				
Seedbank parameters				
Time since fire (TSF)	staySB	outSB	goCont	goSB
TSF ₀	0.1*	0.81*	0*	0*
TSF ₁	0.05*	0.061 [0.044, 0.077]	0*	0*
TSF ₂	0.60 [0.57, 0.63]	0.035 [0.023, 0.046]	0.026 [0.016, 0.037]	0.97 [0.96, 0.98]
TSF ₃	0.85 [0.83, 0.86]	0.035 [0.023, 0.046]	0.026 [0.016, 0.037]	0.97 [0.96, 0.98]
TSF ₄	0.85 [0.83, 0.86]	0.035 [0.023, 0.046]	0.026 [0.016, 0.037]	0.97 [0.96, 0.98]
TSF ₅	0.85 [0.83, 0.86]	0*	0.01*	0.99*
Anthropogenic populations				
Seedbank parameters				
Site	staySB	outSB	goCont	goSB
Sierra del Retín Disturbed	0.60 [0.57, 0.63]	0.061 [0.044, 0.077]	0.11 [0, 0.28]	0.89 [0.72, 1.0]
Prisioneros	0.60 [0.57, 0.63]	0.061 [0.044, 0.077]	0.29 [0.0071, 0.57]	0.71 [0.99, 0.43]
Bujeo	0.60 [0.57, 0.63]	0.061 [0.044, 0.077]	0.16 [0.060, 0.26]	0.84 [0.74, 0.94]
Montera del Torero	0.60 [0.57, 0.63]	0.061 [0.044, 0.077]	0.18 [0, 0.37]	0.82 [0.63, 1.0]
Sierra Carbonera Disturbed	0.60 [0.57, 0.63]	0.061 [0.044, 0.077]	0.16 [0.060, 0.26]	0.84 [0.74, 0.94]

54 2. Seedbank parameters correction factors

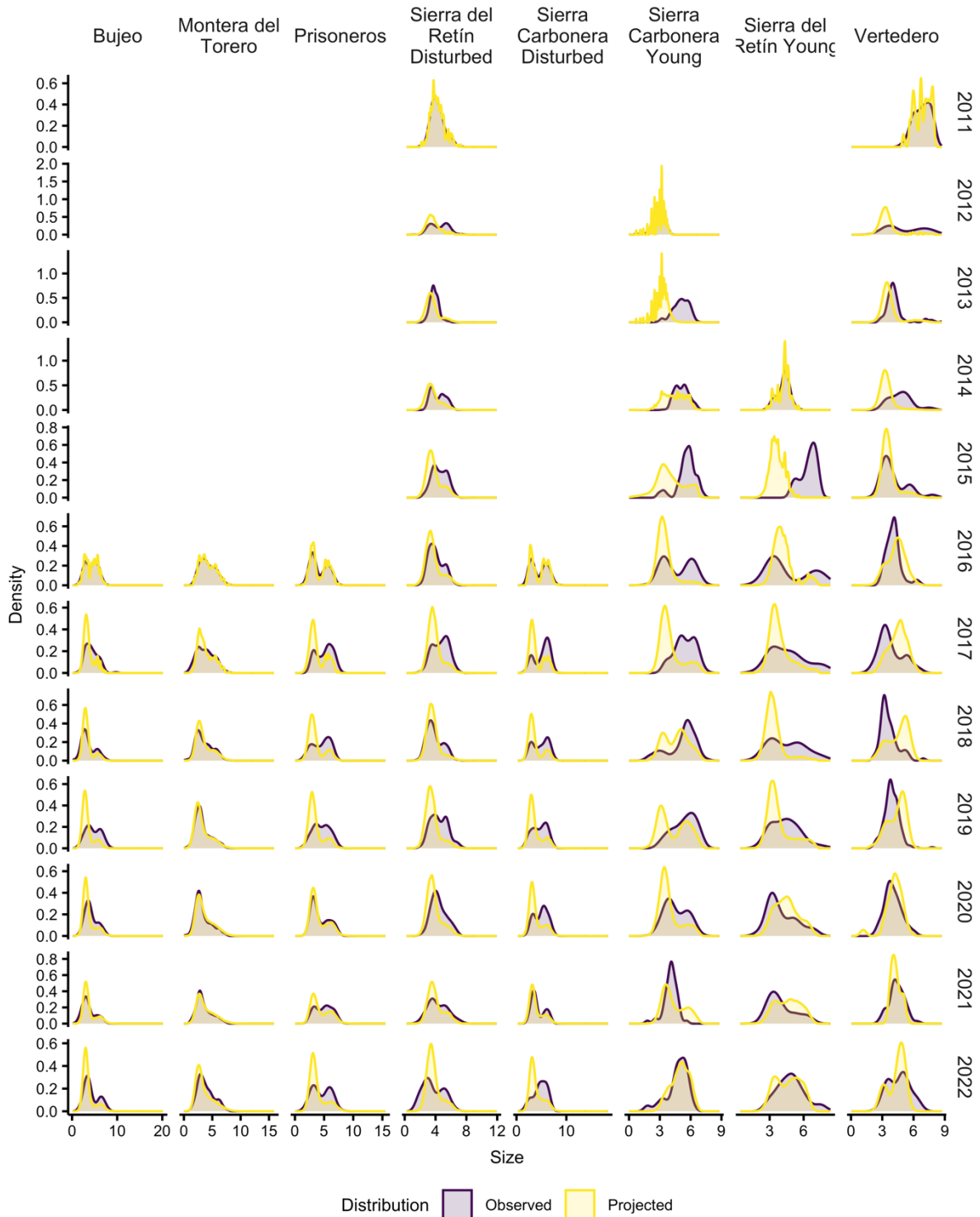
55

56 Accurately estimating seedbank parameters is complex due to the many factors
57 influencing germination and dormancy. Seed mortality is a hidden process that cannot
58 be easily determined in the field without perturbing the populations and is therefore
59 often underestimated. Therefore, to better represent the dewy-pine population
60 dynamics in anthropogenic sites, we computed a correction factor corresponding to
61 the seed aboveground survival (σ_{seed}). σ_{seed} corresponded to the proportion of seeds
62 surviving aboveground and was obtained from data on flower damage ($\sigma_{\text{seed}} = 1 -$
63 flower damage) (Paniw et al., 2017). As anthropogenic populations never returned to
64 TSF₀, we only used σ_{seed} for TSF₄ (0.33). We corrected the seedbank parameter
65 values in anthropogenic habitats by multiplying all four seedbank parameters (i.e.,
66 goCont, outSB, goSB, and staySB) by σ_{seed} . Additionally, previous model calibrations
67 showed the need to further correct several seedbank parameters to mirror the
68 observed dynamics of dewy-pine populations. To do so, we multiplied both goCont
69 and outSB by 0.4 for Sierra Carbonera Disturbed. Moreover, as we estimated plant
70 density within 1-m² quadrats, we avoided unrealistically high recruit numbers by
71 capping the number of recruits to the maximum observed number of seedlings per
72 quadrat during the study period in all natural populations and in two anthropogenic
73 populations: Bujeo and Sierra Carbonera Disturbed. In natural populations, this
74 number was TSF specific; however, data was unavailable for some TSFs in some
75 populations. When unavailable for TSF₀, we set the maximum number of recruits to
76 1.5 times the maximum observed number of seedlings in the populations; in TSF₁, we
77 set it to the maximum observed number of seedlings in the population; and in TSF₂ to
78 the average maximum observed number of seedlings in the population in TSF_{>0}. The

79 correction factors resulted in predicted abundances (out-of-sample predictions)
 80 reflecting well observed abundances, size distributions, and aboveground population
 81 growth rates (Fig. S1; Fig. S2; Fig. 4 in main text).



92 **Figure S1 – Observed and projected aboveground population abundance.** We
 93 projected each natural and anthropogenic population for 500 times across the range
 94 of observed years available for each population (maximum range from 2011 to 2022)
 95 to perform an out-of-sample validation of our individual-based model parameterization.
 96 For each projection, we obtained the average (line) and 25th and 95th (shaded ribbon)
 97 percentile of the aboveground population size. We compared these projected values
 98 to the observed ones (dots).



99 **Figure S2 – Observed and projected distributions of individual size across**
 100 **time.** We projected each population from the first year it was sampled to 2022 and
 101 obtained the site- and year-specific distributions of aboveground individual size, which
 102 we compared to the observed distributions. Size is defined as $\log(\text{number of leaves} \times$
 103 $\text{length of the longest leaf (cm)})$.

104 3. Covariate standardisation and correlation

105

106 We standardised all continuous covariates using the approach described by

107 Gelman (2008):

108

109
$$\text{covariate}_{\text{scaled}(H)} = \frac{(\text{covariate}_{\text{unscaled}(H)} - \mu_{\text{covariate}_{\text{unscaled}(H)}})}{2 \cdot \sigma_{\text{covariate}_{\text{unscaled}(H)}}}$$
 (Equation 1)

110

111 where μ and σ are respectively the mean and standard deviation of a given

112 unscaled covariate in a subset of data from a given habitat H (natural or

113 anthropogenic). In comparison with the common standardisation by one standard

114 deviation, this standardisation approach enables the comparison of the effect sizes

115 of both categorical (i.e. habitat) and continuous covariates (i.e. density-dependent

116 variables).

117

118 We checked for correlations between covariates using the Pearson correlation

119 coefficient (using the `cor` function from the stats R package; R Core Team, 2022).

120 We considered a pair of variables to be correlated when the absolute value of the

121 correlation coefficient was above 0.5. We included only one of the two correlated

122 variables in a model, choosing the first to be retained in the model selection.

123

124 4. Vital-rate model selection

125

126 We assessed the nonlinear response of dewy-pine survival, growth, flowering

127 probability, number of flowers, and seedling size to rainfall, maximum daily

128 temperature, time since fire (TSF), aboveground density of large individuals (size >

129 4.5), and individual size using Generalised Additive Models (GAMs) fitted to
130 demographic data from individual dewy pines growing in natural or anthropogenic
131 habitats. We first assessed whether rainfall and temperature influenced vital rates
132 and in which period. We did this by comparing a null model (i.e., with only year and
133 population random effects, using a random effect basis (bs = "re") in the mgcv
134 package; (Wood, 2017)) with models including cumulative rainfall or average
135 maximum daily temperature across different periods. As each census was done
136 during the flowering period, we assessed rainfall and temperature effect prior to the
137 annual population census for flowering probability, number of flowers, and seedling
138 size; or in the period between two annual censuses for survival and growth (see
139 Table S2 and Table S3). We considered further lagged climatic effects to be
140 captured by changes in plant size and density.

141

142 **Table S2 – Periods of average maximum daily temperature and cumulative**
143 **rainfall considered to assess the effect of temperature and rainfall on dewy-**
144 **pine vital rates.** We investigated the nonlinear response of dewy-pine vital rates to
145 average maximum daily temperature ($\mu_{\max T}$) and cumulative rainfall (\sum_{rain}) in various
146 periods of the years prior (for flowering probability, number of flowers, and seedling
147 size; in regular text) or post the annual population census (for survival and growth; in
148 *italic*).

149

150

151

Period full name	Short name	Start	End	Justification
Previous winter average maximum daily temperature	$\mu_{\max T_prevWinter}$	January	April	Dewy pines rely almost exclusively on insect prey for nutrients (Paniw et al., 2017a). Long periods of above-average temperatures in winter and spring (approximated by this variable) can result in physiological stress for plants and desiccation of leaf mucilage preventing plants from catching and digest prey insects (Paniw et al., 2018).
Previous fall cumulative rainfall	$\sum_{rain_prevFall}$	September	November	Rainfall in fall and winter is a key determinant of plant growth and survival in the Mediterranean shrublands (Paniw et al. 2023). For the dewy pine, in particular, plentiful rain translates to more air humidity, which allows the plants to maintain leaf mucilage to catch and digest prey insects (Adamec, 2009). In addition, abundant rainfall may result in higher invertebrate activity and thus more potential food for plants (Paniw et al., 2017b). Too much rain however may result in prey insects being washed off leaves; and this may occur in particular if plants are exposed (i.e., not protected by surrounding shrubs; Brewer et al., 2021).
Previous winter cumulative rainfall	$\sum_{rain_prevWinter}$	January	April	Same justification as for fall cumulative rainfall. In addition, heavy rainfall in spring may damage or wash away seedlings.

Next summer average maximum daily temperature	$\mu_{\max T_nextSummer}$	May	September	Extremely high summer temperatures may damage and desiccate plants, preventing them to capture prey with leaf mucilage (Paniw et al., 2018), particularly in anthropogenetic habitats where plants are often more exposed (Brewer et al., 2021) and where prey availability may be lower (Paniw et al., 2018)
Next fall cumulative rainfall	$\sum_{rain_nextFall}$	September	November	Same justification as for previous fall rainfall, but considering the period between census at time t and $t+1$ (which is relevant for plant survival and growth)
Next winter cumulative rainfall	$\sum_{rain_nextWinter}$	January	April	Same justification as for previous winter rainfall, but considering the period between census at time t and $t+1$ (which is relevant for plant survival and growth)
Next fall and winter cumulative rainfall	$\sum_{rain_nextFallWinter}$	September	April	Same justification as for previous fall/winter rainfall, but considering the period between census at time t and $t+1$ (which is relevant for plant survival and growth)

152

153 We selected the best model among the possible rainfall and temperature periods

154 using the Akaike Information Criterion (AIC), through the *model.sel* and *AICtab*

155 functions of the MuMIn (Bartoń, 2022) and bbmle R packages (Bolker, 2022); we

156 used a threshold of $\Delta AIC < 2$ to identify models with no strong difference, and

157 selected the model with the lowest number of degrees of freedom if more than one

158 model were within that threshold. If both models with effects of rainfall and

159 temperature performed better than the null model, we calculated Pearson's

160 correlation coefficient using the *cor.test* function of the stats R package (R Core

161 Team, 2022) to check whether the two variables were correlated. If they were (i.e.,
162 correlation coefficient $> |0.5|$), we used the AIC and the number of degrees of
163 freedom to select the best model between the one with rainfall and the one with
164 temperature. Conversely, if the two variables were not correlated (i.e., correlation
165 coefficient $\leq |0.5|$) We compared the models including one of rainfall and
166 temperature to a model with both climatic variables, including their interaction (Table
167 S3). Finally, we performed a forward selection—using the AIC and the degrees of
168 freedom—, progressively adding aboveground density, size (except for seedling
169 size), and time since fire (TSF; for natural populations only) in the model. While
170 Table S3 only shows splines, we included the linear effects of all covariates in the
171 model selection. We then included interactions between covariates in the model
172 selection if at least one of them was retained in the single effect selection.
173 Additionally, we included terms for site-specific random slopes (e.g., random size
174 effect depending on the site).

175 **Table S3 – Example of the model selection process.** We selected the best model
176 to predict a given vital rate (vr) using the Akaike Information Criterion (AIC). We first
177 assessed whether rainfall and temperature affected the vital rate by comparing a null
178 model (with only year and population random effects (**M1**) to models including rainfall
179 or temperature values in various periods of the year (Step 1 for temperature and 2
180 for rainfall). If both models with temperature and rainfall performed better than the
181 null model, we compared them with a model containing both climatic variables (Step
182 3), and also included their interaction (Step 4). We then progressively added size,
183 time since fire (TSF), and aboveground density of large individuals (density) to see if
184 their introgression improved the model (Steps 5–7). Finally, we included interactions
185 between covariates when at least one of the two members of the interaction had
186 been previously retained in the model selection (Steps 8–9). For each step, the *Best*
187 *model according to the AIC* column shows the best model (**M**) according to the AIC.
188 This model is then used as a comparison to the newer models in the next step.
189 Newly added covariates at each time step are shown in green.

Model selection step	Models compared	Best model according to the AIC
1	M1 = vr ~ s(time, bs = "re") + s(site, bs = "re") M2 = vr ~ s($\mu_{\text{maxT_prevWinter}}$, k = 3, bs = "cr") + s(time, bs = "re") + s(site, bs = "re")	M2
2	M3 = vr ~ s(time, bs = "re") + s(site, bs = "re") M4 = vr ~ s($\Sigma_{\text{rain_prevFall}}$, k = 3, bs = "cr") + s(time, bs = "re") + s(site, bs = "re") M5 = vr ~ s($\Sigma_{\text{rain_prevFall}}$, k = 3, bs = "cr") + s(time, bs = "re") + s(site, bs = "re")	M5

3	<p>M2 = $vr \sim s(\mu_{\max T_prevWinter}, k = 3, bs = "cr") + s(\text{time}, bs = "re") + s(\text{site}, bs = "re")$</p> <p>M5 = $vr \sim s(\sum_{\text{rain_prevFall}}, k = 3, bs = "cr") + s(\text{time}, bs = "re") + s(\text{site}, bs = "re")$</p> <p>M6 = $vr \sim s(\mu_{\max T_prevWinter}, k = 3, bs = "cr") + s(\sum_{\text{rain_prevFall}}, k = 3, bs = "cr") + s(\text{time}, bs = "re") + s(\text{site}, bs = "re")$</p>	M6
4	<p>M6 = $vr \sim s(\mu_{\max T_prevWinter}, k = 3, bs = "cr") + s(\sum_{\text{rain_prevFall}}, k = 3, bs = "cr") + s(\text{time}, bs = "re") + s(\text{site}, bs = "re")$</p> <p>M7 = $vr \sim s(\mu_{\max T_prevWinter}, k = 3, bs = "cr") + s(\sum_{\text{rain_prevFall}}, k = 3, bs = "cr") + ti(\mu_{\max T_prevWinter}, \sum_{\text{rain_prevFall}}, k = 3, bs = "cr") + s(\text{time}, bs = "re") + s(\text{site}, bs = "re")$</p>	M7
5	<p>M7 = $vr \sim s(\mu_{\max T_prevWinter}, k = 3, bs = "cr") + s(\sum_{\text{rain_prevFall}}, k = 3, bs = "cr") + ti(\mu_{\max T_prevWinter}, \sum_{\text{rain_prevFall}}, k = 3, bs = "cr") + s(\text{time}, bs = "re") + s(\text{site}, bs = "re")$</p> <p>M8 = $vr \sim s(\mu_{\max T_prevWinter}, k = 3, bs = "cr") + s(\sum_{\text{rain_prevFall}}, k = 3, bs = "cr") + ti(\mu_{\max T_prevWinter}, \sum_{\text{rain_prevFall}}, k = 3, bs = "cr") + s(\text{size}, k = 3, bs = "cr") + s(\text{time}, bs = "re") + s(\text{site}, bs = "re")$</p> <p>M9 = $vr \sim s(\mu_{\max T_prevWinter}, k = 3, bs = "cr") + s(\sum_{\text{rain_prevFall}}, k = 3, bs = "cr") + ti(\mu_{\max T_prevWinter}, \sum_{\text{rain_prevFall}}, k = 3, bs = "cr") + s(\text{density}, k = 3, bs = "cr") + s(\text{time}, bs = "re") + s(\text{site}, bs = "re")$</p> <p>M10 = $vr \sim s(\mu_{\max T_prevWinter}, k = 3, bs = "cr") +$</p>	M9

	<p> $s(\sum \text{rain_prevFall}, k = 3, \text{bs} = \text{"cr"}) +$ $ti(\mu_{\text{maxT_prevWinter}}, \sum \text{rain_prevFall}, k = 3, \text{bs} = \text{"cr"})$ + $s(\text{TSF}, k = 3, \text{bs} = \text{"cr"}) +$ $s(\text{time}, \text{bs} = \text{"re"}) +$ $s(\text{site}, \text{bs} = \text{"re"})$ </p>	
6	<p> M9 = $vr \sim s(\mu_{\text{maxT_prevWinter}}, k = 3, \text{bs} = \text{"cr"}) +$ $s(\sum \text{rain_prevFall}, k = 3, \text{bs} = \text{"cr"}) +$ $ti(\mu_{\text{maxT_prevWinter}}, \sum \text{rain_prevFall}, k = 3, \text{bs} = \text{"cr"})$ + $s(\text{density}, k = 3, \text{bs} = \text{"cr"}) +$ $s(\text{time}, \text{bs} = \text{"re"}) +$ $s(\text{site}, \text{bs} = \text{"re"})$ M11 = $vr \sim s(\mu_{\text{maxT_prevWinter}}, k = 3, \text{bs} = \text{"cr"}) +$ $s(\sum \text{rain_prevFall}, k = 3, \text{bs} = \text{"cr"}) +$ $ti(\mu_{\text{maxT_prevWinter}}, \sum \text{rain_prevFall}, k = 3, \text{bs} = \text{"cr"})$ + $s(\text{density}, k = 3, \text{bs} = \text{"cr"}) +$ $s(\text{size}, k = 3, \text{bs} = \text{"cr"}) +$ $s(\text{time}, \text{bs} = \text{"re"}) +$ $s(\text{site}, \text{bs} = \text{"re"})$ M12 = $vr \sim s(\mu_{\text{maxT_prevWinter}}, k = 3, \text{bs} = \text{"cr"}) +$ $s(\sum \text{rain_prevFall}, k = 3, \text{bs} = \text{"cr"}) +$ $ti(\mu_{\text{maxT_prevWinter}}, \sum \text{rain_prevFall}, k = 3, \text{bs} = \text{"cr"})$ + $s(\text{density}, k = 3, \text{bs} = \text{"cr"}) +$ $s(\text{TSF}, k = 3, \text{bs} = \text{"cr"}) +$ $s(\text{time}, \text{bs} = \text{"re"}) +$ $s(\text{site}, \text{bs} = \text{"re"})$ </p>	M12

7	<p>M12 = $vr \sim s(\mu_{\max T_prevWinter}, k = 3, bs = "cr") +$ $s(\sum rain_prevFall, k = 3, bs = "cr") +$ $ti(\mu_{\max T_prevWinter}, \sum rain_prevFall, k = 3, bs = "cr")$</p> <p>+</p> <p>$s(density, k = 3, bs = "cr") +$ $s(TSF, k = 3, bs = "cr") +$ $s(time, bs = "re") +$ $s(site, bs = "re")$</p> <p>M13 = $vr \sim s(\mu_{\max T_prevWinter}, k = 3, bs = "cr") +$ $s(\sum rain_prevFall, k = 3, bs = "cr") +$ $ti(\mu_{\max T_prevWinter}, \sum rain_prevFall, k = 3, bs = "cr")$</p> <p>+</p> <p>$s(density, k = 3, bs = "cr") +$ $s(TSF, k = 3, bs = "cr") +$ $s(size, k = 3, bs = "cr") +$ $s(time, bs = "re") +$ $s(site, bs = "re")$</p>	M12
8	<p>M12 = $vr \sim s(\mu_{\max T_prevWinter}, k = 3, bs = "cr") +$ $s(\sum rain_prevFall, k = 3, bs = "cr") +$ $ti(\mu_{\max T_prevWinter}, \sum rain_prevFall, k = 3, bs = "cr")$</p> <p>+</p> <p>$s(density, k = 3, bs = "cr") +$ $s(TSF, k = 3, bs = "cr") +$ $s(time, bs = "re") +$ $s(site, bs = "re")$</p> <p>M14 = $vr \sim s(\mu_{\max T_prevWinter}, k = 3, bs = "cr") +$ $s(\sum rain_prevFall, k = 3, bs = "cr") +$ $ti(\mu_{\max T_prevWinter}, \sum rain_prevFall, k = 3, bs = "cr")$</p> <p>+</p> <p>$s(density, k = 3, bs = "cr") +$ $s(TSF, k = 3, bs = "cr") +$ $ti(\mu_{\max T_prevWinter}, density, k = 3, bs = "cr") +$ $s(time, bs = "re") +$ $s(site, bs = "re")$</p> <p>M15 = $vr \sim s(\mu_{\max T_prevWinter}, k = 3, bs = "cr") +$ $s(\sum rain_prevFall, k = 3, bs = "cr") +$ $ti(\mu_{\max T_prevWinter}, \sum rain_prevFall, k = 3, bs = "cr")$</p> <p>+</p> <p>$s(density, k = 3, bs = "cr") +$ $s(TSF, k = 3, bs = "cr") +$ $ti(\mu_{\max T_prevWinter}, TSF, k = 3, bs = "cr") +$ $s(time, bs = "re") +$ $s(site, bs = "re")$</p>	M15

<p>M16 = $vr \sim s(\mu_{\max T_prevWinter}, k = 3, bs = "cr") +$ $s(\sum_{rain_prevFall}, k = 3, bs = "cr") +$ $ti(\mu_{\max T_prevWinter}, \sum_{rain_prevFall}, k = 3, bs = "cr")$</p> <p>+</p> <p>$s(density, k = 3, bs = "cr") +$ $s(TSF, k = 3, bs = "cr") +$ $ti(\mu_{\max T_prevWinter}, size, k = 3, bs = "cr") +$ $s(time, bs = "re") +$ $s(site, bs = "re")$</p> <p>M17 = $vr \sim s(\mu_{\max T_prevWinter}, k = 3, bs = "cr") +$ $s(\sum_{rain_prevFall}, k = 3, bs = "cr") +$ $ti(\mu_{\max T_prevWinter}, \sum_{rain_prevFall}, k = 3, bs = "cr")$</p> <p>+</p> <p>$s(density, k = 3, bs = "cr") +$ $s(TSF, k = 3, bs = "cr") +$ $ti(\sum_{rain_prevFall}, density, k = 3, bs = "cr") +$ $s(time, bs = "re") +$ $s(site, bs = "re")$</p> <p>M18 = $vr \sim s(\mu_{\max T_prevWinter}, k = 3, bs = "cr") +$ $s(\sum_{rain_prevFall}, k = 3, bs = "cr") +$ $ti(\mu_{\max T_prevWinter}, \sum_{rain_prevFall}, k = 3, bs = "cr")$</p> <p>+</p> <p>$s(density, k = 3, bs = "cr") +$ $s(TSF, k = 3, bs = "cr") +$ $ti(\sum_{rain_prevFall}, TSF, k = 3, bs = "cr") +$ $s(time, bs = "re") +$ $s(site, bs = "re")$</p> <p>M19 = $vr \sim s(\mu_{\max T_prevWinter}, k = 3, bs = "cr") +$ $s(\sum_{rain_prevFall}, k = 3, bs = "cr") +$ $ti(\mu_{\max T_prevWinter}, \sum_{rain_prevFall}, k = 3, bs = "cr")$</p> <p>+</p> <p>$s(density, k = 3, bs = "cr") +$ $s(TSF, k = 3, bs = "cr") +$ $ti(\sum_{rain_prevFall}, size, k = 3, bs = "cr") +$ $s(time, bs = "re") +$ $s(site, bs = "re")$</p> <p>M20 = $vr \sim s(\mu_{\max T_prevWinter}, k = 3, bs = "cr") +$ $s(\sum_{rain_prevFall}, k = 3, bs = "cr") +$ $ti(\mu_{\max T_prevWinter}, \sum_{rain_prevFall}, k = 3, bs = "cr")$</p> <p>+</p> <p>$s(density, k = 3, bs = "cr") +$ $s(TSF, k = 3, bs = "cr") +$</p>	
---	--

	<p> $ti(\text{density}, \text{TSF}, k = 3, \text{bs} = \text{"cr"}) +$ $s(\text{time}, \text{bs} = \text{"re"}) +$ $s(\text{site}, \text{bs} = \text{"re"})$ </p> <p> M21 = $vr \sim s(\mu_{\text{maxT_prevWinter}}, k = 3, \text{bs} = \text{"cr"}) +$ $s(\sum \text{rain_prevFall}, k = 3, \text{bs} = \text{"cr"}) +$ $ti(\mu_{\text{maxT_prevWinter}}, \sum \text{rain_prevFall}, k = 3, \text{bs} = \text{"cr"})$ </p> <p>+</p> <p> $s(\text{density}, k = 3, \text{bs} = \text{"cr"}) +$ $s(\text{TSF}, k = 3, \text{bs} = \text{"cr"}) +$ $ti(\text{density}, \text{size}, k = 3, \text{bs} = \text{"cr"}) +$ $s(\text{time}, \text{bs} = \text{"re"}) +$ $s(\text{site}, \text{bs} = \text{"re"})$ </p> <p> M22 = $vr \sim s(\mu_{\text{maxT_prevWinter}}, k = 3, \text{bs} = \text{"cr"}) +$ $s(\sum \text{rain_prevFall}, k = 3, \text{bs} = \text{"cr"}) +$ $ti(\mu_{\text{maxT_prevWinter}}, \sum \text{rain_prevFall}, k = 3, \text{bs} = \text{"cr"})$ </p> <p>+</p> <p> $s(\text{density}, k = 3, \text{bs} = \text{"cr"}) +$ $s(\text{TSF}, k = 3, \text{bs} = \text{"cr"}) +$ $ti(\text{TSF}, \text{size}, k = 3, \text{bs} = \text{"cr"}) +$ $s(\text{time}, \text{bs} = \text{"re"}) +$ $s(\text{site}, \text{bs} = \text{"re"})$ </p>	
9	<p> M15 = $vr \sim s(\mu_{\text{maxT_prevWinter}}, k = 3, \text{bs} = \text{"cr"}) +$ $s(\sum \text{rain_prevFall}, k = 3, \text{bs} = \text{"cr"}) +$ $ti(\mu_{\text{maxT_prevWinter}}, \sum \text{rain_prevFall}, k = 3, \text{bs} = \text{"cr"})$ </p> <p>+</p> <p> $s(\text{density}, k = 3, \text{bs} = \text{"cr"}) +$ $s(\text{TSF}, k = 3, \text{bs} = \text{"cr"}) +$ $ti(\mu_{\text{maxT_prevWinter}}, \text{TSF}, k = 3, \text{bs} = \text{"cr"}) +$ $s(\text{time}, \text{bs} = \text{"re"}) +$ $s(\text{site}, \text{bs} = \text{"re"})$ </p> <p> M23 = $vr \sim s(\mu_{\text{maxT_prevWinter}}, k = 3, \text{bs} = \text{"cr"}) +$ $s(\sum \text{rain_prevFall}, k = 3, \text{bs} = \text{"cr"}) +$ $ti(\mu_{\text{maxT_prevWinter}}, \sum \text{rain_prevFall}, k = 3, \text{bs} = \text{"cr"})$ </p> <p>+</p> <p> $s(\text{density}, k = 3, \text{bs} = \text{"cr"}) +$ $s(\text{TSF}, k = 3, \text{bs} = \text{"cr"}) +$ $ti(\mu_{\text{maxT_prevWinter}}, \text{TSF}, k = 3, \text{bs} = \text{"cr"}) +$ $ti(\mu_{\text{maxT_prevWinter}}, \text{density}, k = 3, \text{bs} = \text{"cr"}) +$ $s(\text{time}, \text{bs} = \text{"re"}) +$ $s(\text{site}, \text{bs} = \text{"re"})$ </p> <p> M24 = $vr \sim s(\mu_{\text{maxT_prevWinter}}, k = 3, \text{bs} = \text{"cr"}) +$ $s(\sum \text{rain_prevFall}, k = 3, \text{bs} = \text{"cr"}) +$ </p>	M15

	$ti(\mu_{\max T_prevWinter}, \sum_{\text{rain_prevFall}}, k = 3, bs = "cr")$	
	$+$ $s(\text{density}, k = 3, bs = "cr") +$ $s(\text{TSF}, k = 3, bs = "cr") +$ $ti(\mu_{\max T_prevWinter}, \text{TSF}, k = 3, bs = "cr") +$ $ti(\mu_{\max T_prevWinter}, \text{size}, k = 3, bs = "cr") +$ $s(\text{time}, bs = "re") +$ $s(\text{site}, bs = "re")$	
	$\mathbf{M25} = vr \sim s(\mu_{\max T_prevWinter}, k = 3, bs = "cr") +$ $s(\sum_{\text{rain_prevFall}}, k = 3, bs = "cr") +$ $ti(\mu_{\max T_prevWinter}, \sum_{\text{rain_prevFall}}, k = 3, bs = "cr")$	
	$+$ $s(\text{density}, k = 3, bs = "cr") +$ $s(\text{TSF}, k = 3, bs = "cr") +$ $ti(\mu_{\max T_prevWinter}, \text{TSF}, k = 3, bs = "cr") +$ $ti(\sum_{\text{rain_prevFall}}, \text{density}, k = 3, bs = "cr") +$ $s(\text{time}, bs = "re") +$ $s(\text{site}, bs = "re")$	
	$\mathbf{M26} = vr \sim s(\mu_{\max T_prevWinter}, k = 3, bs = "cr") +$ $s(\sum_{\text{rain_prevFall}}, k = 3, bs = "cr") +$ $ti(\mu_{\max T_prevWinter}, \sum_{\text{rain_prevFall}}, k = 3, bs = "cr")$	
	$+$ $s(\text{density}, k = 3, bs = "cr") +$ $s(\text{TSF}, k = 3, bs = "cr") +$ $ti(\mu_{\max T_prevWinter}, \text{TSF}, k = 3, bs = "cr") +$ $ti(\sum_{\text{rain_prevFall}}, \text{TSF}, k = 3, bs = "cr") +$ $s(\text{time}, bs = "re") +$ $s(\text{site}, bs = "re")$	
	$\mathbf{M27} = vr \sim s(\mu_{\max T_prevWinter}, k = 3, bs = "cr") +$ $s(\sum_{\text{rain_prevFall}}, k = 3, bs = "cr") +$ $ti(\mu_{\max T_prevWinter}, \sum_{\text{rain_prevFall}}, k = 3, bs = "cr")$	
	$+$ $s(\text{density}, k = 3, bs = "cr") +$ $s(\text{TSF}, k = 3, bs = "cr") +$ $ti(\mu_{\max T_prevWinter}, \text{TSF}, k = 3, bs = "cr") +$ $ti(\sum_{\text{rain_prevFall}}, \text{size}, k = 3, bs = "cr") +$ $s(\text{time}, bs = "re") +$ $s(\text{site}, bs = "re")$	
	$\mathbf{M28} = vr \sim s(\mu_{\max T_prevWinter}, k = 3, bs = "cr") +$ $s(\sum_{\text{rain_prevFall}}, k = 3, bs = "cr") +$	

	$ \begin{aligned} & \text{ti}(\mu_{\text{maxT_prevWinter}}, \Sigma_{\text{rain_prevFall}}, k = 3, \text{bs} = \text{"cr"}) \\ + & \\ & \text{s}(\text{density}, k = 3, \text{bs} = \text{"cr"}) + \\ & \text{s}(\text{TSF}, k = 3, \text{bs} = \text{"cr"}) + \\ & \text{ti}(\mu_{\text{maxT_prevWinter}}, \text{TSF}, k = 3, \text{bs} = \text{"cr"}) + \\ & \text{ti}(\text{density}, \text{TSF}, k = 3, \text{bs} = \text{"cr"}) + \\ & \text{s}(\text{time}, \text{bs} = \text{"re"}) + \\ & \text{s}(\text{site}, \text{bs} = \text{"re"}) \\ \mathbf{M29} = \text{vr} \sim & \text{s}(\mu_{\text{maxT_prevWinter}}, k = 3, \text{bs} = \text{"cr"}) + \\ & \text{s}(\Sigma_{\text{rain_prevFall}}, k = 3, \text{bs} = \text{"cr"}) + \\ & \text{ti}(\mu_{\text{maxT_prevWinter}}, \Sigma_{\text{rain_prevFall}}, k = 3, \text{bs} = \\ \text{"cr"}) + & \\ & \text{s}(\text{density}, k = 3, \text{bs} = \text{"cr"}) + \\ & \text{s}(\text{TSF}, k = 3, \text{bs} = \text{"cr"}) + \\ & \text{ti}(\mu_{\text{maxT_prevWinter}}, \text{TSF}, k = 3, \text{bs} = \text{"cr"}) + \\ & \text{ti}(\text{density}, \text{size}, k = 3, \text{bs} = \text{"cr"}) + \\ & \text{s}(\text{time}, \text{bs} = \text{"re"}) + \\ & \text{s}(\text{site}, \text{bs} = \text{"re"}) \\ \mathbf{M30} = \text{vr} \sim & \text{s}(\mu_{\text{maxT_prevWinter}}, k = 3, \text{bs} = \text{"cr"}) + \\ & \text{s}(\Sigma_{\text{rain_prevFall}}, k = 3, \text{bs} = \text{"cr"}) + \\ & \text{ti}(\mu_{\text{maxT_prevWinter}}, \Sigma_{\text{rain_prevFall}}, k = 3, \text{bs} = \text{"cr"}) \\ + & \\ & \text{s}(\text{density}, k = 3, \text{bs} = \text{"cr"}) + \\ & \text{s}(\text{TSF}, k = 3, \text{bs} = \text{"cr"}) + \\ & \text{ti}(\mu_{\text{maxT_prevWinter}}, \text{TSF}, k = 3, \text{bs} = \text{"cr"}) + \\ & \text{ti}(\text{TSF}, \text{size}, k = 3, \text{bs} = \text{"cr"}) + \\ & \text{s}(\text{time}, \text{bs} = \text{"re"}) + \\ & \text{s}(\text{site}, \text{bs} = \text{"re"}) \end{aligned} $	
--	--	--

191 5. Vital-rate estimation results

192

193 **Table S4 – Most parsimonious generalised additive models for dewy-**
194 **pine vital rates.** For natural ($n = 3$) and anthropogenic ($n = 5$) populations, we
195 estimated survival (σ), growth of aboveground plants (φ), flowering probability (ρ_{fi}),
196 number of flowers (n_{flowers}), and seedling size (Φ) as a function of monthly average
197 daily maximum temperature in a given period ($\mu_{\text{maxT_period}}$), monthly cumulative
198 rainfall in a given period ($\Sigma_{\text{rain_period}}$), aboveground density of large individuals
199 (density), individual size, and—for natural populations—time since fire (TSF). We
200 selected the best model to predict a given vital rate using the Akaike Information
201 Criterion (AIC). The function $s(x_{\text{edf}})$ is the spline smoothing function (i.e. simple
202 effect) of x , and $ti(x, y_{\text{edf}})$ is the tensor product smoothing function of x and y . We
203 used a cubic regression spline ($bs = "cr"$ in the `mgcv` package; Wood, 2011; Wood et
204 al., 2016; Wood, 2017) for all smoothing parameters, with a dimension $k = 3$ (except
205 for the size effect on the number of flowers, where we used $k = 4$ to force a decline in
206 the number of flowers of large individuals and avoid an ever-increasing number of
207 flowers). Additionally, all models include a year and site random effect. edf is the
208 corresponding effective degrees of freedom (Wood, 2017), which represents the
209 amount of nonlinearity in the model component ($edf = 1$ corresponds to a linear fit),
210 and n in the sample size. For the intercept and linear predictors (i.e., outside of s and
211 ti smoothing functions), we report the estimated β -coefficients and the standard
212 error.

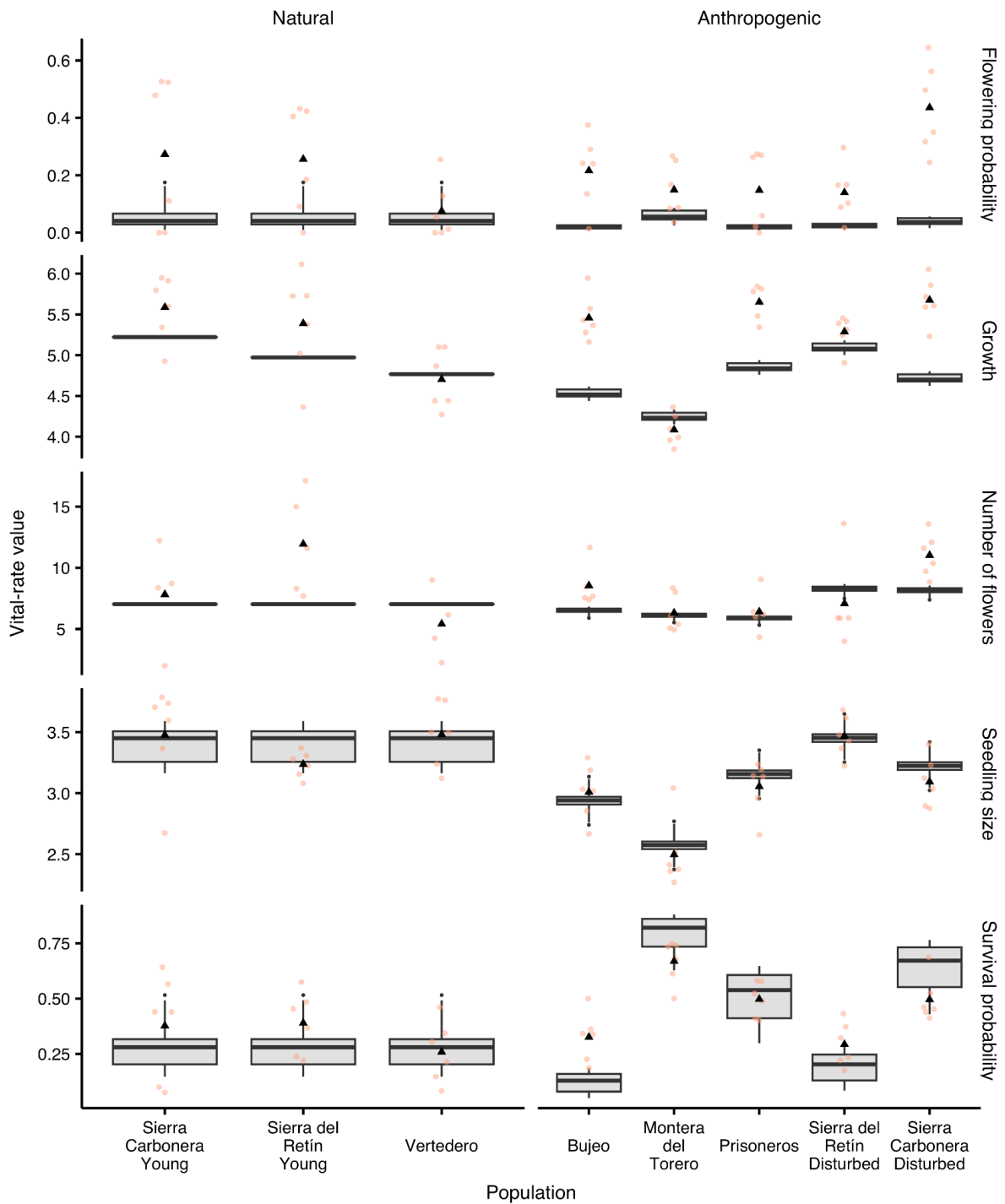
213

Vital rate	Family (link function)	Most parsimonious model	<i>n</i>
Natural populations			
σ	Binomial (logit)	-1.1 _(0.28) + 0.27 _(0.47) $\mu_{\max T_nextSummer}$ + 0.11 _(0.48) $\sum_{rain_nextFall}$ + ti($\sum_{rain_nextFall}$, $\mu_{\max T_nextSummer}$ edf=0.88) + s(size edf=1.7) + s(TSF edf=0.00018) + s($\mu_{\max T_nextSummer}$, site edf=1.5, bs = "re") + ti(size, TSF edf=2.1) + ti($\sum_{rain_nextFall}$, density edf=2.7) - 1.4 _(0.46) $\sum_{rain_nextFall}$ *TSF + ti($\mu_{\max T_nextSummer}$, size edf=0.74) - 0.26 _(0.096) $\mu_{\max T_nextSummer}$ *density + ti($\mu_{\max T_nextSummer}$, TSF edf=0.93) + ti($\sum_{rain_nextFall}$, size edf=1.7) + s(time edf=3.8, bs = "re") + s(site edf=0.00010, bs = "re")	1493
γ	Scaled <i>t</i> (identity)	5.1 _(0.12) + s($\sum_{rain_nextFall}$ edf=0.000063) + 1.5 _(0.14) size + s(TSF edf=1.7) - 0.074 _(0.018) density + s(size, site edf=1.6, bs = "re") + ti($\sum_{rain_nextFall}$, TSF edf=0.81) + ti($\sum_{rain_nextFall}$, density edf=2.1) + ti(size, density edf=0.83) + s(time edf=0.000019, bs = "re") + s(site edf=1.8, bs = "re")	482
ρ_{fi}	Binomial (logit)	-4.0 _(0.57) + 0.93 _(0.95) $\sum_{rain_prevFall}$ + ti($\sum_{rain_prevFall}$, $\mu_{\max T_prevWinter}$ edf=1.5) + 5.5 _(0.44) size + s(TSF edf=0.0000079) + ti(TSF, $\mu_{\max T_prevWinter}$ edf=0.91) + ti(TSF, density edf=0.58) + ti($\sum_{rain_prevFall}$, TSF edf=0.61) + ti($\sum_{rain_prevFall}$, density edf=1.3) + ti(size, density edf=1.2) + s(time edf=3.8, bs = "re") + s(site edf=0.000041, bs = "re")	1487
$n_{flowers}$	Negative binomial (log)	2.0 _(0.052) + s($\mu_{\max T_prevWinter}$ edf=0.00041) + s(size edf=2.8) - 0.40 _(1.4) TSF + s(time edf=0.0013, bs = "re") + s(site edf=0.000056, bs = "re")	185
Φ	Scaled <i>t</i> (identity)	3.4 _(0.073) + s($\mu_{\max T_prevWinter}$ edf=0.66) + s(density edf=0.49) + 0.16 _(0.079) TSF + s(density, site edf=0.000064, bs = "re") + s(TSF, site edf=0.69, bs = "re") + ti($\mu_{\max T_prevWinter}$, density edf=1.3) + ti($\mu_{\max T_prevWinter}$, TSF edf=0.76) + ti(density, TSF edf=0.69) + s(time edf=4.8, bs = "re") + s(site edf=0.000071, bs = "re")	745
Anthropogenic populations			
σ	Binomial (logit)	-0.55 _(0.60) + s($\sum_{rain_nextFall}$ edf=0.015) - 1.8 _(0.41) $\mu_{\max T_nextSummer}$ + ti($\sum_{rain_nextFall}$, $\mu_{\max T_nextSummer}$ edf=0.00017) + s(size edf=1.9) + s(size, site edf=3.6, bs = "re") + s($\sum_{rain_nextFall}$, site edf=3.2, bs = "re") + ti($\sum_{rain_nextFall}$, size edf=0.92) + 0.11 _(0.037) size*density + s(time edf=4.5, bs = "re") + s(site edf=3.9, bs = "re")	6008
γ	Scaled <i>t</i> (identity)	5.0 _(0.13) + s($\mu_{\max T_nextSummer}$ edf=0.37) + s(size edf=1.6) - 0.028 _(0.0053) density + s(size, site edf=3.9, bs = "re") + s($\mu_{\max T_nextSummer}$, site edf=3.9, bs = "re") + s(time edf=3.9, bs = "re") + s(site edf=3.8, bs = "re")	3202
ρ_{fi}	Binomial (logit)	-4.7 _(0.36) + s($\sum_{rain_prevWinter}$ edf=0.50) + s(size edf=2.0) + s(density, edf=1.6) + s(size, site edf=3.6, bs = "re") + s($\sum_{rain_prevWinter}$, site edf=2.4, bs = "re") + s(density, site edf=2.7, bs = "re") + s(time edf=5.0, bs = "re") + s(site edf=3.0, bs = "re")	6254
$n_{flowers}$	Negative binomial (log)	1.9 _(0.072) + s($\sum_{rain_prevFall}$ edf=0.0012) + s(size edf=2.8) + s($\sum_{rain_prevFall}$, site edf=4.0, bs = "re") + s(size, site edf=3.7, bs = "re") + s(time edf=3.0, bs = "re") + s(site edf=0.015, bs = "re")	899
Φ	Scaled <i>t</i> (identity)	3.0 _(0.14) + s($\mu_{\max T_prevWinter}$ edf=0.50) - 0.057 _(0.012) density + s($\mu_{\max T_prevWinter}$, site edf=2.9, bs = "re") + s(density, site edf=1.9, bs = "re") + ti($\mu_{\max T_prevWinter}$, density edf=0.64) + s(time edf=5.5, bs = "re") + s(site edf=3.9, bs = "re")	2608

215 *Among-site variation in average vital rates and climate effects*

216

217 Dewy-pine vital rates varied between natural and anthropogenic habitat as
218 well as between sites. Among-site variation was larger in anthropogenic than in
219 natural conditions, possibly because of the among-population differences in the level
220 of anthropogenic disturbance. This variation was especially large for survival rates,
221 which ranged from 0.11 [0.058, 0.20] in Bujeo to 0.80 [0.72, 0.86] in Montera del
222 Torero, while it remained stable at 0.27 [0.17, 0.40] on average in natural
223 populations (Fig. S3).



224

225

Figure S3 – Among-site variation in average vital-rate values in natural

226

and anthropogenic populations. The boxplots represent the distribution of the

227

average values of predicted site-specific survival, growth, and flowering rates, as

228

well as the number of flowers and seedling size estimated for each year. The

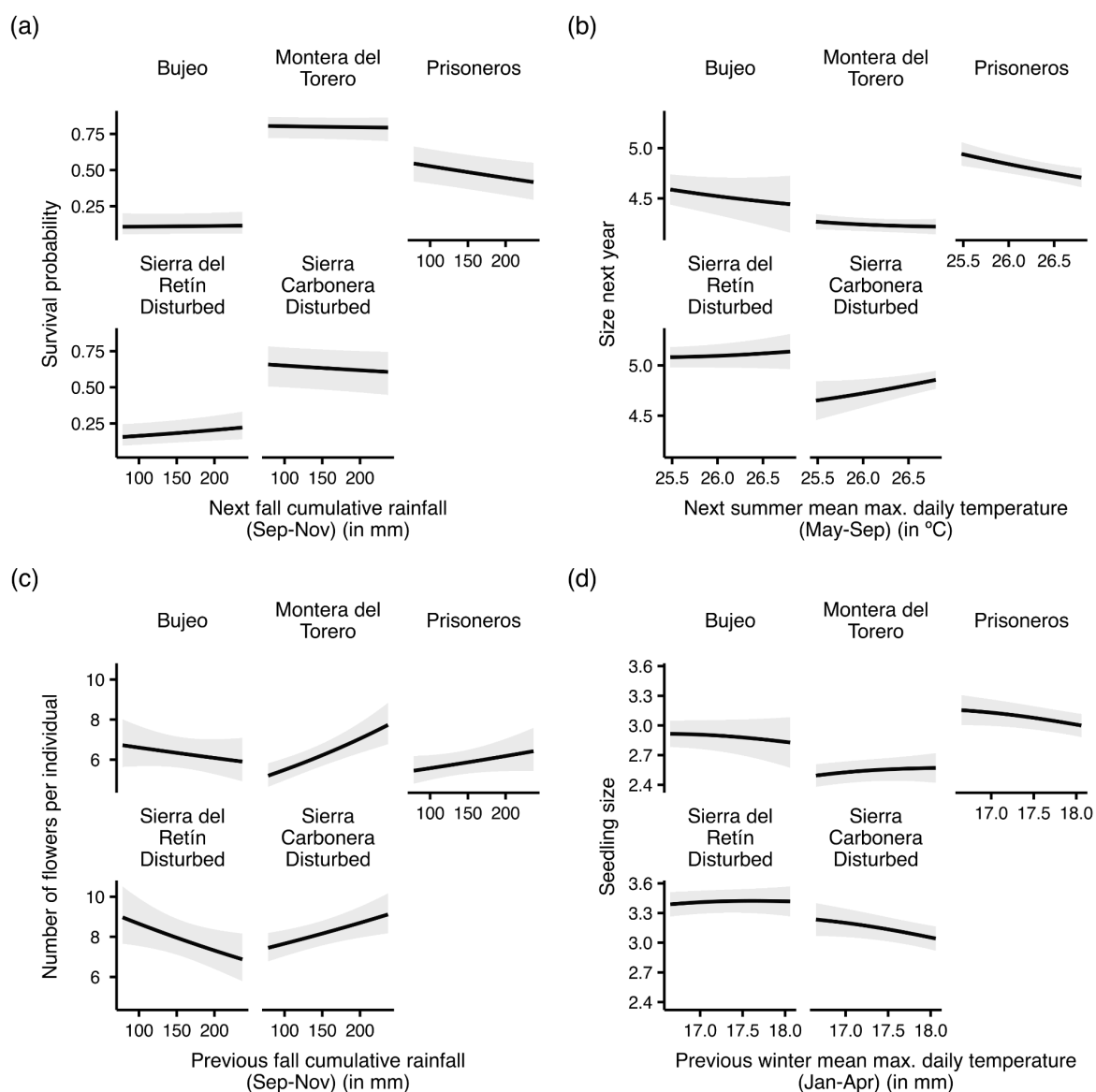
229

whiskers represent the 2.5th and 97.5th percentiles and the black triangle the mean

230 estimate. We kept covariates at their mean values (scaled value = 0) except for the
231 number of flowers, where we used the mean size of reproducing individuals when
232 doing predictions. The coloured dots represent the observed average vital rates in
233 each population and year.

234

235 In anthropogenic habitats, we found among-site disparities in the direction of
236 association between climatic variables and survival, growth, number of flowers per
237 individual, and seedling size (Fig. S4). For instance, the number of flowers was
238 positively associated with increasing rainfall in Montera del Torero population (e.g.
239 from 5.5 [5.0, 6.1] under 100 mm of rain to 7.0 [6.3, 7.8] under 200 mm), but
240 negatively in Sierra del Retín Disturbed (e.g. from 8.7 [7.5, 9.9] to 7.3 [6.4, 8.4]). In
241 contrast, there was no such among-site variation in natural habitats. For example,
242 seedlings were bigger with higher winter temperatures (January–April); seedling size
243 increased from 3.0 [2.8, 3.3] under 16 °C to 3.4 [3.3, 3.6] under 18 °C (Fig. S5).



244

245

Figure S4 – Among-site variation in the association between climatic

246

variables and vital rates in anthropogenic populations. We predicted the values

247

of (a) survival probability, (b) size in the next year, (c) number of flowers per

248

individual, and (d) seedling size for a range of rainfall and temperature values in

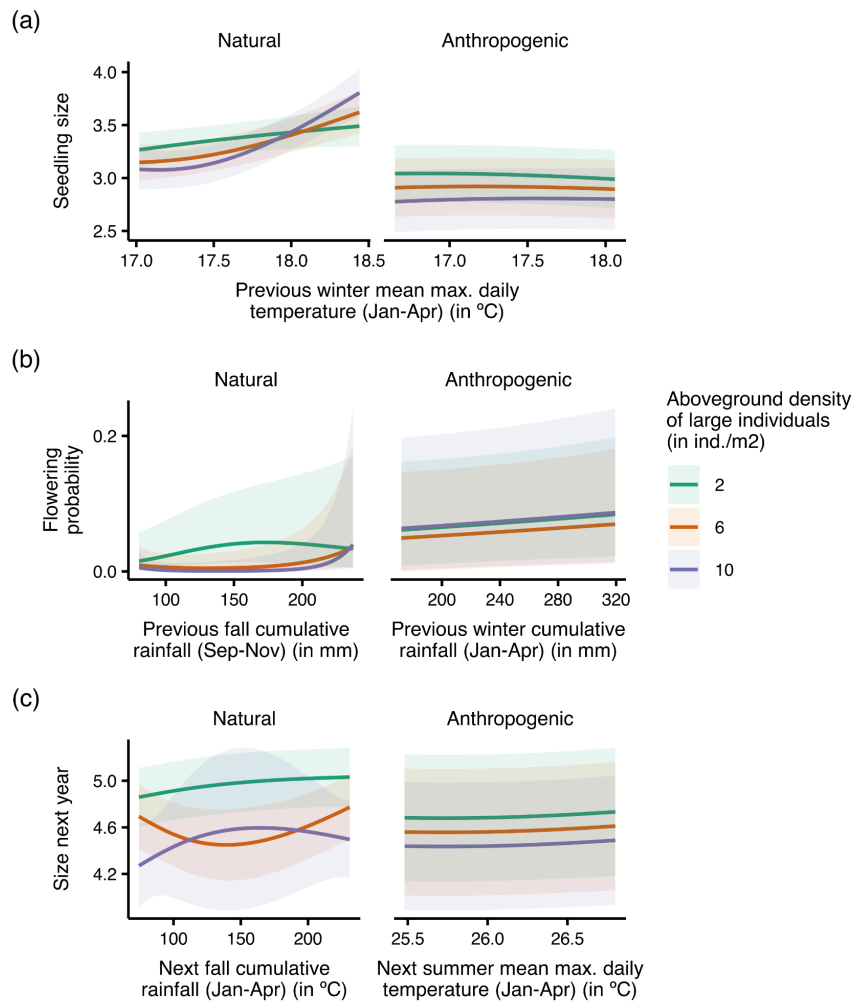
249

each anthropogenic population of dewy pines. The lines represent the average vital-

250

rate value and the shaded ribbon the 95% confidence interval. We kept all other

251 covariates at their mean values (scaled value = 0) except for the number of flowers,
 252 where we used the mean size of reproducing individuals.



253

254 **Figure S5 – Density-dependent variation in vital-rate responses to**

255 **climate.** We predicted the values of (a) seedling size, (b) flowering probability, and

256 (c) size in the next year for a range of rainfall and temperature values and three

257 levels of aboveground densities in natural and anthropogenic habitats. The lines

258 represent the average vital-rate value and the shaded ribbon the 95% confidence

259 interval. We kept all other covariates at their mean values (scaled value = 0) except

260 for the number of flowers, where we used the mean size of reproducing individuals.

261

262 *Vital-rate responses to large aboveground individual density and climate-*
263 *density interactions*

264

265 Seedling size decreased with higher numbers of large individuals aboveground (from
266 3.0 [2.8, 3.3] at 2 ind./m² to 2.8 [2.5, 3.1] at 10 ind./m² in anthropogenic populations
267 and from 3.4 [3.2, 3.5] to 3.1 [3.0, 3.3] in natural ones; Fig. S5a; Table S5). Density
268 also mediated the association between seedling size and winter temperature in
269 natural populations, with a stronger positive correlation between the two variables
270 with 6 ind./m² (3.2 [3.1, 3.4] at 17.5 °C and 3.7 [3.4, 3.9] at 18.5 °C) than with 2
271 ind./m² (3.4 [3.2, 3.5] and 3.5 [3.3, 3.7]) (Fig. S5a; Table S5). Additionally, with high
272 densities in natural populations, flowering probability was low except for high
273 amounts of rainfall (e.g. with 6 ind./m², 0.19 [0.035, 0.60] for 150 mm of rainfall and
274 0.37 [0.096, 0.76] for 200 mm; but with 2 ind./m², 0.71 [0.43, 0.88] and 0.71 [0.38,
275 0.90]) (Fig. S5b; Table S5), and the pattern was similar for growth (e.g. with 6
276 ind./m², 4.5 [4.1, 4.8] for 150 mm of rainfall and 4.6 [4.3, 4.9] for 200 mm; but with 2
277 ind./m², 5.0 [4.7, 5.2] and 5.0 [4.8, 5.3]) (Fig. S5c; Table S5).

278

279 *Vital-rate responses to time since fire and size*

280

281 As expected from previous work and observations, individuals in natural populations
282 had a short lifespan, as indicated by the decrease in survival with time since fire
283 (TSF) (0.42 [0.28, 0.57] and 0.29 [0.18, 0.42] respectively 3 and 7 years after a fire)
284 and size (0.26 [0.16, 0.40] with a size of 5.0 and 0.22 [0.12, 0.37] with 6.2) (Fig.
285 S6a,b; Table S5). This early decline in survival was accompanied by investment into
286 reproduction from early post-fire stages, with flowering probability decreasing from

287 0.16 [0.038, 0.48] to 0.051 [0.016, 0.15] respectively 3 and 7 years after a fire and
288 the number of flowers per individual from 10 [8.2, 13] to 7.6 [6.8, 8.4] (Fig. 5c,d;
289 Table S5). Dewy pines growing in natural conditions also appeared to reproduce
290 throughout most of their lifetime, as both flowering probabilities and number of
291 flowers continuously increased with size (individuals had a probability of flowering of
292 0.17 [0.061, 0.38] and 2.9 [2.4, 3.5] flowers with a size of 5.0, which respectively
293 increased to 0.74 [0.47, 0.90] and 7.8 [6.9, 8.7] with 6.2) (Fig. S6e,f; Table S5). In
294 contrast, the largest individuals had the highest survival in anthropogenic habitats
295 (0.61 [0.32, 0.84] and 0.75 [0.46, 0.91] with sizes of 5.0 and 6.2; Fig. S6b; Table S5),
296 but did not invest as much in reproduction with both flowering probability and number
297 of flowers declining after reaching a peak for a size of 7.3 (probability of flowering of
298 0.69 [0.34, 0.91]) and 8.2 (19 [13, 28] flowers) (Fig. S6e,f; Table S5).

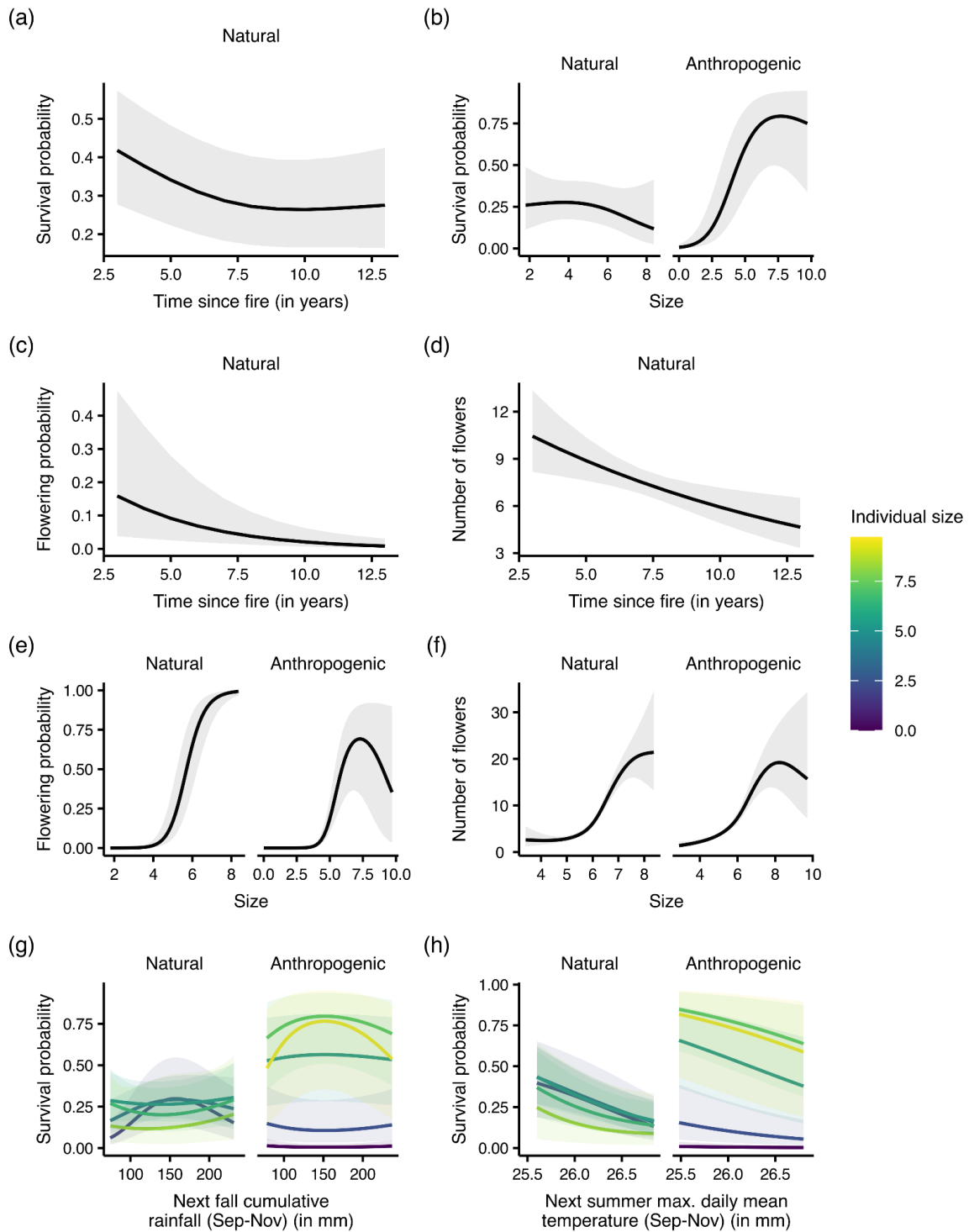
299

300 *Vital-rate responses to size-climate interactions*

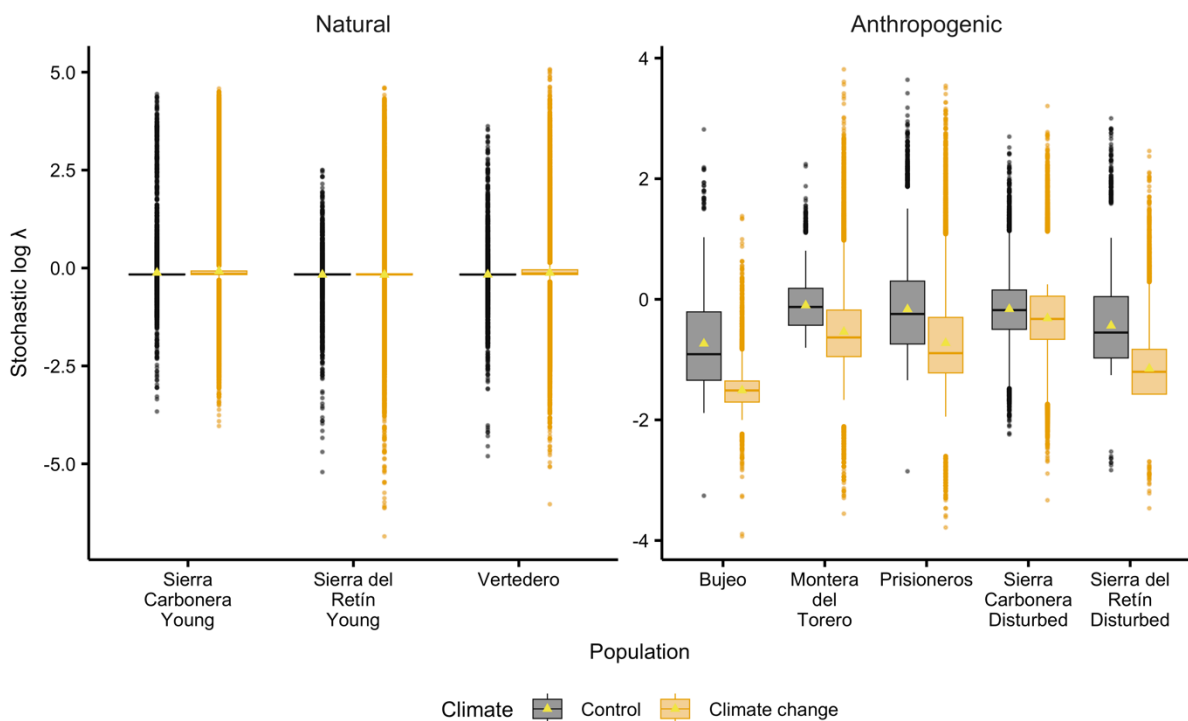
301

302 In natural populations, small individuals survived best at intermediate rainfall (e.g.
303 0.29 [0.18, 0.43] with 150 mm of rain for an individual of size 3.4) than for high or low
304 amounts of rainfall (0.18 [0.098, 0.30] with 80 mm and 0.26 [0.14, 0.43] with 210
305 mm), while large individuals survived best at low or high rainfall (e.g., for an
306 individual of size 6.6, 0.26 [0.13, 0.45] with 80 mm, 0.20 [0.10, 0.37] with 150 mm,
307 and 0.26 [0.13, 0.45] with 210 mm; Fig. S6g; Table S5). Additionally, survival rates
308 decreased faster with summer temperature for large than for small individuals (from
309 0.60 [0.32, 0.83] at 25 °C to 0.26 [0.13, 0.44] at 26 °C with a size of 6.6, and from
310 0.57 [0.32, 0.79] to 0.34 [0.22, 0.49] with a size of 3.4; Fig. S6h; Table S5). We also
311 found size dependence in the association between survival and rainfall in

312 anthropogenic populations, where large individuals survived best at intermediate
 313 amounts of rain in fall (e.g., for an individual with a size of 6.6, 0.67 [0.37, 0.88] at 80
 314 mm of rain, 0.78 [0.49, 0.93] at 150 mm, and 0.73 [0.44, 0.91] at 210 mm), while
 315 small individuals were not affected by changes in rainfall (Fig. S6g; Table S5).



316 **Figure S6 – Vital-rate responses to time since fire, size, and size-climate**
 317 **interactions.** We predicted the values of survival and flowering probability as well as
 318 the number of flowers per individual for a range of number of years since the last fire
 319 (time since fire) in natural habitats (a, c, d) and for a range of individual sizes in both
 320 natural and anthropogenic habitats (b, e, f). Finally, we predicted the values of
 321 survival probability for a range of individual sizes as well as (h) rainfall and (g)
 322 temperature values. The lines represent the average vital-rate value and the shaded
 323 ribbon the 95% confidence interval. In each case, we kept all other covariates at their
 324 mean values (scaled value = 0) except for the number of flowers, where we used the
 325 mean size of reproducing individuals.



326 **Figure S7 – Site-specific population growth rate.** For each population, we
 327 calculated the stochastic growth rate $\log \lambda_s$ as the average of all annual $\log \lambda$ in each
 328 of 500 projections.

329 **References – Appendix S1**

330

331 Bartoń, K. (2022). MuMIn: Multi-Model Inference. R. [https://CRAN.R-](https://CRAN.R-project.org/package=MuMIn)
332 [project.org/package=MuMIn](https://CRAN.R-project.org/package=MuMIn)

333 Bolker, B. (2022). Bbmle: Tools for General Maximum Likelihood Estimation. R.
334 <https://CRAN.R-project.org/package=bbmle>

335 Conquet, E., Ozgul, A., Blumstein, D. T., Armitage, K. B., Oli, M. K., Martin, J. G. A.,
336 Clutton-Brock, T. H., & Paniw, M. (2023). Demographic Consequences of
337 Changes in Environmental Periodicity. *Ecology*, **104**(3), e3894.
338 <https://doi.org/10.1002/ecy.3894>

339 Gelman, A. (2008). Scaling Regression Inputs by Dividing by Two Standard
340 Deviations. *Statistics in Medicine*, **27**(15), 2865–73.
341 <https://doi.org/10.1002/sim.3107>

342 Gómez-González, S., Paniw, M., Antunes, K., & Ojeda, F. (2018). Heat Shock and
343 Plant Leachates Regulate Seed Germination of the Endangered Carnivorous
344 Plant *Drosophyllum Lusitanicum*. *Web Ecology*, **18**(1), 7–13.
345 <https://doi.org/10.5194/we-18-7-2018>

346 Paniw, M., Gil-Cabeza, E., & Ojeda, F. (2017a). Plant Carnivory beyond Bogs:
347 Reliance on Prey Feeding in *Drosophyllum Lusitanicum* (Drosophyllaceae) in
348 Dry Mediterranean Heathland Habitats. *Annals of Botany*, **119**(6), 1035–41.
349 <https://doi.org/10.1093/aob/mcw247>

350 Paniw, M., Quintana-Ascencio, P. F., Ojeda, F., & Salguero-Gómez, R. (2017b).
351 Interacting Livestock and Fire May Both Threaten and Increase Viability of a
352 Fire-Adapted Mediterranean Carnivorous Plant. *Journal of Applied Ecology*,
353 **54**(6), 1884–94. <https://doi.org/10.1111/1365-2664.12872>

- 354 R Core Team. (2022). R: A Language and Environment for Statistical Computing.
355 Vienna, Austria: R Foundation for Statistical Computing. [https://www.R-](https://www.R-project.org/)
356 [project.org/](https://www.R-project.org/)
- 357 Wood, S. N. (2011). Fast Stable Restricted Maximum Likelihood and Marginal
358 Likelihood Estimation of Semiparametric Generalized Linear Models. *Journal*
359 *of the Royal Statistical Society Series B: Statistical Methodology*, **73**(1), 3–36.
360 <https://doi.org/10.1111/j.1467-9868.2010.00749.x>
- 361 Wood, S. N. (2017). *Generalized Additive Models: An Introduction with R, Second*
362 *Edition*. CRC Press.
- 363 Wood, S. N., Pya, N., & Säfken, B. (2016). Smoothing Parameter and Model
364 Selection for General Smooth Models. *Journal of the American Statistical*
365 *Association*, **111**(516), 1548–63.
366 <https://doi.org/10.1080/01621459.2016.1180986>

1 **Appendix S2 – Current and future rainfall and temperature data in dewy-pine**
2 **populations**

3

4 1. Current rainfall and temperature data

5

6 We modelled the response of dewy-pine vital rates to rainfall and maximum
7 daily temperature using observed daily climatic data at dewy-pine population
8 locations (Table 1) from the E-OBS dataset from the EU-FP6 project UERRA and the
9 Copernicus Climate Change Service (Cornes et al., 2018; accessible at
10 https://surfobs.climate.copernicus.eu/dataaccess/access_eobs.php). We used the
11 ncdf4 R package to process the raw netCDF weather data (Pierce, 2021), and
12 transformed the daily rainfall and maximum daily temperature into monthly
13 cumulative rainfall and average maximum daily temperature. For each population,
14 we then obtained monthly cumulative rainfall and average maximum temperature
15 data from the year prior the first census (i.e., 2010 for Sierra del Retín Disturbed and
16 Vertedero, 2011 for Sierra Carbonera Young, 2014 for Sierra del Retín Young, and
17 2015 for all other populations). To do so, we averaged the recorded climate values
18 within a buffer of 0.1×1.5 degrees around the GPS location of each population.

19

20

21

22

23

24

25

Table S1 – Description of dewy-pine populations. Longitude and latitude of

26 population locations are given in decimal degrees.

Population	Habitat type	Description*	Latitude	Longitude	First sampled	Last fire*	% bare ground [#]
Sierra Carbonera Young	Natural	Little browsed heathland patch (4 fires 1975-2008)	36.209722	-5.36	2012	2011	8.67 (±9.01)
Sierra del Retín Young	Natural	Little browsed heathland patch (1 fire 1975-2008)	36.1769444	-5.8330555	2015	2013	5.01 (±6.38)
Vertedero	Natural	Little browsed heathland patch (1 fire 1975-2008); surrounded by browsed areas but was fenced in after 2009 fire to prevent browsing	36.121667	-5.49	2011	2009	NA
Sierra del Retín Disturbed	Anthropogenic	Moderately browsed heathland patch (1 fire 1975-2008); located in military zone in a regularly cleared area (every 3 years) along a road to avoid wildfire ignitions	36.198056	-5.823611	2011	1996	NA
Prisioneros	Anthropogenic	Located on abandoned quarry; frequent browsing by goats	36.105	-5.4863888	2016	1950	56.80 (±22.09)
Bujeo	Anthropogenic	On a regularly cleared area (every 3 years) along a dirt road to avoid wildfire ignitions; frequent browsing by goats	36.072461	-5.52654	2016	1950	73.87 (±25.47)
Montera del Torero	Anthropogenic	On an old firebreak made by vegetation removal with bulldozers (mechanical uprooting); moderate browsing	36.226389	-5.585278	2016	1950	62.93 (±21.96)

Sierra Carbonera Disturbed	Anthropogenic	In a small uprooted, open patch close to old (abandoned) military premises; moderate browsing	36.106388	-5.3605555	2016	1950	22.67 (±22.99)
----------------------------	---------------	---	-----------	------------	------	------	----------------

27 *Source: Paniw et al., 2017. See also [REDIAM](#) - *Áreas recorridas por el fuego en*
28 *Andalucía (1975-actualidad)*; Browsing was determined based on observations of
29 dung/droppings of ungulates at the study sites during each visit (frequent browsing:
30 droppings found in > 60% of plots on average; moderate browsing: droppings found
31 in 30-60% of plots on average; little browsing: droppings found in < 30% of plots on
32 average)

33 #Source: Gómez-González et al., 2018. % bare soil cover in a site was calculated as
34 the number of 25 grids (10×10 cm each, arranged in a 50-cm square) that were bare
35 soil. In each site in 2017, 30 of such 50-cm squares were located adjacent to
36 randomly sampled dewy pine plants.

37

38 2. Projected rainfall and temperature data

39

40 To project dewy-pine populations under climate change, we used projected
41 rainfall and temperature values at dewy-pine population locations from 11 global
42 circulation models (GCM; see Table 2) from the Coupled Model Intercomparison
43 Project 6 (CMIP6; Eyring et al., 2016; Pascoe et al., 2020; Waliser et al., 2020)
44 available from the Earth System Grid Federation (ESFG; Petrie et al., 2021;
45 available at <https://aims2.llnl.gov/search>). For each model, we selected the best
46 variant using the GCMeval tool (Parding et al., 2020; accessible at
47 <https://gcmeval.met.no/>). For each GCM, we downloaded data for the intermediate
48 and worst scenario of atmospheric greenhouse gas Representative Concentration

49 Pathway (RCP), corresponding to a level of radiative forcing reaching 4.5 (RCP 4.5)
50 or 8.5 (RCP 8.5) Watts per square metre (Wm^{-2}) by 2100, respectively. We
51 processed the raw data from each climate projection model using the ncd4 R
52 package (Pierce, 2021) to obtain monthly cumulative rainfall and average maximum
53 temperature in each population by averaging the values recorded within a buffer of
54 0.1×1.5 degrees around the population coordinates (i.e., 1.5 times the grid
55 resolution).

56

57 Most GCMs comprised projected rainfall and temperature values beyond the values
58 observed in our populations. To avoid predicting vital rates using values of climate
59 variables outside the observed range, we capped these values to the maximum and
60 minimum observed. For example, while the observed maximum cumulative rainfall in
61 fall was 245 mm, six of the considered GCM predicted greater values in some years,
62 ranging from 250 to 463 mm; we transformed these values to the maximum
63 observed (245 mm). This allowed us to investigate the response of dewy-pine
64 populations to increases in the frequency of extreme climatic conditions, rather than
65 changes in absolute rainfall and temperature values.

66 **Table S2 – List of global circulation models used to project dewy-pine**
 67 **populations under climate change.**

Source ID	Experiment	Variant	Version	Institution	Modelling centre	Citation
CanESM5	ssp585	r1i1p1f1	20190429	Canadian Centre for Climate Modelling and Analysis, Environment and Climate Change Canada, Victoria, BC V8P 5C2, Canada	CCCma	(Swart et al., 2019)
EC_Earth3	ssp585	r4i1p1f1	20200425	AEMET, Spain; BSC, Spain; CNR-ISAC, Italy; DMI, Denmark; ENEA, Italy; FMI, Finland; Geomar, Germany; ICHEC, Ireland; ICTP, Italy; IDL, Portugal; IMAU, The Netherlands; IPMA, Portugal; KIT, Karlsruhe, Germany; KNMI, The Netherlands; Lund University, Sweden; Met Eireann, Ireland; NLeSC, The Netherlands; NTNU, Norway; Oxford University, UK; surfSARA, The Netherlands; SMHI, Sweden; Stockholm University, Sweden; Unite ASTR, Belgium; University College Dublin, Ireland; University of Bergen, Norway; University of Copenhagen, Denmark; University of Helsinki, Finland; University of Santiago de Compostela, Spain; Uppsala University, Sweden; Utrecht University, The Netherlands; Vrije Universiteit Amsterdam, the Netherlands;	EC-Earth-Consortium	(EC-Earth Consortium (EC-Earth), 2019)

				Wageningen University, The Netherlands. Mailing address: EC-Earth consortium, Rossby Center, Swedish Meteorological and Hydrological Institute/SMHI, SE-601 76 Norrkoping, Sweden		
FGOALS_G3	ssp585	r1i1p1f1	20190818	Chinese Academy of Sciences, Beijing 100029, China	CAS	(Li, 2019)
GFDL_ESM4	ssp585	r1i1p1f1	20180701	National Oceanic and Atmospheric Administration, Geophysical Fluid Dynamics Laboratory, Princeton, NJ 08540, USA	NOAA-GFDL	(John et al., 2018)
GISS_E2_1_G	ssp585	r1i1p1f2	20200115	Goddard Institute for Space Studies, New York, NY 10025, USA	NASA-GISS	(NASA Goddard Institute for Space Studies (NASA/GISS), 2020)
INM_CM4_8	ssp585	r1i1p1f1	20190603	Institute for Numerical Mathematics, Russian Academy of Science, Moscow 119991, Russia	INM	(Volodin et al., 2019)
IPSL_CM6A_LR	ssp585	r1i1p1f1	20190903	Institut Pierre Simon Laplace, Paris 75252, France	IPSL	(Boucher et al., 2019)
MIROC6	ssp585	r1i1p1f1	20191016	JAMSTEC (Japan Agency for Marine-Earth Science and Technology, Kanagawa 236-0001, Japan), AORI (Atmosphere and Ocean Research Institute, The University of Tokyo, Chiba 277-8564, Japan), NIES (National Institute for Environmental Studies, Ibaraki 305-8506, Japan), and R-	MIROC	(Shiogama et al., 2019)

				CCS (RIKEN Center for Computational Science, Hyogo 650-0047, Japan)		
MPI_ESM1_2_LR	ssp585	r10i1p1f1	20190710	Max Planck Institute for Meteorology, Hamburg 20146, Germany	MPI-M	(Wieners et al., 2019)
MRI_ESM2_0	ssp585	r1i1p1f1	20191108	Meteorological Research Institute, Tsukuba, Ibaraki 305-0052, Japan	MRI	(Yukimoto et al., 2019)
NorESM2_MM	ssp585	r1i1p1f1	20191108	NorESM Climate modeling Consortium consisting of CICERO (Center for International Climate and Environmental Research, Oslo 0349), MET-Norway (Norwegian Meteorological Institute, Oslo 0313), NERSC (Nansen Environmental and Remote Sensing Center, Bergen 5006), NILU (Norwegian Institute for Air Research, Kjeller 2027), UiB (University of Bergen, Bergen 5007), UiO (University of Oslo, Oslo 0313) and UNI (Uni Research, Bergen 5008), Norway. Mailing address: NCC, c/o MET-Norway, Henrik Mohns plass 1, Oslo 0313, Norway	NCC	(Bentsen et al. 2019)

68

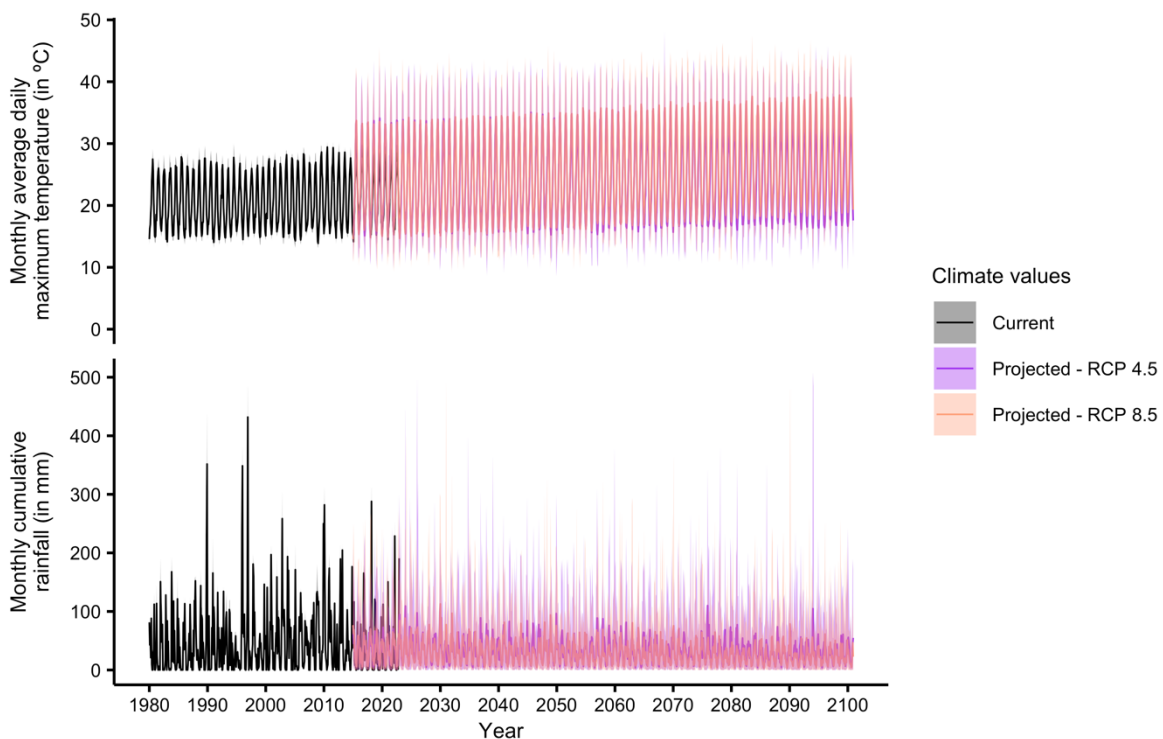
69 **3. Current and future climatic trends**

70

71 Temperatures have increased in the past decades, with an average trend

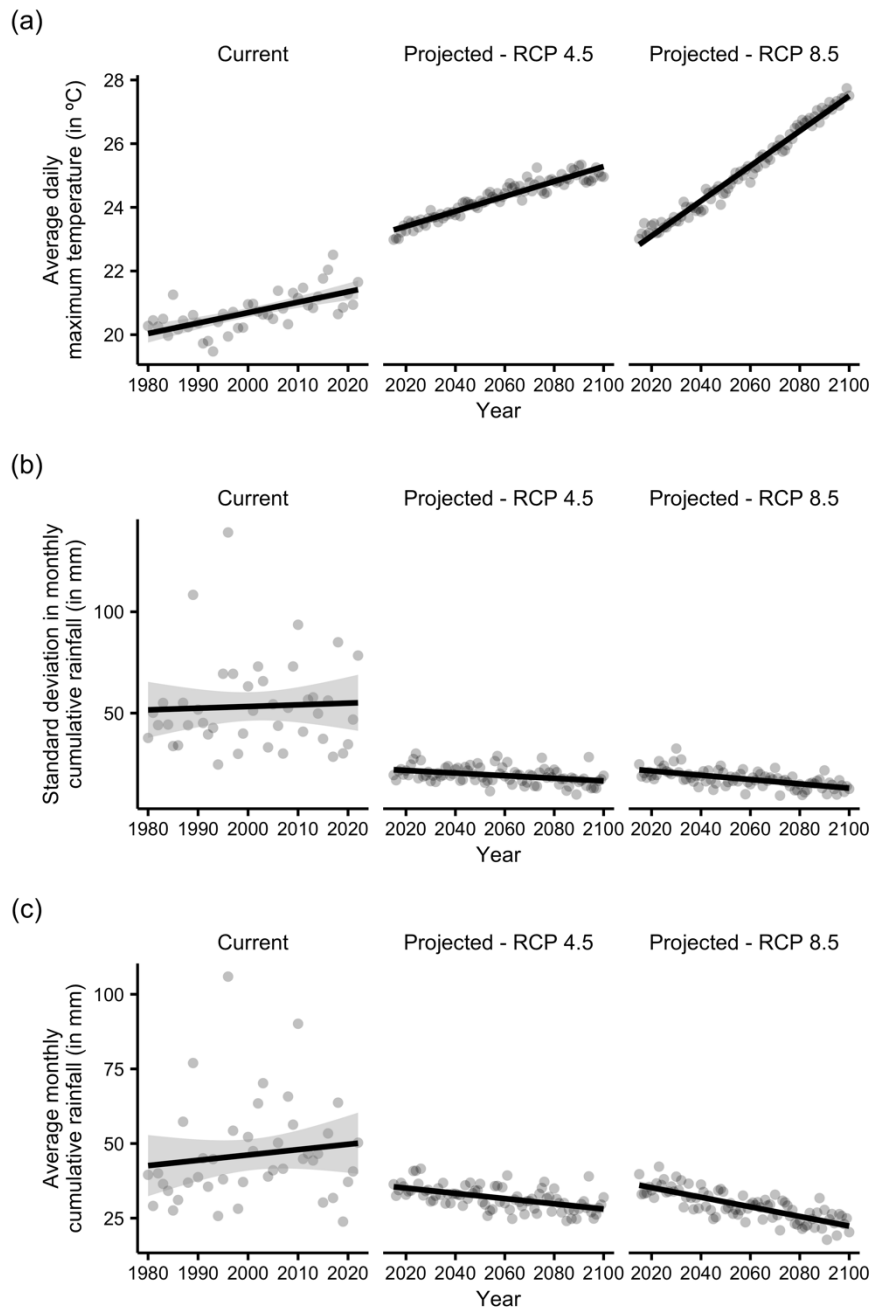
72 (mean and 95% confidence interval) of 0.033 °C [0.021; 0.044] per year between

73 1980 and 2022. This trend will continue and intensify in the future, as climate-change
 74 models predict an increase of 0.055 °C [0.053; 0.057] per year on average between
 75 2015 and 2100 under the RCP 8.5 global change scenario (Moss et al., 2010; van
 76 Vuuren et al., 2011; Riahi et al., 2011). Average monthly cumulative rainfall and its
 77 variability show opposite trends between the current and projected conditions. Both
 78 the yearly mean and variability increased on average between 1980 and 2022 (0.18
 79 [-0.23, 0.59] and 0.083 mm [-0.47, 0.63] per year, respectively) but are predicted to
 80 decrease until 2100 according to future projections under the RCP 8.5 scenario (-
 81 0.16 [-0.19, -0.13] and -0.11 mm [-0.14, -0.077]). Notably, while the RCP 4.5 global
 82 change scenario predicts a more moderate increase in temperature, both scenarios
 83 show the same trend for the 30 years of our projections (Fig. S1; Fig. S2a).



84 **Figure S1 – Current and projected monthly temperature and rainfall data.**
 85 We obtained current data on daily maximum temperature and daily rainfall amounts
 86 from the E-OBS dataset from the EU-FP6 project UERRA and the Copernicus
 87 Climate Change Service. We extracted the projected rainfall and temperature values

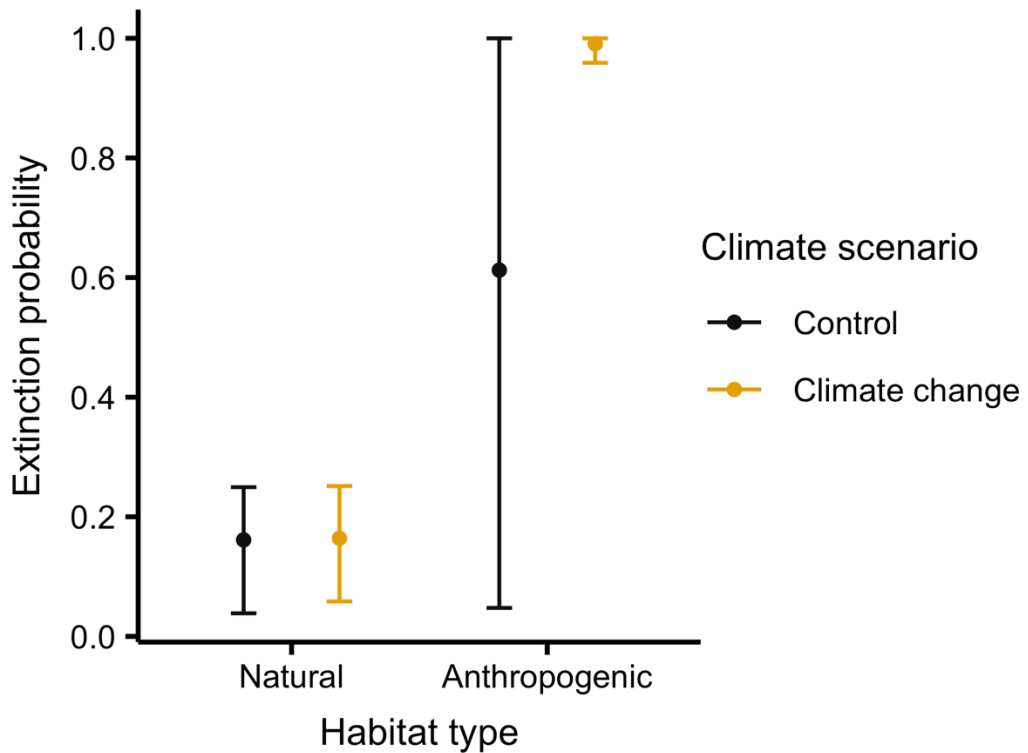
88 under the RCP 4.5 and 8.5 global change scenarios from 11 global change models
89 from the Coupled Model Intercomparison Project 6 (CMIP6; available from the Earth
90 System Grid Federation).



91 **Figure S2 – Current and projected trends in temperature and rainfall.** We
92 investigated yearly changes in (a) average daily maximum temperature, (b) standard
93 deviation in monthly cumulative rainfall, and (c) average monthly cumulative rainfall,
94 for the current (1980–2022) and projected conditions (2015–2100) under the RCP

95 4.5 and 8.5 global change scenarios. Dots represent the observed values and lines
96 and shaded ribbons represent the mean and 95% confidence interval of linear
97 models fitted to each data subset.

98



99

100 **Figure S3 – Demographic consequences of climate change in natural**
101 **and anthropogenic populations of dewy pines under scenario RCP4.5.** We
102 projected each natural and anthropogenic population 500 times for 30 years under a
103 control (keeping temperature and rainfall conditions as currently observed) and two
104 climate-change scenarios (RCP4.5 and RCP8.5). Here, we show results for scenario
105 RCP4.5 (see Figure 5 in the main text for RCP8.5). We computed, for each
106 population, the probability of quasi-extinction (p_{q-ext}). Here we summarise these
107 metrics per habitat type, and the variability in the values therefore correspond to
108 among-population and among-projection differences.

109

110 **References – Appendix S2**

111

112 Bentsen, M., Olivière, D. J. L., Seland, Ø., Toniazzi, T., Gjermundsen, A., Graff, L. S.,
113 Debernard, J. B., Gupta, A. K., He, Y., Kirkevåg, A., Schwinger, J., Tjiputra,
114 J., Aas, K. S., Bethke, I., Fan, Y., Griesfeller, J., Grini, A., Guo, C., Ilicak, M.,
115 ... Schulz, M. (2019). *NCC NorESM2-MM Model Output Prepared for CMIP6*
116 *ScenarioMIP ssp585*. Version 20191108. Earth System Grid Federation.
117 <https://doi.org/10.22033/ESGF/CMIP6.8321>

118 Boucher, O., Denvil, S., Levavasseur, G., Cozic, A., Caubel, A., Foujols, M.-A.,
119 Meurdesoif, Y., Cadule, P., Devilliers, M., Dupont, E., & Lurton, T. (2019).
120 IPSL IPSL-CM6A-LR Model Output Prepared for CMIP6 ScenarioMIP ssp585.
121 Version 20190903. Earth System Grid Federation.
122 <https://doi.org/10.22033/ESGF/CMIP6.5271>

123 Cornes, R. C., van der Schrier, G., van den Besselaar, E. J. M., & Jones, P. D.
124 (2018). An Ensemble Version of the E-OBS Temperature and Precipitation
125 Data Sets. *Journal of Geophysical Research: Atmospheres*, **123**(17), 9391–
126 409. <https://doi.org/10.1029/2017JD028200>

127 EC-Earth Consortium (EC-Earth). (2019). *EC-Earth-Consortium EC-Earth3 Model*
128 *Output Prepared for CMIP6 ScenarioMIP ssp585*. Version 20200425. Earth
129 System Grid Federation. <https://doi.org/10.22033/ESGF/CMIP6.4912>

130 Eyring, V., Bony, S., Meehl, G. A., Senior, C. A., Stevens, B., Stouffer, R. J., &
131 Taylor, K. E. (2016). Overview of the Coupled Model Intercomparison Project
132 Phase 6 (CMIP6) Experimental Design and Organization. *Geoscientific Model*
133 *Development*, **9**(5), 1937–58. <https://doi.org/10.5194/gmd-9-1937-2016>

134 Gómez-González, S., Paniw, M., Antunes, K., & Ojeda, F. (2018). Heat Shock and

135 Plant Leachates Regulate Seed Germination of the Endangered Carnivorous
136 Plant *Drosophyllum Lusitanicum*. *Web Ecology*, **18**(1), 7–13.

137 John, J. G., Blanton, C., McHugh, C., Radhakrishnan, A., Rand, K., Vahlenkamp, H.,
138 Wilson, C., Zadeh, N. T., Dunne, J. P., Dussin, R., Horowitz, L. W., Krasting,
139 J. P., Lin, P., Malyshev, S., Naik, V., Ploshay, J., Shevliakova, E., Silvers, L.
140 Stock, C., Winton, M., & Zeng, Y. (2018). *NOAA-GFDL GFDL-ESM4 Model*
141 *Output Prepared for CMIP6 ScenarioMIP ssp585*. Version 20180701. Earth
142 System Grid Federation. <https://doi.org/10.22033/ESGF/CMIP6.8706>

143 Li, L. (2019). *CAS FGOALS-G3 Model Output Prepared for CMIP6 ScenarioMIP*
144 *ssp585*. Version 20190818. Earth System Grid Federation.
145 <https://doi.org/10.22033/ESGF/CMIP6.3503>

146 Moss, R. H., Edmonds, J. A., Hibbard, K. A., Manning, M. R., Rose, S. K., van
147 Vuuren, D. P., Carter, T. R., Emori, S., Kainuma, M., Kram, T., Meehl, G. A.,
148 Mitchell, J. F. B., Nakicenovic, N., Riahi, K., Smith, S. J., Stouffer, R. J.,
149 Thomson, A. M., Weyant, J. P., & Wilbanks, T. J. (2010). The next generation
150 of scenarios for climate change research and assessment. *Nature*, 463, 747–
151 756. <https://doi.org/10.1038/nature08823>

152 NASA Goddard Institute for Space Studies (NASA/GISS). (2020). *NASA-GISS*
153 *GISS-E2.1G Model Output Prepared for CMIP6 ScenarioMIP ssp585*. Version
154 20200115. Earth System Grid Federation.
155 <https://doi.org/10.22033/ESGF/CMIP6.7460>

156 Paniw, M., Quintana-Ascencio, P. F., Ojeda, F., & Salguero-Gómez, R. (2017b).
157 Interacting Livestock and Fire May Both Threaten and Increase Viability of a
158 Fire-Adapted Mediterranean Carnivorous Plant. *Journal of Applied Ecology*,
159 **54**(6), 1884–94. <https://doi.org/10.1111/1365-2664.12872>

160 Parding, K. M., Dobler, A., McSweeney, C. F., Landgren, O. A., Benestad, R.,
161 Erlandsen, H. B., Mezghani, A., Gregow, H., Rätty, O., Viktor, E., El Zohbi, J.,
162 Christensen, O. B., & Loukos, H. (2020). GCMeval – An Interactive Tool for
163 Evaluation and Selection of Climate Model Ensembles. *Climate Services*,
164 **18**(April), 100167. <https://doi.org/10.1016/j.cliser.2020.100167>

165 Pascoe, C., Lawrence, B. N., Guilyardi, E., Juckes, M., & Taylor, K. E. (2020).
166 Documenting Numerical Experiments in Support of the Coupled Model
167 Intercomparison Project Phase 6 (CMIP6). *Geoscientific Model Development*,
168 **13**(5), 2149–67. <https://doi.org/10.5194/gmd-13-2149-2020>

169 Petrie, R., Denvil, S., Ames, S., Levavasseur, G., Fiore, S., Allen, C., Antonio, F.,
170 Berger, K., Bretonnière P.-A., Cinquini, L., Dart, E., Dwarakanath, P., Drukem,
171 K., Evans, B., Franchistéguy, L., Gardoll, S., Gerbier, E., Greenslade, M.,
172 Hassell, D., ... Wagner, R. (2021). Coordinating an Operational Data
173 Distribution Network for CMIP6 Data. *Geoscientific Model Development*,
174 **14**(1), 629–44. <https://doi.org/10.5194/gmd-14-629-2021>

175 Pierce, D. (2021). Ncdf4: Interface to Unidata netCDF (Version 4 or Earlier) Format
176 Data Files. R. <https://CRAN.R-project.org/package=ncdf4>

177 Riahi, K., Rao, S., Krey, V., Cho, C., Chirkov, V., Fischer, G., Kindermann, G.,
178 Nakicenovic, N., & Rafaj, P. (2011). RCP 8.5—A Scenario of Comparatively
179 High Greenhouse Gas Emissions. *Climatic Change*, **109**(1), 33.
180 <https://doi.org/10.1007/s10584-011-0149-y>

181 Shiogama, H., Abe, M., & Tatebe, H. (2019). *MIROC MIROC6 Model Output*
182 *Prepared for CMIP6 ScenarioMIP ssp585. Version 20191016*. Earth System
183 Grid Federation. <https://doi.org/10.22033/ESGF/CMIP6.5771>

184 Swart, N. C., Cole, J. N. S., Kharin, V. V., Lazare, M., Scinocca, J. F., Gillett, N. P.,

185 Anstey, J., Arora, V., Christian, J. R., Jiao, Y., Lee, W. G., Majaess, F.,
186 Saenko, O. A., Seiler, C., Seinen, C., Shao, A., Solheim, L., von Salzen, K.,
187 Yango, D., Winter, B., & Sigmond, M. (2019). *CCCma CanESM5 Model*
188 *Output Prepared for CMIP6 ScenarioMIP ssp585*. Version 20190429. Earth
189 System Grid Federation. <https://doi.org/10.22033/ESGF/CMIP6.3696>

190 van Vuuren, D. P., Edmonds, J., Kainuma, M., Riahi, K., Thomson, A., Hibbard, K.,
191 Hurtt, G. C., Kram, T., Krey, V., Lamarque, J.-L., Masui, T., Meinshausen, M.,
192 Nakicenovic, N., Smith, S. J. & Rose, S. K. (2011). The representative
193 concentration pathways: an overview. *Climatic Change*, **109**, 5.
194 <https://doi.org/10.1007/s10584-011-0148-z>

195 Volodin, E., Mortikov, E., Gritsun, A., Lykossov, V., Galin, V., Diansky, N., Gusev, A.,
196 Kostykin, S., Iakovlev, N., Shestakova, A., & Emelina, S. (2019). *INM INM-*
197 *CM4-8 Model Output Prepared for CMIP6 ScenarioMIP ssp585*. Version
198 20190603. Earth System Grid Federation.
199 <https://doi.org/10.22033/ESGF/CMIP6.12337>

200 Waliser, D., Gleckler, P. J., Ferraro, R., Taylor, K. E., Ames, S., Biard, J., Bosilovich,
201 M. G., Brown, O., Chepfer, H., Cinquini, L., Durack, P.J., Eyring, V., Mathieu,
202 P.-P., Lee, T., Pinnock, S., Potter, G. L., Rixen, M., Saunders, R., Schulz, J.,
203 Thépaut, J.-N., Tuma, M. (2020). Observations for Model Intercomparison
204 Project (Obs4MIPs): Status for CMIP6. *Geoscientific Model Development*,
205 **13**(7), 2945–58. <https://doi.org/10.5194/gmd-13-2945-2020>

206 Wieners, K.-H., Giorgetta, M., Jungclaus, J., Reick, C., Esch, M., Bittner, M., Gayler,
207 V., Haak, H., de Vrese, P., Raddatz, T., Mauritsen, T., von Storch, J.-S.,
208 Behrens, J., Brovkin, V., Claussen, M., Crueger, T., Fast, I., Fiedler, S.,
209 Hagemann, S., ... Roeckner, E. (2019). *MPI-M MPI-ESM1.2-LR Model Output*

210 *Prepared for CMIP6 ScenarioMIP ssp585. Version 20190710. Earth System*
211 Grid Federation. <https://doi.org/10.22033/ESGF/CMIP6.6705>
212 Yukimoto, S., Koshiro, T., Kawai, H., Oshima, N., Yoshida, K., Urakawa, S., Tsujino,
213 H., Deushi, M., Tanaka, T., Hosaka, M., Yoshimura, H., Shindo, E., Mizuta,
214 R., Ishii, M., Obata, A., & Adachi, Y. (2019). *MRI MRI-ESM2.0 Model Output*
215 *Prepared for CMIP6 ScenarioMIP ssp585. Version 20191108. Earth System*
216 Grid Federation. <https://doi.org/10.22033/ESGF/CMIP6.6929>

1 **Appendix S3 – Individual-based model description**

2

3 The model description follows the ODD (Overview, Design concepts, Details)
4 protocol for describing individual- and agent-based models (Grimm et al., 2006), as
5 updated by (Grimm et al., 2020).

6

7 1. Purpose and patterns

8

9 The purpose of the model is to predict population growth rates and extinction
10 probabilities of dewy-pine (*Drosophyllum lusitanicum*) populations in natural and
11 anthropogenic habitats in response to projected changes in rainfall and temperature
12 values. We evaluate our model by its ability to reproduce the observed dynamics in
13 the mean changes in aboveground abundance in each population, or at least follow
14 a similar trend.

15

16 2. Entities, state variables, and scales

17

18 *Entities and state variables*

19

20 The **environment** is a single entity representing the population. Its role is to
21 describe the environment (e.g. climate variables) and keep track of simulated time.
22 Environment state variables correspond to dynamic global variables and are
23 presented in Table 1.

24 **Table 1 – Environment state variables**

Variable name	Variable type and units	Range	Meaning
<i>time_sim</i>	Integer; dynamic	≥1	Number of years that passed since the start of the projection
<i>year_obs</i>	Integer; dynamic (e.g. 2020)	≥2016	Current year in the projection
<i>year</i>	Integer; dynamic (e.g. 2020)	≥2016	Year randomly sampled from the available observed years
<i>TSF</i>	Integer; dynamic	≥0	Number of years since the last fire
<i>TSFcat</i>	Categorical; dynamic (0–4)	{0, 1, 2, 3, 4}	Post-fire habitat stage, with any number of years after a fire ≥ 4 corresponding to 4
<i>corr_seed_surv</i>	Probability; dynamic	[0, 1]	Correction factor representing the survival probability of seeds above the ground
<i>summerT</i>	Real number; °C; dynamic	≥0	Average minimum daily temperature in summer (May–September) following the annual survey in May
<i>prevwinterT</i>	Real number; °C; dynamic	≥0	Average minimum daily temperature in winter (January–April) prior to the annual survey in May
<i>fallR</i>	Integer; mm; dynamic	≥0	Cumulative rainfall in fall (September–November) following the annual survey in May
<i>prevfallR</i>	Integer; mm; dynamic	≥0	Cumulative rainfall in fall (September–November) prior to the annual survey in May
<i>prevwinterR</i>	Integer; mm; dynamic	≥0	Cumulative rainfall in winter (January–April) prior to the annual survey in May
<i>extinction</i>	Binary; dynamic	{0, 1}	Current state of the population: extinct (1) or not (0)

25

26 **Plants** are entities representing the aboveground—as opposed to seeds—individual

27 dewy pines in the population. They correspond to individuals from the seedling stage

28 in the species life cycle. The state variables unique to each plant are presented in
 29 Table 2.

30

31 **Table 2 – Plant state variables**

Variable name	Variable type and units	Range	Meaning
<i>ID</i>	Character string; static	NA	Unique identifier of the plant
<i>quadratID</i>	Character string; static	NA	Unique identifier of the quadrat corresponding to the location of the plant
<i>size</i>	Real number; dynamic	≥ 0	Plant size in the current time step, corresponding to $\log(\text{number of leaves} \times \text{length of the longest leaf in cm})$
<i>survival</i>	Binary; dynamic	{0, 1}	State of the plant at the next time step: alive (1) or dead (0)
<i>sizeNext</i>	Real number; dynamic	≥ 0	Plant size in the next time step, corresponding to $\log(\text{number of leaves} \times \text{length of the longest leaf in cm})$
<i>flowering</i>	Binary; dynamic	{0, 1}	Reproductive state of the plant in the current time step: flowering (1) or not (0)
<i>nbFlowers</i>	Integer; dynamic	≥ 0	Number of flowers on the plant
<i>nb_seeds</i>	Integer; dynamic	≥ 0	Number of seeds per flower produced by the plant

32

33 Seeds are entities representing individuals before they germinate and become
 34 seedlings. Because they are concerned by different processes, we divided seeds
 35 between two types of entities: **Seedbank seeds** are entities representing the seeds
 36 in the soil seedbank and **produced seeds** are entities representing the individuals
 37 that have been produced by aboveground reproducing dewy pines in the current
 38 time step. Their state variables are presented in Table 3 and Table 4.

39 **Table 3 – Seedbank seed state variables**

Variable name	Variable type and units	Range	Meaning
<i>ID</i>	Character string; static	NA	Unique identifier of the seed
<i>quadratID</i>	Character string; static	NA	ID of the quadrat corresponding to the location of the seed
<i>size</i>	Real number; dynamic	≥ 0	Size of the seedling growing from the germinating seed in the next time step, corresponding to $\log(\text{number of leaves} \times \text{length of the longest leaf in cm})$
<i>outSB</i>	Binary; dynamic	{0, 1}	Seed germination (1) or not (0)
<i>staySB</i>	Binary; dynamic	{0, 1}	Seed dormancy (1) or not (0)

40

41 **Table 4 – Produced seed state variables**

Variable name	Variable type and units	Range	Meaning
<i>ID</i>	Character string; static	NA	Unique identifier of the seed
<i>quadratID</i>	Character string; static	NA	ID of the quadrat corresponding to the location of the seed
<i>size</i>	Real number; dynamic	≥ 0	Size of the seedling growing from the germinating seed in the next time step, corresponding to $\log(\text{number of leaves} \times \text{length of the longest leaf in cm})$
<i>goCont</i>	Binary; dynamic	{0, 1}	Seed germination (1) or not (0)
<i>goSB</i>	Binary; dynamic	{0, 1}	Seed entering the seedbank (1) or not (0)

42

43 **Quadrats** are two-dimensional squares representing the monitoring units in which
44 plants are censused in a population. Quadrats are only associated with one dynamic
45 state variable, *abLarge*, an integer (≥ 0) corresponding to the number of plants with a
46 size > 4.5 present in a quadrat.

47

48 *Scales*

49

50 The model is spatially explicit and represents a population in a two-dimensional
51 space extending over 40 m² divided in 1-m² quadrats. These quadrats are discrete
52 units in which individual plants and seeds are distributed, and correspond to the units
53 in which dewy pines are monitored every year—more specifically in four separated
54 transects of ten quadrats each.

55

56 The model represents time via discrete time steps, each corresponding to one year,
57 to replicate the annual surveys that take place in May in the various populations.

58

59 3. Process overview and scheduling

60

61 *Process overview*

62

63 The model covers the life cycle of dewy pines. At each time step, the
64 **environment** updates the environmental variables and simulation time; the **plants**
65 reproduce, survive, and grow; the **seedbank seeds** germinate or stay dormant; and
66 the **produced seeds** germinate or go to the seedbank. The **quadrats** get new
67 aboveground density values.

68 *Schedule summary*

69

70 Throughout the model, the update of each state variable is done simultaneously for
71 all entities, as each process in a given entity (i.e., environment, seeds, and plants) is
72 assumed to be independent from the processes in another entity.

73

74 At each timestep, the model resets the ensemble of **seeds produced** to zero. The
75 population of **plants** is also reset if a fire occurred, as all aboveground individuals
76 are burned. The **environment** then updates the environmental variables (rainfall and
77 temperature) as well as the simulation year and the number of years after the last
78 fire. The latter two are used to update the correction factor representing seed
79 survival (*corr_seed_surv*).

80

81 Aboveground **plants** then reproduce (see *Reproduction* submodel); that is, they
82 flower and produce a certain number of flowers, which in turn produce seeds. The
83 number of flowers is capped to the user-selected value if needed. The fate of the
84 **seeds produced** is updated; they can either germinate, contribute to the seedbank,
85 or die (i.e., none of the two former processes). **Produced seeds** that do not die are
86 then assigned an ID, and those that germinate a size, and the maximum ID number
87 is updated.

88

89 After reproducing, **plants** survive and grow (*Survival and growth* submodel). The
90 size is capped or adjusted if needed. Seedbank processes take place next
91 (*Seedbank* submodel), with **seedbank seeds** germinating, staying dormant, or dying
92 (i.e., none of the two former processes). Seeds that germinate are attributed a size.

93 **Produced seeds** that were assigned to go dormant are added to the seedbank, and
94 those that germinate are added to the aboveground population after capping their
95 number in each **quadrat**.

96

97 After each timestep, the population growth rate and mean change in aboveground
98 population abundance are calculated and the yearly individual data is merged to the
99 full data. The **environment** updates the simulation time and the extinction status to 1
100 if the quasi-extinction threshold is reached, and the size of each surviving **plant** is
101 updated to its size at the next time step. Finally, the aboveground density in each
102 **quadrat** is updated.

103

104 *Schedule details*

105

106 The schedule follows the processes of the dewy-pine life cycle during a year from
107 the annual census occurring in May. This census occurs during the flowering period
108 and the model replicates this by starting with the *Reproduction* submodel. The
109 *Survival and growth* and *Seedbank* submodels could come in any order after
110 reproduction took place, as they are independent from each other.

111

112 In natural populations, the schedule depends on the fire regime. Reproduction does
113 not happen until the second year after a fire occurs, and only survival and growth, as
114 well as germination or dormancy in the seedbank, are represented in the year of a
115 fire and the following year.

116 4. Design concepts

117

118 1. Basic principles

119

120 This model relies on previous knowledge on the life cycle of dewy pines
121 (Paniw et al., 2017; Conquet et al., 2023) to perform a population viability analysis
122 (PVA), a modelling approach commonly used in population ecology. By projecting
123 population dynamics into the future, a PVA aims at assessing the probability of
124 persistence of populations and allows for the introduction of stochasticity in
125 environmental conditions (e.g. fire return, or sampling from a distribution of
126 temperature and rainfall values). While this model is designed for plant populations
127 and does not include any representation of social organisation or individual's
128 decision processes, it allows to take into account demographic stochasticity (by
129 sampling demographic processes from distributions), which is often unaccounted for
130 in PVAs due to the use of simplified population models such as matrix population
131 models (MPM) or integral projection models (IPM).

132

133 2. Emergence

134

135 Changes in aboveground population size emerge from individual fate, which in turn
136 emerges from the relationship between demographic processes (e.g. survival or
137 reproduction) and individual traits (plant size), density, and environmental variables.
138 Individual traits and density vary with changes in demographic processes affecting
139 individual fate. How the various demographic processes interact to shape individual
140 life histories is imposed by previous empirical observations on the species' life cycle.

141 Seedbank processes emerge from the simulated sequence of post-fire habitat
142 stages (in natural populations) or from site-specific parameters that do not vary
143 through time parameters (in anthropogenic populations).

144

145 3. Adaptation

146

147 Individuals do not make any decisions based on objectives in this model.

148

149 4. Objectives

150

151 Individuals do not use any fitness measure to make decisions.

152

153 5. Learning

154

155 Learning is not implemented in this model.

156

157 6. Prediction

158

159 Prediction is not implemented in this model.

160

161 7. Sensing

162

163 Sensing is not implemented in this model.

164 8. Interaction

165

166 Interactions between individuals in this model are mediated by competition for
167 resources (e.g. light or prey) and facilitation (e.g. provision of shade). These
168 interactions are represented by the effect of density at the beginning of year t on
169 demographic processes, and in turn individual fate, from time t to $t+1$. Here, density
170 corresponds more specifically to the number of aboveground individuals of size > 4.5
171 in a given 1-m² quadrat, as we expect from observations that individuals further than
172 the quadrat are too far to affect focal plants, and that smaller individuals only have a
173 small effect on other individuals.

174

175 9. Stochasticity

176

177 Stochasticity occurs at several levels of the model. First, if the user chooses to
178 project the population under current climatic conditions, the sequence of years of the
179 desired length will be created by randomly sampling from the list of observed years.
180 If the user chooses to project the population under future climate-change conditions,
181 this random sampling of observed years is used to obtain the sequence of years to
182 be used as random effects in the submodels, that is, the years representing the
183 variation in demographic processes that is not explained by environmental
184 conditions, individual traits, or density.

185

186 Additionally, all demographic processes governing the fate of both aboveground
187 **plants** and **produced and seedbank seeds** are stochastic. For each **plant**, the
188 survival, size (at the next time step or after germinating), flowering status, and

189 number of flowers are sampled from binomial, scaled Student t , and Poisson
190 distributions with parameters obtained from predictions of generalised additive
191 models and depending on the environmental conditions, individual traits, and
192 density. For each **seed**, whether it germinates, stays dormant, or contributes to the
193 seedbank is sampled from a binomial distribution with parameters depending on the
194 site in which the simulation is performed or the time since last fire. The number of
195 seeds per flower for each **plant** is sampled from a Poisson distribution with a fixed
196 mean previously used in population projections for this system (Paniw et al., 2017;
197 Conquet et al., 2023).

198

199 Moreover, the location of each seed in the seedbank at the start of the simulation is
200 attributed randomly, with each quadrat having the same probability

201 $\frac{1}{\text{total number of quadrats}}$ to be designated as a seed's location. In subsequent years, all

202 **produced seeds** are assigned to the quadrat of the parent **plant**. This approach
203 allows us to reproduce the lack of active dispersal mechanisms in dewy pines,
204 leading most seeds to fall and establish next to the mother plant.

205

206 Finally, when the number of **plants** to add to the population is higher than the
207 capping threshold set by the user, the new individuals to be removed from the
208 recruits are sampled at random.

209

210 10. Collectives

211

212 There are no collectives in this model.

213

214 11. Observation

215

216 The two main outputs of this model are (1), for each simulation the yearly population
217 growth rates ($\log \lambda = \frac{N_t}{N_{t-1}}$, where N_t is the total population size—above ground and in
218 the seedbank—in year t and N_{t-1} in year $t-1$) that can be used to calculate the
219 stochastic growth rate over the whole simulation ($\log \lambda_S = \frac{\sum_{t=2}^T \log \lambda_t}{T}$ where T is the
220 number of simulated years), and (2) whether the population went extinct within the
221 number of simulated years, which can be used to obtain the probability of quasi-
222 extinction (proportion of simulations where the population went under the quasi-
223 extinction threshold, i.e., $10 >$ aboveground individuals and $50 >$ seeds in the
224 seedbank) across a number of simulations defined by the user.

225 In addition, the output of the model contains the full individual data across the whole
226 simulation, the mean change in aboveground population abundance (i.e. the
227 population growth rate without taking the seedbank into account), as well as
228 population size and population density (i.e. number of individuals of size > 4.5 per 1-
229 m² quadrat).

230

231 5. Initialization

232

233 For both habitats (natural and anthropogenic) and all scenarios (control and
234 climate change) the initial number of aboveground **plants**, as well as their size and
235 location (**quadrat**) corresponds to that observed in the population and first year
236 chosen by the user for the simulation, as does the density in each **quadrat**. The
237 number of **seeds** present in the seedbank when starting the simulation is defined by
238 the user (by default 10,000 for natural populations and 3,000 for anthropogenic

239 populations), and the **seeds** are initially assigned randomly to their **quadrat**. The
240 number of **produced seeds** and the extinction status are initialised at 0. The
241 sequence of yearly population growth rates, mean change in aboveground
242 population abundance, and population density are initialised with NAs.

243

244 In both scenarios, the required number of years (set by the user) is sampled among
245 the years observed in the full individual data (e.g. 30 samples of years 2016–2021).
246 This sequence of years is used to represent random year variation (i.e., random
247 effects in vital-rate models). However, the sequence of yearly temperature and
248 rainfall values depends on the scenario. Under the control scenario, these values
249 correspond to the observed climate in each year of the sampled sequence. When
250 the population is projected under climate change, the temperature and rainfall values
251 reflect the projected climate values obtained from the global circulation models
252 (GCM) from the first year defined by the user and following a chronological order
253 until the end of the simulation.

254

255 Finally, projecting natural populations requires to initialise a sequence of post-fire
256 habitat stages (0–4). In the first year, this corresponds to the stage observed in the
257 first year of the simulation (defined by the user). The following stages are determined
258 by a Markov chain (Fig. S1; see also Paniw et al., 2017; Conquet et al., 2023), where
259 the transition from the last to the first stage (fire year) depends on the probability of
260 fire return (p), which is set by the user (1/30 by default). The sequence of number of
261 years since the last fire (TSF) is initialised using the observed number in the first

262 year of the simulation, with the subsequent TSFs being inferred from the sequence
 263 of post-fire habitat stages.

264 Environment at t

		1	2	3	4	5
Environment at $t+1$	1	0	0	0	0	p
	2	1	0	0	0	0
	3	0	1	0	0	0
	4	0	0	1	0	0
	5	0	0	0	1	$1-p$

265
266
267
268
269

270 **Figure S1 - Markov chain determining the succession of post-fire**
 271 **habitats for the dewy pine population.** The first four states (from the fire year to
 272 the third year after a fire) constitute the deterministic part of the Markov chain and
 273 thus always follow each other in a sequence of 1 to 4 (probability of transition = 1).
 274 The fifth state (from the fourth year after a fire) is stochastic, and the transition from
 275 this state depends on the fire frequency p (i.e., the population will remain in state 5
 276 until a fire occurs).

277

278 6. Input data

279

280 The model uses as input data individual-based data on dewy pines
 281 (aboveground **plants**) in the population chosen by the user. These data have been
 282 collected during annual population surveys occurring in May since at least 2016
 283 (earlier for some populations, see Appendix S2). These surveys enabled us to obtain
 284 data on individuals' survival, size (log[length of the longest leaf x number of leaves]),
 285 reproductive status, and number of flowers (Paniw et al., 2017). Additionally, the
 286 model uses input data containing values from 2016 to 2050 of (1) average daily

287 minimum temperature (in °C) in summer and fall following a census and fall and
288 winter prior to a census, and (2) cumulative rainfall (in mm) in fall and winter
289 following a prior to a census. Details on data sources and preparation can be found
290 in Appendix S2.

291

292 7. Submodels

293

294 *Reproduction*

295

296 Flowering: Individuals can reproduce from two years after a fire occurred in natural
297 populations (Paniw et al., 2017). The reproductive status of individuals (0 or 1) is
298 drawn from a binomial distribution which probability is predicted from a generalised
299 additive model (GAM) describing the observed relationship between flowering
300 probability and winter mean daily maximum temperature, fall cumulative rainfall,
301 individual size, aboveground density of individuals with size > 4.5, and time since last
302 fire in natural populations (see Appendix S1: Table S5 for the full equation linking the
303 various covariates to flowering probability).

304

305 Number of flowers per individual: Reproductive individuals (i.e., flowering = 1) can
306 produce flowers, their number being drawn from a negative binomial distribution
307 which probability is predicted from a generalised additive model (GAM) describing
308 the observed relationship between the number of flowers and winter mean daily
309 maximum temperature, individual size, and time since last fire in natural populations
310 (see Appendix S1: Table S5 for the full equation linking the various covariates to the
311 number of flowers per individual).

312

313 Number of seeds per flower: The number of seeds for each flower is drawn from a
314 Poisson distribution with a mean fixed at 9.8, which corresponds to the value used in
315 previous population projections of the dewy-pine system (Paniw et al., 2017;
316 Conquet et al., 2023).

317

318 *Survival and growth*

319

320 Survival: Individual survival (0 or 1) is sampled from a binomial distribution which
321 probability is predicted from a generalised additive model (GAM) describing the
322 observed relationship between survival and summer mean daily maximum
323 temperature, fall cumulative rainfall, individual size, aboveground density of
324 individuals with size > 4.5, and time since last fire in natural populations (see
325 Appendix S1: Table S5 for the full equation linking the various covariates to survival).

326

327 Growth: The size of surviving individuals in the following year is sampled from a
328 truncated scaled Student *t* distribution with location (i.e. mean), scale (i.e. standard
329 deviation) and degrees of freedom obtained from a generalised additive model
330 describing the observed relationship between individuals' size in the next year and
331 fall cumulative rainfall, individual size, aboveground density of individuals with size >
332 4.5, and time since last fire in natural populations (see Appendix S1: Table S5 for the
333 full equation linking the various covariates to growth). The minimum or maximum
334 observed sizes were assigned to individuals with infinite size values.

335 *Seedbank*

336

337 Continuous germination and contribution to the seedbank: For each **produced seed**,
338 whether it germinated directly without going to the seedbank (0 or 1) was sampled
339 from a binomial distribution with a mean determined by the probability to germinate
340 when produced (goCont) which depended on time since last fire (in natural
341 populations) or site (in anthropogenic populations) (see Appendix S1: Table S1 for
342 details on the mean values). Among the seeds that will not germinate, seeds that will
343 contribute to the seedbank in the next year (0 or 1) were then sampled from a
344 binomial distribution with a mean determined by 1-goCont. The rest of the seeds
345 were considered dead and removed from the population. In anthropogenic
346 populations, the probabilities of continuous germination and contribution to the
347 seedbank were corrected for seed survival (i.e., multiplied by 0.33) and, in one
348 population (Sierra Carbonera Disturbed), further multiplied by 0.4 to replicate more
349 accurately the observed population dynamics.

350

351 Germination from the seedbank: For each **seedbank seed**, whether it germinated
352 from the seedbank (0 or 1) was sampled from a binomial distribution with a mean
353 depending on time since last fire (in natural populations) or site (in anthropogenic
354 populations) (see Appendix S1: Table S1 for details on the mean values). In
355 anthropogenic populations, the probability of germination from the seedbank was
356 corrected for seed survival (i.e., multiplied by 0.33) and, in one population (Sierra
357 Carbonera Disturbed), further multiplied by 0.4 to replicate more accurately the
358 observed population dynamics.

359

360 Dormancy: For each **seedbank seed**, whether it remained dormant in the seedbank
361 (0 or 1) was sampled from a binomial distribution with a mean depending on time
362 since last fire (in natural populations) or site (in anthropogenic populations) (see
363 Appendix S1: Table S1 for details on the mean values). In anthropogenic
364 populations, the probability of dormancy was corrected for seed survival (i.e.,
365 multiplied by 0.33) to replicate more accurately the observed population dynamics.

366

367 Seedling size: The size of a germinating seed is sampled from a truncated scaled
368 Student *t* distribution with location (i.e. mean), scale (i.e. standard deviation) and
369 degrees of freedom obtained from a generalised additive model describing the
370 observed relationship between seedling size and winter mean daily maximum
371 temperature, aboveground density of individuals with size > 4.5, and time since last
372 fire in natural populations (see Appendix S1: Table S5 for the full equation linking the
373 various covariates to seedling size). The minimum or maximum observed sizes were
374 assigned to individuals with infinite size values.

375 **References – Appendix S3**

376

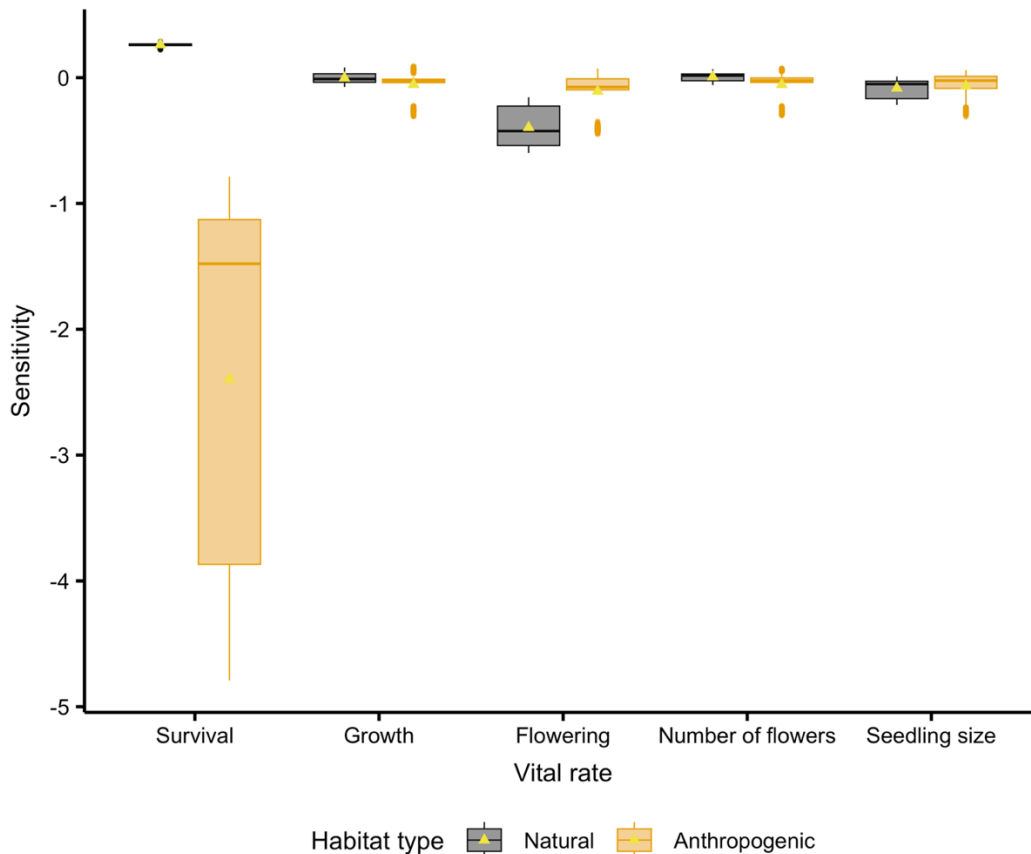
377 Conquet, E., Ozgul, A., Blumstein, D. T., Armitage, K. B., Oli, M. K., Martin, J. G. A.,
378 Clutton-Brock, T. H., & Paniw, M. (2023). Demographic Consequences of
379 Changes in Environmental Periodicity. *Ecology*, **104**(3), e3894.
380 <https://doi.org/10.1002/ecy.3894>

381 Grimm, V., Berger, U., Bastiansen, F., Eliassen, S., Ginot, V., Giske, J., Goss-
382 Custard, J., Grand, T., Heinz, S. K., Huse, G., Huth, A., Jepsen, J. U.,
383 Jørgensen, C., Mooij, W. M., Müller, B., Pe'er, G., Piuu, C., Railsback, S. F.,
384 Robbins, A. M., ... DeAngelis, D. L. (2006). A Standard Protocol for
385 Describing Individual-Based and Agent-Based Models. *Ecological Modelling*,
386 **198**(1), 115–26. <https://doi.org/10.1016/j.ecolmodel.2006.04.023>

387 Grimm, V., Railsback, S. F., Vincenot, C. E., Berger, U., Gallagher, C., DeAngelis, D.
388 L., Edmonds, B., Ge, J., Giske, J., Groeneveld, J., Johnston, A. S. A., Milles,
389 A., Nabe-Nielsen, J., Polhill, J. G., Radchuk, V., Rohwäder, M.-S., Stillman, R.
390 A., Thiele, J. C., & Ayllón, D. (2020). The ODD Protocol for Describing Agent-
391 Based and Other Simulation Models: A Second Update to Improve Clarity,
392 Replication, and Structural Realism. *Journal of Artificial Societies and Social*
393 *Simulation*, **23**(2), 7. <https://doi.org/10.18564/jasss.4259>

394 Paniw, M., Quintana-Ascencio, P. F., Ojeda, F., & Salguero-Gómez, R. (2017).
395 Interacting Livestock and Fire May Both Threaten and Increase Viability of a
396 Fire-Adapted Mediterranean Carnivorous Plant. *Journal of Applied Ecology*,
397 **54**(6), 1884–94. <https://doi.org/10.1111/1365-2664.12872>

1 Appendix S4 – Results from sensitivity analyses



2

3 **Figure S1 – Sensitivity of stochastic population growth rate across 30**

4 **years ($\log \lambda_s$) to climate-change effects in different vital rates.** We projected

5 each natural and anthropogenic population 100 times for 30 years by changing

6 temperature and rainfall values as projected under the RCP 8.5 climate-change

7 scenario in specific vital rates while keeping climatic drivers at their past observed

8 values for the remaining vital rates. We then calculated % changes in $\log \lambda_s$

9 compared to a control scenario where climatic drivers are at their past observed

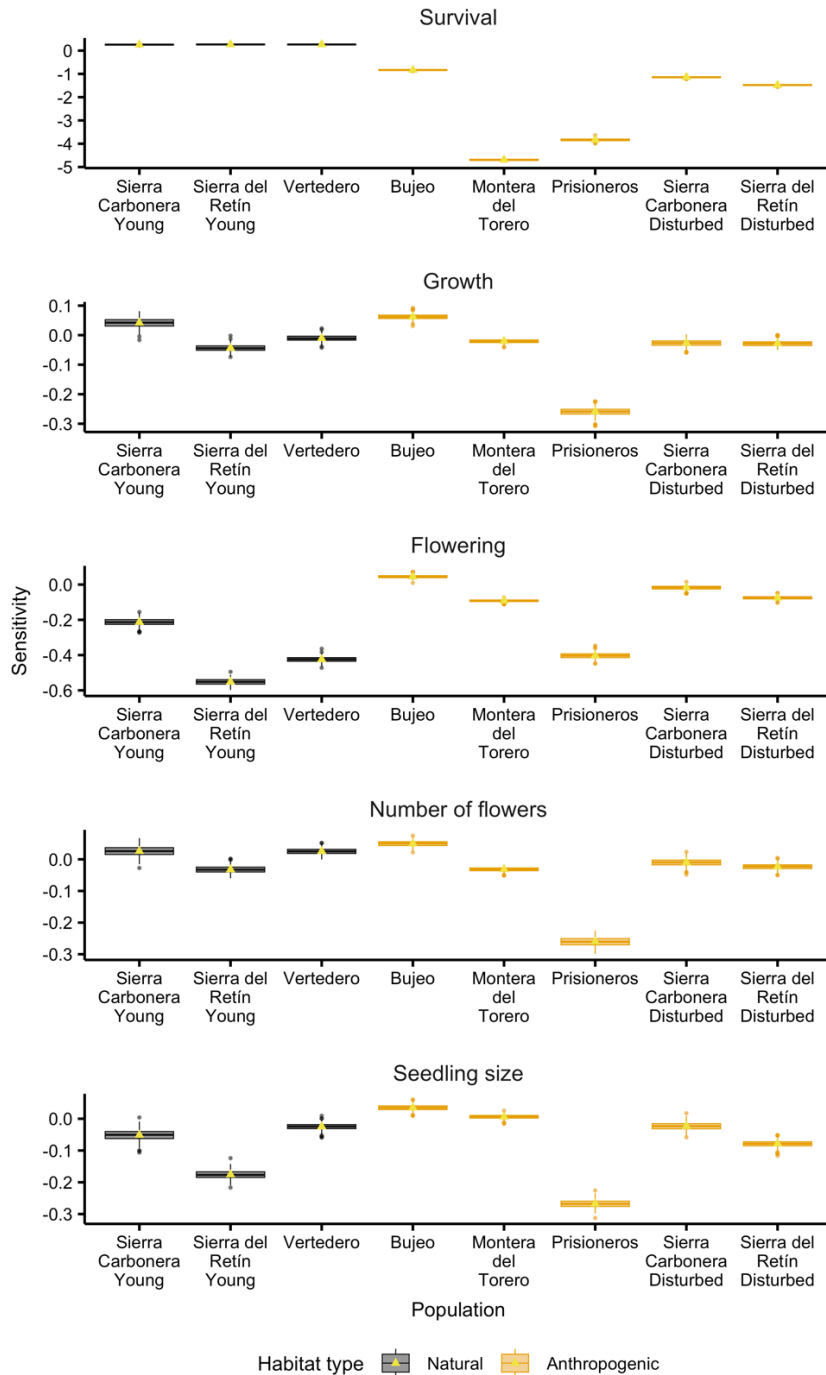
10 values for all vital rates (500 $\log \lambda_s$ for each population). We calculated 500

11 sensitivity values for each population by randomly sampling 100 $\log \lambda_{s_control}$ from

12 the 500 available and comparing them to the 100 available $\log \lambda_{s_perturbed}$. Here

13 we summarise these changes per vital rate, with the triangles representing averages

14 across populations and sensitivity simulations.



15

16 **Figure S2 – Sensitivity of stochastic population growth rate across 30**

17 **years ($\log \lambda_s$) to climate-change effects in different vital rates across**

18 **populations.** We projected each natural and anthropogenic population 100 times for

19 30 years by changing temperature and rainfall values as projected under the RCP

20 8.5 climate-change scenario in specific vital rates while keeping climatic drivers at

21 their past observed values for the remaining vital rates. We then calculated %

22 changes in $\log \lambda_S$ compared to a control scenario where climatic drivers are at their
23 past observed values for all vital rates (500 $\log \lambda_S$ for each population). We
24 calculated 500 sensitivity values for each population by randomly sampling 100 \log
25 $\lambda_{S_control}$ from the 500 available and comparing them to the 100 available \log
26 $\lambda_{S_perturbed}$. Here we summarise these changes per vital rate and population, with
27 the triangles representing averages across 500 sensitivity values.

28